Mechanisms underlying Formin-2 function in the motility of neuronal growth cones

A Thesis Submitted in partial fulfillment of the requirements for the degree of Doctor of Philosophy

By

Ketakee Ghate

20112003

Indian Institute of Science Education and Research

(IISER), Pune

2019

Declaration

I declare that this written submission represents my research work in my own words and where others' ideas or works have been included, I have adequately cited and referenced the original sources. I also declare that I have adhered to all principles of academic honesty and integrity and have not misrepresented or fabricated or falsified any idea/data/fact/source in my submission. I understand that violation of the above will because for disciplinary action by the Institute and can also evoke penal action from the sources which have thus not been properly cited or from whom proper permission has not been taken when needed.

Date: 11/03/2019

Ketakee Ghate

Reg. No: 20112003

Certificate

It is certified that the work incorporated in the thesis entitled "**Mechanisms underlying Formin-2 function in the motility of neuronal growth cones**" submitted by Ketakee Ghate was carried out by the candidate, under my supervision. The work presented here or any part of it has not been included in any other thesis submitted previously for the award of any degree or diploma from any other University or institution.

Date: 11/03/2019

Dr. Aurnab Ghose

Thesis advisor

Acknowledgements

I joined IISER, Pune in August 2011 as a part of the first Integrated Ph.D. programme. Since then, it has been an excellent learning experience and a privilege to be a part of the IISER family. I would like to take this opportunity to express my deepest appreciation to everyone who has been directly or indirectly a part of this experience.

First and foremost, I would like to thank my thesis advisor Dr. Aurnab Ghose for being an incredible mentor and giving me the opportunity to work with him. I am really grateful to him for giving the freedom to explore new ideas during my Ph.D. I have learned from him patience; optimism and scientific thinking which have helped me grow professionally as well as personally. I sincerely thank him for his constant support, encouragement and constructive criticism which has always helped and improved my scientific communications and research perspective.

I would like to thank my RAC members Dr. Richa Rikhy and Dr.Surendra Ghaskadbi for their critical inputs and suggestions. I am also grateful to Dr. Mayurika Lahiri for her support and assistance regarding animal cell culture which gave me an opportunity to work with mouse fibroblasts. I would also like to express my deepest regards to Prof. Nishikant Subhedar who was an important part of this journey and our lab who taught me a tremendous passion for pursuing neuroscience.

I sincerely thank Dr. Shamik Sen and Kavitha Sthanam (IIT, Bombay) for their help with measuring PAA gel stiffness. I also thank Dr. David Odde (University of Minnesota) for kindly sharing the flow-tracker code and for assistance with the analysis. I also thank Denis Tsygankov (the University of North Carolina at Chapel Hill) for his prompt assistance with CellGeo analysis.

Additionally, IISER, Pune provided me with state of the art infrastructure which allowed me to carry out my experiments with great ease. To facilitate this, a number of people helped me

with ordering, procurement of reagents and even instrumentation. I would like to thank all of them; Mrunalini, Mahesh, Piyush, Kalpesh, Roopali, and Shabnam for their help and assistance.

I would like to express special thanks to IISER microscopy facility without which any work in this project would not have been possible. Thanks to very kind and prompt help from Vijay Vitthal who not only taught me working with microscopes but who was also extremely helpful with any microscopy query and analysis. I would also like to thank other staff at the microscopy facility; Santosh, Aditi, and Rahul for helping me from time to time.

I thank all my past and present lab members; Abhishek, Sampada, Ajesh, Tanushree, Dhriti, Aditi and Devika for their input and suggestions. I thank Abhishek once again for helping me with several techniques in the lab during the first few years of my Ph.D. I especially thank Sampada for being my partner and sharing silly jokes and laughs in the lab. I also learned a lot from Sampada scientifically which inspired me in my research. I thank Tanushree, Dhriti, Aditi, and Devika for our scientific and non-scientific discussions that made the lab life really enjoyable.

I made some really great friends during my Ph.D. at IISER. I especially would like to thank Sayali, Aditi, and Sampada for our entertaining coffee times and accompanying discussions. I thank them for their relentless support for my adventures in science and otherwise! I also met many wonderful people during this time that helped me grow as a scientist and as a person through our interactions. I would like to thank Chaitanya, Shubhankar, Manasi, Niraja, Libi, Rupa, Trupti and many others who directly or indirectly assisted me in my Ph.D.

I also thank my friends outside IISER who supported me and motivated me from time to time. I thank Ketaki, Shalmali, Gauri, Anuja, Sumedha and Amba for our random meetings and discussions that helped me refresh and relieve the work stress.

Last but definitely not the least; I would like to express my deepest appreciation to my family. I thank my mother, father, and sister, for supporting my every decision and keeping me motivated to pursue my passion for research.

Contents

List of figures

Abstract

Stereotyped wiring of the nervous system during development is accomplished by guidance cues which tightly control and shape neuronal trajectories and instruct the growth cone to make appropriate synaptic contacts. Tight regulation of growth cone steering is achieved by remodelling the underlying growth cone cytoskeleton that regulates polarity, protrusion, substrate adhesion and generation of coordinated traction forces. However, exact mechanisms of this regulation still remain less characterized in growth cones.

In the following thesis, we focus on Formin-2 (Fmn2), a member of the formin family of actin-binding proteins. Earlier work from our group has shown that perturbation of Fmn2 in the developing chick spinal cord results in defective trajectories of spinal commissural neurons *in vivo*. In this study we show that Fmn2 transcript is not only enriched in the spinal cord but also higher expression coincides with the developmental window of commissural interneuron pathfinding in the spinal cord. Depletion of Fmn2 affects growth cone motility *in vitro* and results in a reduced lifetime of growth cone filopodia. On the other hand, reduction in Fmn2 does not affect the filopodial elongation and initiation rates suggesting a role in substrate adhesion based stability of filopodia.

To understand the slow growth cone movement, in this study we have investigated growth cone substrate-dependent interactions in neurons that suggested the importance of Fmn2 in regulating growth cone point contacts. Earlier work has suggested that force-based maturation of point contacts is compromised upon Fmn2 depletion, implicating Fmn2 in the molecular clutch mechanism. Supporting this hypothesis, the current study reveals a regulatory role for Fmn2 in the generation of traction forces by growth cones. Additionally, retrograde flow of F-actin was found to be elevated upon knockdown of Fmn2, indicating slipping of the molecular clutch and further underscoring Fmn2 function as a component of the molecular clutch.

Supporting studies in mouse fibroblasts show Fmn2 localization to ventral stress fibres and juxta focal adhesions suggesting its role in mediating their interaction. This crosstalk is further highlighted by knockdown studies that suggest a role in mechanotransduction-dependent stability of adhesions. This interaction is further exemplified by our observations of leading-edge stabilization defects during cell spreading of Fmn2 depleted cells.

Taken together this study identifies Fmn-2 as a regulator of the molecular clutch in neuronal growth cones. It is likely that this function of Fmn-2 underlies its role in growth cone motility and consequent development of neural circuits.

1. Synopsis

1.1 Introduction

The emergence of the stereotyped neuronal circuit is essential for functional nervous system in adult organisms. Individual cells composing the nervous system characterized as neurons play an important role in building the nervous system very early during the embryonic development. A dynamic, sensory and polarised structure present distally at the neuronal cell known as the growth cone integrates biochemical signals presented by the surrounding tissue to guide itself during neuronal development (Huber et al., 2003). The growth cone encounters diffused chemical and substrate-bound cues during the development which act as a roadmap for the formation of precise connections of the neuron with the appropriate target. This ability of the growth cone to steer towards or away depending on the cue is however imparted to it by the tight spatiotemporal regulation of its underlying cytoskeleton, actin, and microtubules (Dent and Gertler, 2003).

The growth cone is characterized by the presence of thin, finger-like filopodia and flat, veil-like lamellipodia, characterized by the presence of unbranched and branched actin filaments respectively. Growth cones also have a microtubule rich central region that extends to the axonal shaft (Lowery and Van Vactor, 2009). Several studies that perturbed these cytoskeletal elements revealed the importance of these structures in driving directed motility of growth cone (Vitriol and Zheng, 2012; Gomez and Letourneau, 2014). In order to move forward, growth cones form integrin-based attachments with the underlying substrate which allow traction forces generated by the cytoskeletal dynamics to transmit onto the substrate

and achieve directional motility of the growth cone. Studies perturbing actin polymerization affected growth cone dynamics highlighting the importance of actin dynamics in regulating growth cone motility (Marsh and Letourneau, 1984; Forscher and Smith, 1988).

Over the years several actin and microtubule-associated proteins have been studied in the context of regulating growth cone motility, substrate adhesion downstream of guidance cues and generation of traction forces necessary for the growth cone to move forward (Lowery and Van Vactor, 2009, Dent et al., 2011, Kerstein et al., 2015). An array of actin regulatory proteins has been implicated in neurons as well as in other cell types to elongate, bundle and protect barbed ends of actin filaments. However, how an actin nucleator can link actin dynamics to the substrate adhesions and modulate cell motility is still poorly understood.

In this study, we identify Fmn2 is a potential candidate that regulates spinal cord development in the chick embryo. We further dissect the role of Fmn2 in regulating neuronal motility by regulating the crosstalk between dynamic actin cytoskeleton in the growth cone and the integrin-mediated substrate adhesions formed by exploratory growth cone. We also study mouse fibroblasts to achieve better resolution of Fmn2 localization and function and we show its functional consistency in modulating the interaction between adhesions and actin architecture.

1.2 Objectives

1. Wiring of the nervous system is a complex process that takes place early during development of an organism. As the growth cone is the central part driving the development of the nervous system, it is important to understand its regulation in order to study neuronal circuit formation. As demonstrated by several studies over the years, actin remodelling in the growth cone is the key to the guidance of neurons. Thus, one of the objectives of this study was to screen for expression of actin nucleators in the developing nervous system and study their role in the growth cone motility. Here we identify a formin family member, Fmn2 which was previously known to be enriched in the mammalian nervous system (Leader and Leder, 2000) as an important regulator of spinal cord development. As previously shown by our group, Fmn2 is important for proper development of commissural interneuron trajectories *in vivo*. This function of Fmn2 is likely to be driven by its ability to regulate growth cone morphology (Sahasrabudhe et al., 2016). In this thesis, we show the role of Fmn2 in maintaining filopodial stability essential for proper growth cone dynamics and motility (Chapter 2).

2. Regulation of neuronal motility is a key factor during development which is a tightly modulated interplay between dynamic actin and integrin-mediated substrate adhesions. During growth cone advance, the dynamic actin retrograde flow is physically coupled to integrin-mediated point contacts to achieve actin polymerization-driven neuronal motility. In this study, we describe the unique role of Fmn2 in regulating growth cone point contact dynamics and modulating actin retrograde flow. Our studies indicate the role of Fmn2 as a molecular clutch in growth cone motility by regulating actin cytoskeleton and point contacts thereby modulating traction forces generated by the growth cone (Chapter 3).

3. Our studies indicate the role of Fmn2 as a molecular clutch in neuronal growth cones modulating actin dynamics as well as point contacts. However, observing precise localization of Fmn2 that facilitates this communication was challenging to study in neurons for which we utilized mouse fibroblasts to gain better insight into localization and functional insights of Fmn2. Our main objective of this study was to understand how Fmn2 might be communicating with the actin cytoskeleton and focal adhesions to regulate the molecular clutch behaviour observed in neurons. Our studies in fibroblasts show that Fmn2 localizes to contractile ventral stress fibres in these cells just next to the adjacent focal adhesions giving it perfect access to regulate the crosstalk between F-actin and focal adhesions. We also found that similar to neuronal growth cones Fmn2 is necessary for the stability of focal adhesions in mouse fibroblasts further confirming its functional role in regulating substrate adhesions (Chapter 4).

1.3 Major findings

1.3.1 Fmn2 transcript is enriched in developing chick spinal cord and is required to maintain filopodial stability.

To study the role of cytoskeleton regulators in developing spinal cord, we took a candidate based approach and we screened a number of actin nucleators for their enrichment in developing spinal cord of chick embryo. We found Fmn2 not only highly expressed in the spinal cord, but we show that its enrichment is sustained along the window of commissural interneuron development. *In vivo* studies performed following this observation further confirmed the importance of Fmn2 in shaping commissural trajectories during development (Sahasrabudhe et al., 2016). *In vitro* studies showed the importance of Fmn2 in maintaining neuronal morphology (Sahasrabudhe et al., 2016) which leads us to study filopodial dynamics more carefully. In this study, we show that Fmn2 is essential for stabilization of filopodial

protrusions in growth cones, but it is dispensable for the initiation and elongation of them. This observation was further confirmed by studying tip adhesion marker pFAK (Y 397) and bead pulling assay which showed compromised tip adhesions upon reduced Fmn2 levels (Sahasrabudhe et al., 2016).

1.3.2 Fmn2 modulates persistent motility of neuronal growth cones by modulating the molecular clutch.

Loss of filopodial stability caused by lack of Fmn2 was attributed to weak engagement with the underlying substrate. This was further confirmed by loss of pFAK (Y 397) staining at the filopodial tips and by the failure of bead pulling by contractile filopodia as shown by our group (Sahasrabudhe et al., 2016). These observations and the *in vivo* guidance defect caused by loss of Fmn2 (Sahasrabudhe et al., 2016) directed us to study individual neuronal motility in cultured neurons upon Fmn2 knockdown. Our studies indeed confirm that Fmn2 regulated growth cone speed and directionality necessary for persistent growth cone motility. A common principle of cell motility is that cells should be able to exert traction forces onto the underlying substrate in order to move ahead. The actin cytoskeleton is the major player of generating these forces and relaying them on the underlying substrate via ECM based ligand-receptor interactions. The popular 'molecular clutch' hypothesis combining these two aspects, postulates that integrin-mediated focal contacts mechanically couple retrograde actin flow inside the cell acting as a molecular clutch thereby modulating actin dynamics to drive cell motility.

In the current thesis, we show that Fmn2 is necessary for regulating point contact stability in the growth cones. We immunolabelled several proteins that are known to be recruited at the point contacts such as paxillin, focal adhesion kinase (FAK) and vinculin which all indicated that loss of Fmn2 causes compromised formation of point contacts. Stability marker such as autophosphorylated pFAK (Y 397) staining further indicated unstable point contacts in the growth cone upon loss of Fmn2. As suggested by the 'molecular clutch' hypothesis, weak clutch engagement would result in increased retrograde flow causing affected growth cone motility. To test this, we studied actin retrograde flow on Fmn2 depleted background and we observed that loss of Fmn2 indeed increases the retrograde flow in the growth cone lamellipodia. Our experiments further confirmed Fmn2 as a possible player in modulating molecular clutch as we observed the importance of Fmn2 in maintaining growth cone traction forces.

1.3.3 Fmn2 localizes to contractile stress fibres in fibroblasts and stabilizes focal adhesion formation on ECM substrates.

We studied mouse fibroblasts to further understand the localization of Fmn2 with respect to actin and focal adhesions. Our overexpression studies in these cells showed Fmn2 expression at the contractile ventral stress fibres caging the nucleus of the cell. Fmn2 not only decorates these stress fibres but also situates itself right next to the focal adhesions present on either end of these stress fibres giving it perfect access to modulate the two. Similar to neurons, we observed that Fmn2 is necessary for stabilization of focal adhesions in fibroblasts cultured on ECM substrates. To study the role of Fmn2 in communicating actin and focal contacts we employed a well-characterized cell spreading assay that suggested a role of Fmn2 in stabilizing leading edge possibly by stabilizing nascent focal contacts during cell spreading which further highlights its important role in cross-talk between substrate contacts and the dynamic actin cytoskeleton.

1.4 Discussion

Growth cone motility underlying nervous system development is a fascinating area of research and for several years various actin and microtubule regulators have been studied to understand mechanisms that build the neural circuits (Lowery and Van Vactor, 2009, Dent et al., 2011). Studies show the involvement of actin cytoskeleton in growth cone motility downstream of guidance cues and also modulation of substrate point contacts (Kerstein et al., 2015) but the involvement of an actin regulator in linking both these processes has not been shown.

Here we identify actin nucleator Fmn2 in chick spinal cord that regulates actin dynamics and growth cone point contact dynamics in neuronal growth cones. We also show that the traction forces generated by the growth cone as a result of physical interaction between actin retrograde flow and integrin-mediated point contacts are altered upon reduction of Fmn2. Our independent studies in mouse fibroblasts also indicate the involvement of Fmn2 in stabilizing integrin-mediated focal adhesions as well as mediating actin and focal adhesion interaction.

Taken together, this study describes Fmn2, an actin regulator, as a promising candidate that is involved in regulating the molecular clutch underlying the motility in neuronal growth cones.

2. Enrichment of Formin-2 in developing chick nervous system and its role in maintaining filopodial stability

2.1 Introduction

2.1.1 Growth cone as the vehicle

Establishment of an effective neural network is achieved by regulated navigation of neurons to their appropriate targets by sensing the tissue environment. This guidance is achieved by a highly motile and dynamic structure at the tip of the neuron known as growth cone which senses surface bound or diffusible chemical cues and remodels the underlying cytoskeleton in order to steer through the surrounding tissue (Dent and Gertler, 2003). The growth cone is a highly motile structure that is characterized primarily by the presence of actin and microtubule polymers. The growth cone can be divided into three distinct zones which are characterized by specific organisations of actin and microtubules. The peripheral zone, also known as the 'P' zone, is characterized by exploratory and dynamic rod-like filopodia and sheet-like lamellipodia, structures that are dominated by polymerizing actin. The transition zone or 'T' zone separates actin-rich peripheral zone from microtubule dominated central zone that emerges from the axonal shaft and is characterized by the presence of actin arcs and

occasional invasion by exploratory microtubules from the central zone (Lowery and Van Vactor, 2009) (Fig. 2.1). Importance of cytoskeletal structures in growth cone guidance has been demonstrated *in vivo* using drug-based and genetic inhibition of actin (Bentley et al., 1986) and microtubules (Yamada et al., 1970). Exploring the cellular environment is an essential part of accurate axonal guidance, is mainly achieved by filopodia which are thin, finger-like projections enriched with unbranched, parallel oriented actin filaments and the veil like flat region of growth cone periphery known as lamellipodia enriched with branched actin network drives the overall movement of the growth cone. Studies showing the importance of lamellipodial and filopodial dynamics to growth cone advancement (Argio et al., 1984, Argio et al., 1985) emphasizing the role of these structures in growth cone motility.

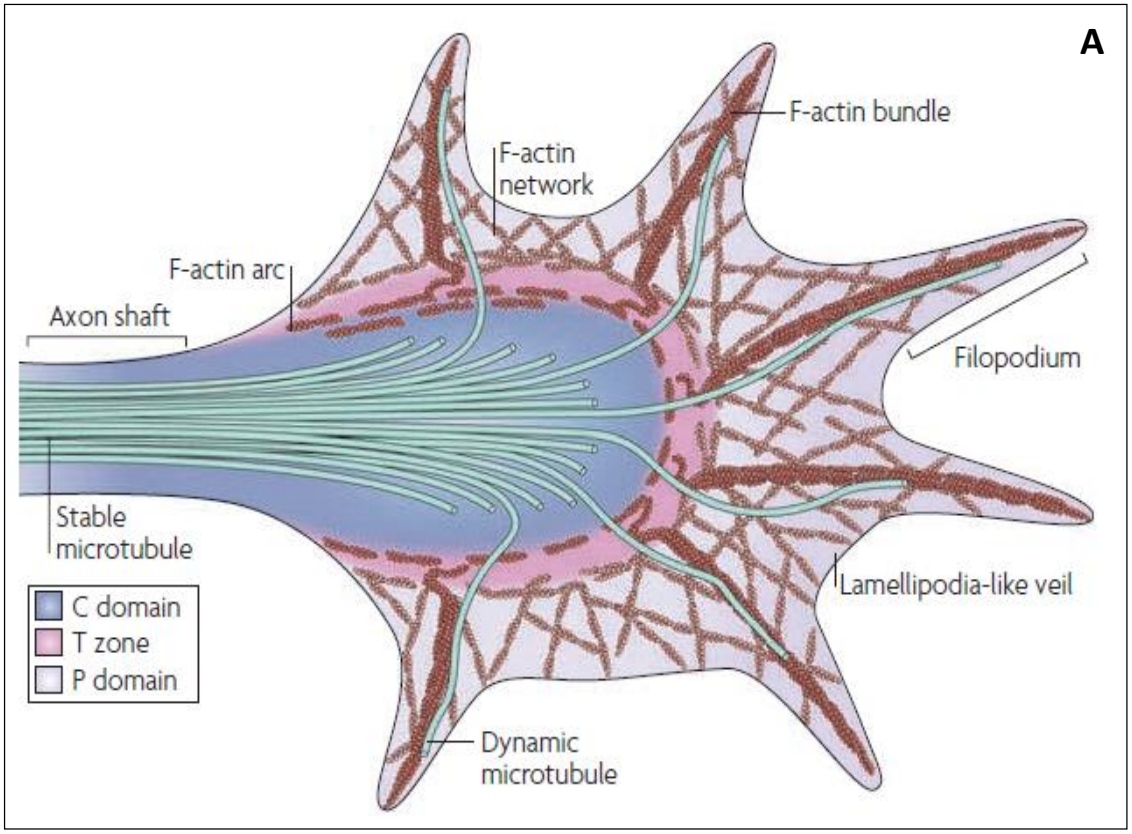

Figure 2.1: Cytoskeletal organisation in the neuronal growth cone. (A) Schematic of a typical growth cone depicting actin-rich peripheral domain with dynamic filopodia and lamellipodia, followed by small but distinct transition zone characterized by actin arcs and

further the microtubule rich central zone emerging into the axonal shaft (Reproduced from Lowery and Van Vactor 2009).

2.1.2 Actin dynamics in growth cones

Actin is central to various cellular processes such as cell motility, endocytosis, cell-substrate adhesion, and wound healing. Monomeric actin referred to as globular or G-actin binds to other monomers to form long polymeric filamentous or F-actin. F-actin filaments are polar and intrinsically dynamic with one end of the filament growing due to the addition of G-actin subunits (barbed end) and another end from which the subunits dissociate in ADP bound state (pointed end). Even though *de novo* actin can polymerize, the formation of actin polymer from them is not thermodynamically favourable. To achieve this, cells utilize a number of actin-binding proteins. Over years, groups of proteins that can nucleate new actin filaments (actin nucleators such as Formins, Spir, Cobl), elongate existing filaments (ENA/VASP), bundle existing filaments (Fascin) or sever existing filaments (Cofilin) to generate more barbed ends have been characterized (Pak et al.,2008; Dent et al.,2011). Apart from a large repertoire of actin-binding proteins, motor proteins such as Myosin utilise actin filaments as tracts and cause the retrograde flow of actin, the process of continuous movement of F-actin from the leading edge of the cell to the centre of the growth cone (Lowery and Van Vactor, 2009). Given the peripheral domain enriched in actin, understanding regulation of actin assembly and dynamics plays a key role in studying growth cone velocity modulation and directional motility.

2.1.3 Actin nucleators in growth cones

In order to achieve formation of complex actin structures, actin subunits have to be organised into filaments which is achieved by a repertoire of proteins. Arp2/3 is a protein complex which is well studied and is known to generate branched actin filaments that are found in lamellipodia. However, to orchestrate the polymerization of unbranched actin filaments, several groups of actin-associated proteins have been characterized. Two major families that are known to form such actin filaments are formins, proteins with the presence of distinctive FH1-FH2 domain and WH2 domain containing proteins which can be further grouped into Spire and Cordon-bleu (Cobl) (Fig. 2.2).

Arp2/3 along with several accessory proteins known as nucleation promoting factors polymerize an actin filament by serving as a seed that sits on another existing actin filament at a distinct angle generating branched actin meshwork (Campellone and Welch, 2010). WH2 domain containing family of nucleators typically consists of a tandem cluster of three or more actin monomers that serve as a template for nucleation of the actin filament. Formins, however, have a more unique function as they can not only recruit actin monomers due to their characteristic FH1-FH2 domain but can remain associated with them and elongate them serving also as anti-capping proteins to protect actin filaments (Higgs and Peterson, 2005; Yang and Svitkina, 2011).

Studies have highlighted the role of some of formin family members in filopodia formation such as Diaphanous 2 (Diaph2) and DAAM (Dent et al., 2007). Another member of the formin family, Formin-2 (Fmn2) was originally found to be enriched in neuronal tissue (Leader and Leder, 2000), however little is known about its function in neuronal growth cones. Contractile actin networks generated by Fmn2 are also implicated in generating accurate spindle positioning and meiosis in the fly oocyte (Rosales-Nieves et al., 2006) and mammalian systems (Leader et al., 2002; Schuh and Ellenberg, 2008). Recent studies associate mutations in FMN2 affect human intellectual and cognitive abilities and are linked with compromised dendritic spines and synaptic density in mice (Law et al., 2014; Mozhui et al., 2008). Taken together actin nucleators are essential in generating actin structures which are not only the key in maintaining growth cone architecture but their impact on higher-order neuronal circuits demand a thorough investigation of their function on the formation of the neural network.

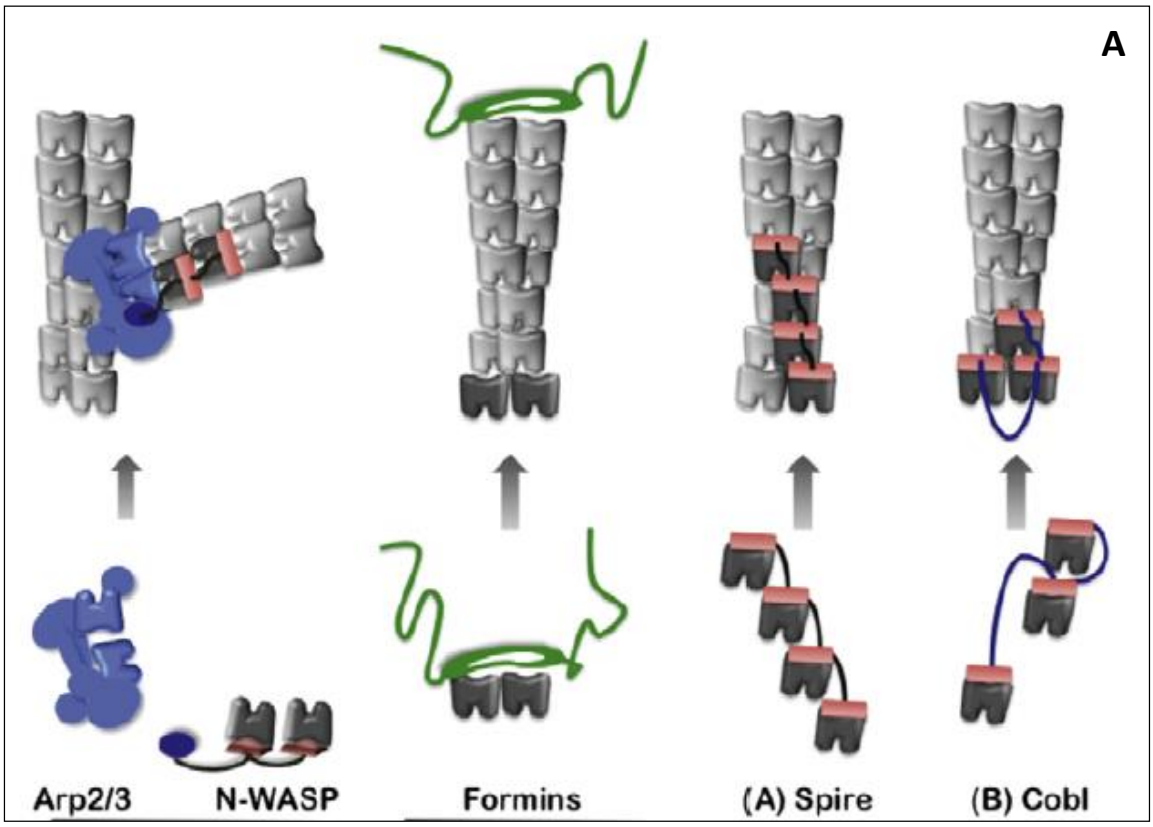

Figure 2.2: Families of actin nucleators. (A) Schematic depicting modes of nucleation in case of each protein family. Arp2/3 along with nucleation-promoting factor N-WASP can generate branched actin filaments. Formins act as nucleators as well as elongators and WH2 family proteins, Spire and Cobl serve as a seed for nucleation of the new filament (Reproduced from Chesarone and Goode 2009).

2.2 Results

2.2.1 Fmn2 is enriched in developing chick spinal cord

To explore the role of actin nucleators in developing a central nervous system of chick embryo (*Gallus gallus*), we first wanted to study the spatiotemporal expression of actin nucleators in our model system for which we chose 2 formin family members Fmn2 and Diaph3; spire family members Spir1 and Spir2 and Cobl.

In order to address this, we employed quantitative real-time PCR (qRT PCR) using SYBR green enzyme as a method of assessment since it is significantly beneficial over the endpoint PCR as it is a sensitive method that generates fluorescent readout in real time as the PCR reaction progresses. SYBR green dye in the enzyme mixture binds to the double-stranded PCR product generated during the reaction and thus the fluorescent readout provides a proxy to assess the enrichment level of a transcript. The PCR cycle where the readout is maximum known as threshold (C_t) values, are generated and are inversely proportional to the enrichment of the transcript. For example, a transcript that expresses abundantly in the tissue will be more enriched and hence will attain the Ct value faster.

Whole brain, spinal cord and heart tissue from 6^{th} day old fertilised chicken egg (HH25/26) were dissected and total RNA from the tissue was extracted using Trizol-chloroform extraction method. cDNA from 2 µg total RNA was synthesized *in vitro* and was further used as a template for qRT PCR. A two-fold serial dilution system of cDNA was employed to determine the exponential range of amplification in order to get an accurate estimate of transcript level. To get a relative estimate of the transcript of a gene of interest i.e. the selected actin nucleators, housekeeping gene β-actin was used as a control in the similar dilution system. The relative abundance of the actin nucleators' transcripts was calculated, without efficiency correlation, using formula $R = 2^{-\Delta\Delta C}{}_t$ (Livak and Schmittgen, 2001) where the ΔC_t value was determined by the difference between C_t values of housekeeping and nucleator gene and $\Delta\Delta C_t$ value was determined by normalising ΔC_t values of spinal cord and heart tissue to that of the brain tissue.

This screening across tissues showed a clear abundance of Fmn2 mRNA in chick central nervous system furthermore indicating higher enrichment in spinal cord tissue when the relative abundance was normalised to the same in brain tissue (Fig. 2.3 A).

During development neurons from one half of the spinal cord move along the midline, cross the midline and then move in specific trajectories to the contralateral half of the spinal cord which requires tight regulation of cytoskeleton in the sensory growth cone. We speculated changes in levels of actin nucleators during this developmental window in the spinal cord. To address this, we screened Fmn2, Diaph3, Spir1, Spir2 and Cobl in developmental stages ranging from 50 hrs post fertilization to 4th day (HH14 – HH22) of developing chick which demarcates the axogenesis of spinal commissural neurons, a population of dorsal interneurons, in the spinal cord (Fig. 2.3 C).

Embryos of these stages were exploited to extract total RNA using Trizol-chloroform extraction method. Similar to the tissue screening, cDNA from 2 µg total RNA was synthesized *in vitro* and was further used as a template for qRT PCR with the two-fold serial dilution system. Keeping the housekeeping gene β-actin consistent, the relative abundance of the actin nucleators' transcripts was calculated, with the same formula $R = 2^{-\Delta\Delta C}{}_t$ (Livak and Schmittgen, 2001) where the ΔC_t value was calculated by the difference between the C_t values of housekeeping and nucleator gene and $\Delta\Delta C_t$ value was calculated by normalising ΔC_t values of stages HH 19 and HH 22 to that of stage HH 14.

This mRNA expression screen revealed sustained expression of Fmn2 as well as Spir2 transcript in the developing spinal cord indicating a functional co-operation between them during axogenesis (Fig. 2.3 B). However, in this study, we decided to focus more on understanding the role of Fmn2 in neuronal development.

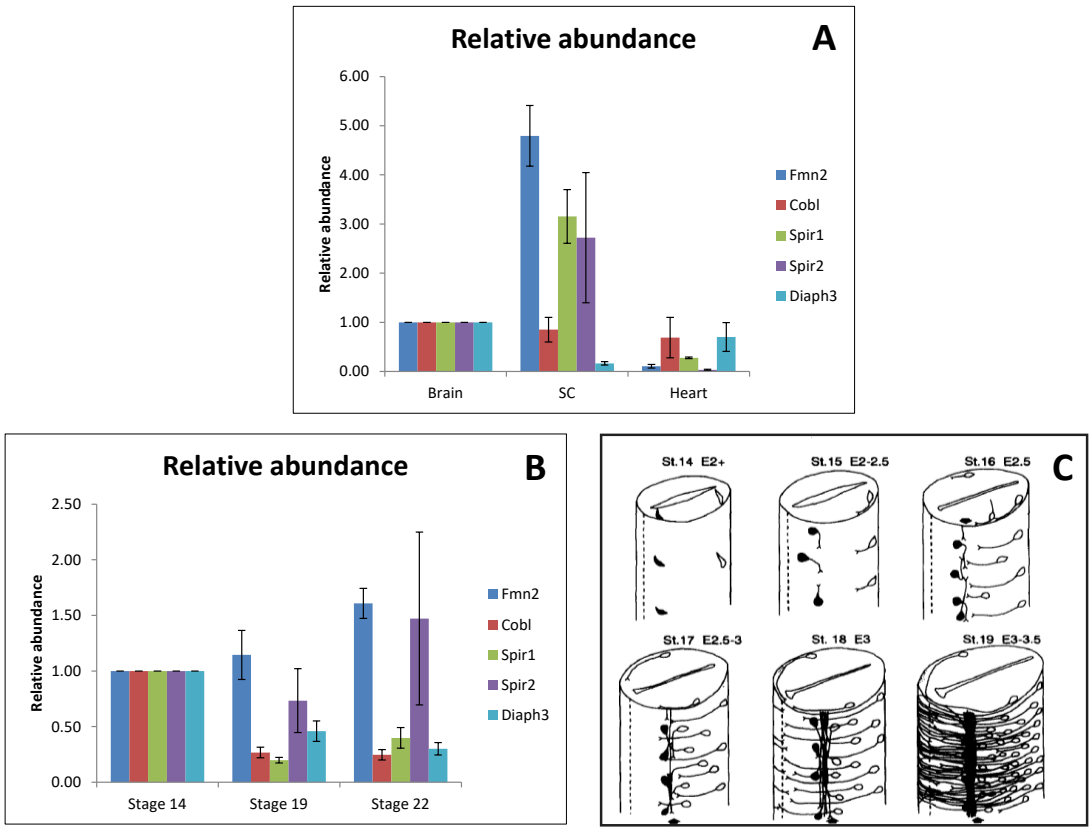

Figure 2.3: Expression of actin nucleators in the chick embryo. (A) Relative abundance of transcripts in neural tissue and heart. Despite a being an actin-rich muscular tissue heart does not show enrichment of actin nucleators as much as neural tissue, further concentrating the transcript levels in the spinal cord (The graph represents average relative abundance of 3 technical replicates. Each replicate utilised RNA from 3 different embryos). (B) Relative abundance of actin nucleators during the development of chick embryo. Fmn2 levels are sustained along with similar pattern in Spir-2 transcript (The graph represents the average relative abundance of 9 technical replicates. Each replicate utilised RNA from 3 different embryos). (C) Schematic of spinal cord development. The stages here depict the development of commissural axons and the stages coincide with the ones used in the screen in (B) (Reproduced from Yaginuma et al., 1994).

2.2.2 Fmn2 localizes to actin structures in neuronal growth cone

Knockdown of Fmn2 results in trajectory defects in spinal commissural neurons *in vivo* (Sahasrabudhe et al., 2016) suggesting the role of Fmn2 in neuronal motility or affected detection of guidance cues. However, to understand these cellular mechanisms in detail, it is essential to first know the localization of Fmn2 protein in spinal neurons.

Dissected chick spinal neurons were cultured on the fibronectin-coated glass for 24 hrs and immunolabelled with chick Fmn2 (gFmn2) specific antibody and phalloidin conjugated with Alexa Fluor 568 to stain endogenous gFmn2 and F-actin respectively and imaged using epifluorescence microscopy. To analyse the localization of gFmn2 a 2-pixel wide line was drawn on actin-rich filopodia in Fiji, an image analysing software, followed by analysing the grey scale values in both antibody channels (Fig. 2.4 E).

This analysis reveals that gFmn2 is present in the central region of growth cone as well as it is present in the actin-rich peripheral region where it decorates the actin bundles in finger-like filopodial protrusions of growth cones (Fig. 2.4 C). This observation indicates the importance of gFmn2 in maintaining and regulating actin architecture in spinal chick growth cones.

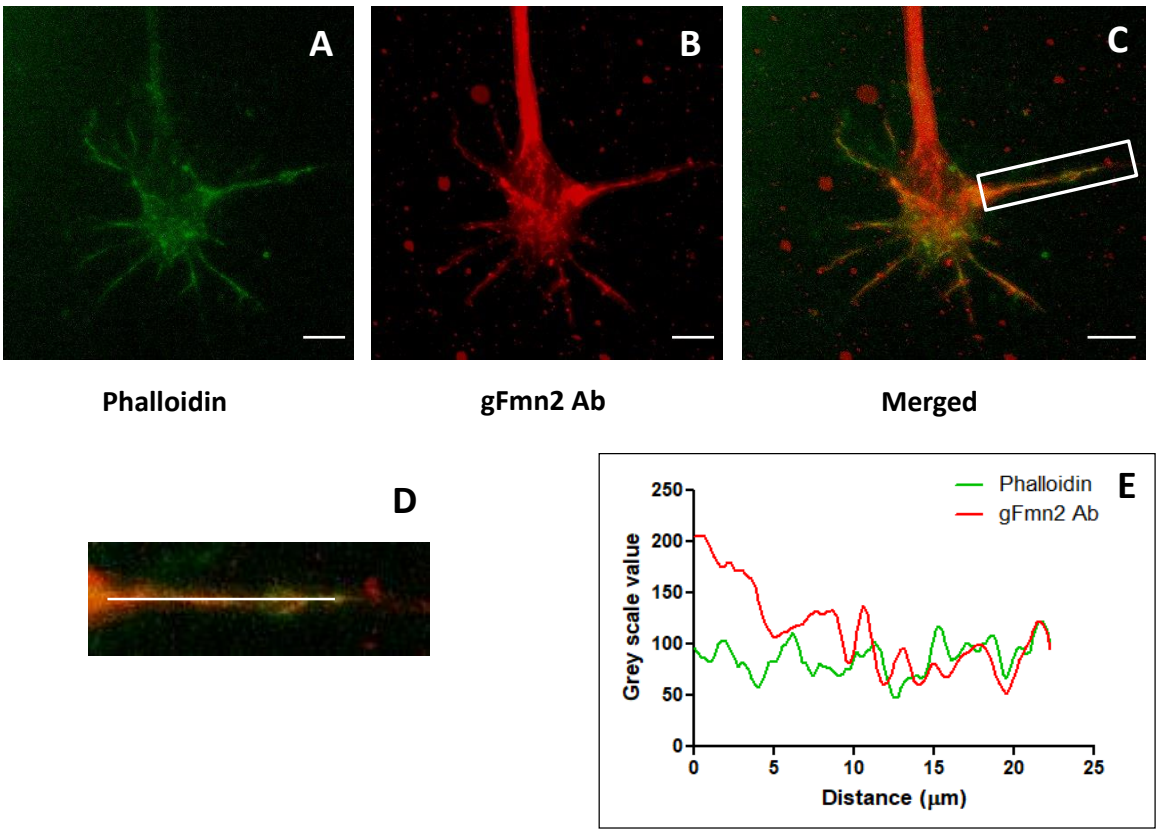

Figure 2.4: Fmn2 localizes to actin structures in chick spinal growth cones. (A) Phalloidin labelling actin structures in the growth cone. (B) Antibody specific against chick Fmn2 decorating actin structures. (C) Merged image of the two channels showing co-localization of gFmn2 to actin. (D) Zoomed image of filopodia from inset marked in (C). (E) Greyscale values from line scan across the filopodia in (D) revealing localization of endogenous gFmn2 to actin-rich filopodia (N = 3) (Scale bar = 5 µm).

2.2.3 Fmn2 is necessary for the stability of growth cone filopodia

As previously described by our group, we have characterised two independent morpholinos that targeted translation of gFmn2 transcript in the chick embryo. Using these morpholinos we successfully achieved up to 70% knockdown in gFmn2 protein. In addition, the rescue experiments performed *in vivo* confirmed the specificity of the morpholino (Sahasrabudhe et al., 2016).

In the current thesis, to assess Fmn2 function, we have utilised the same translational blocking morpholino under those identical conditions and concentrations.

In vitro studies with fixed spinal neurons showed the role of Fmn2 in maintaining neuronal morphology (Sahasrabudhe et al., 2016). Morpholino-mediated knockdown of gFmn2 resulted in smaller growth cones with reduced filopodia number and lengths (Sahasrabudhe et al., 2016). Even though this study indicated that gFmn2 regulates actin cytoskeleton underlying growth cone morphology, the precise function of gFmn2 in filopodia dynamics could not be elucidated.

To understand the role of gFmn2 in dynamic filopodia, we imaged the morpholino transfected growth cones live and tracked filopodial dynamics. The emergence of a finger like a membrane protrusion up to 2 µm long was considered as an initiation event. The time taken to attain the maximum length by a new protrusion or existing filopodia (> 2 µm) was considered as the elongation rate.

Spinal neurons were electroporated with either control morpholino with a random sequence or against chick Fmn2 with a reporter plasmid pCAG-GFP and plated on the fibronectin-coated glass. Neurons with GFP signal were imaged after 24 hrs to track filopodial initiation events or elongation rates; however, for easier manual tracking of the protrusions, the DIC channel of the corresponding growth cones was assessed. The 30 min time-lapse movies with 1 sec time interval were carefully substacked according to emergence and elongation of a protrusion. In Fiji, one-pixel wide line of length 2 µm was overlayed next to the protrusion to be analysed and a montage was created of the substack. The initiation events were manually calculated from these montages as well as the elongation rates were measured by measuring the change in filopodia length per unit time (Fig. 2.5).

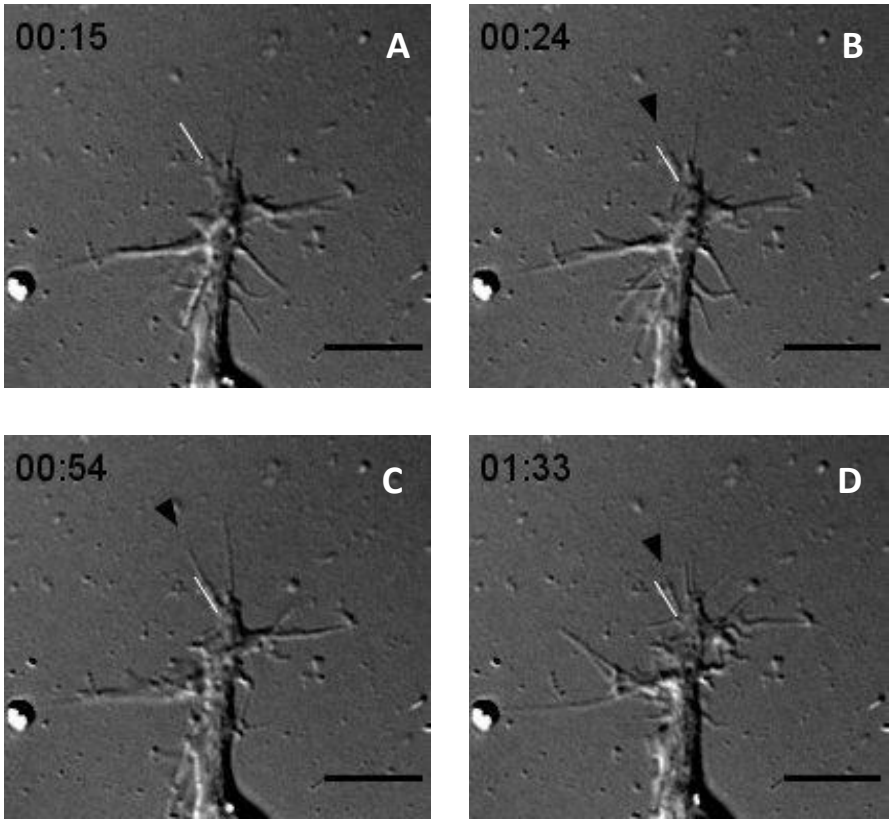

Figure 2.5: Filopodial dynamics in spinal neurons. DIC images tracking dynamics of a filopodial protrusion (pointed by arrowhead) emerging near the white line which was used as a measure of length (2 µm) for the protrusion to be called filopodia. (A) The region of the growth cone before the emergence of filopodia. (B) Initiation event – the protrusion emerged and grew up to 2 µm. (C) The maximum length attained by the protrusion. Time from initiation frame up to this frame was considered as elongation rate. (D) The filopodia retracted and shortened below the while line i.e. 2 µm cut off, thus finishing the entire lifetime of that particular filopodium (Scale bar = 5 µm).

Formins are known to nucleate and elongate actin bundles (Campellone and Welch, 2010) therefore perturbation of them could lead to filopodial initiation or elongation defects as shown in case of DAAM (Matusek et al., 2008). Interestingly, our analysis of filopodial dynamics showed gFmn2 is dispensable for initiation and elongation of filopodia of spinal neurons (Fig. 2.6).

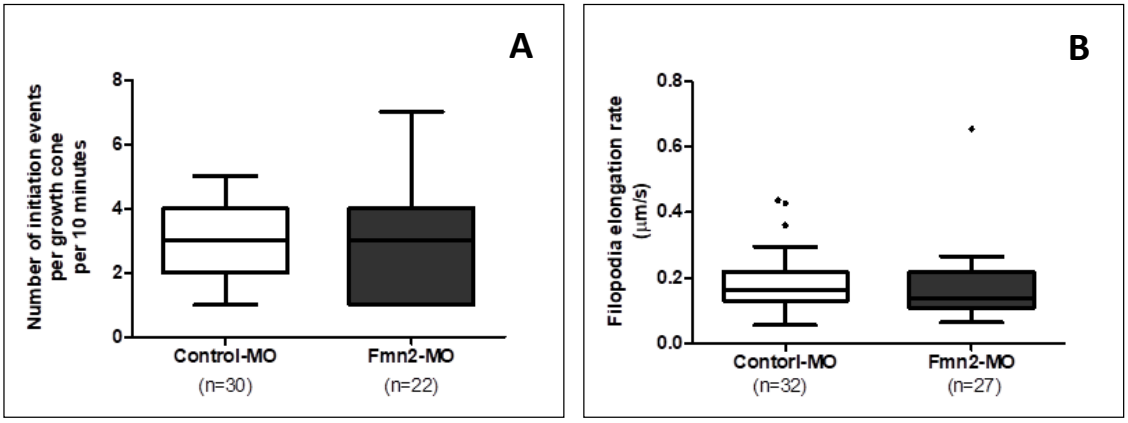

Figure 2.6: Fmn2 is dispensable for filopodia initiation and elongation. (A) and (B) showing a non-significant change in filopodial initiation or elongation upon gFmn2 knockdown (Numbers in brackets on graphs depict independent events analysed across 10 control growth cones and 15 gFmn2 knockdown growth cones imaged in 3 independent experiments).

Further careful analysis of these montages to determine the lifespan of these growth cone filopodia which was measured by tracking a filopodial protrusion (> 2 µm) elongating followed by subsequent retraction resulting in the filopodia shortening (< 2 µm) revealed the role of gFmn2 in a filopodial lifetime (Fig. 2.5). Loss of gFmn2 not only affects the filopodial lifetime in neuronal growth cone but also increases the overall population of short-lived filopodia (Fig. 2.7).

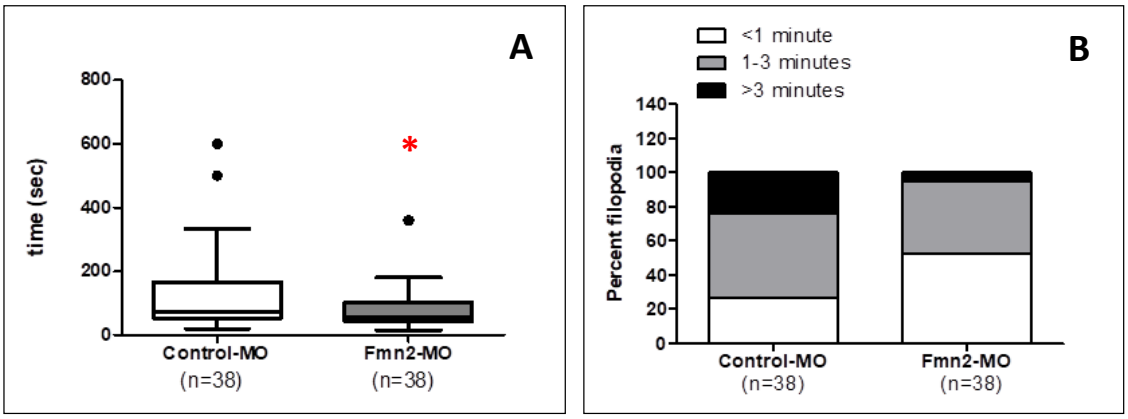

Figure 2.7: Fmn2 is required for stabilization of growth cone filopodia. (A) Loss of gFmn2 resulting in a reduced lifetime of growth cone filopodia (P = 0.0264). (B) Binning of entire filopodial population analysed depending upon their lifetime showed the elevated percent of short-lived filopodia (Numbers in brackets on graphs depict independent events analysed across 10 control growth cones and 15 gFmn2 knockdown growth cones imaged in 3 independent experiments).

Taken together, these results show that the absence of gFmn2 does not affect initiation events or elongation rates but the overall filopodial lifetime indicating that gFmn2 is necessary for filopodia lifetime.

2.3 Discussion

Growth cone guidance is essential for the construction of accurate neural circuits and precision of that depend highly upon spatiotemporal regulation of underlying cytoskeleton. Growth cones are specialised sensory structures that are enriched in actin and microtubules which make understating interplay of these cytoskeletal elements key in studying neural mechanisms.

Actin forms filopodia and lamellipodia, dynamic regions of growth cones essential in driving guided cell motility (Dent et al., 2011), therefore over years number of regulatory proteins of actin are studied in growth cones to dissect mechanisms underlying motility (Lowery and Van Vactor 2009).

Using a screen for spatiotemporal expression of a few actin nucleators in developing chick nervous system we show enrichment of Fmn2 in the spinal cord of chick embryo which points to a possible role of Fmn2 in neuronal development in chick embryos. Fmn2 was initially characterized in the mammalian nervous system (Leader and Leder, 2000) but it is not well studied for its cellular function in neurons. Our screen in developing spinal cord for expression of Fmn2 indicates its potential role in the development of spinal commissural neurons as the expression time window of Fmn2 coincides with that of the commissural axogenesis (Yaginuma et al., 1990) suggesting a plausible role in the development of this interneuronal population in the spinal cord. Further studies from our lab have demonstrated *in vivo* defects in commissural neurons at the spinal cord midline which supports our hypothesis of the role of Fmn2 in their development (Sahasrabudhe et al., 2016).

Immunofluorescence studies on cultured spinal neurons reveal localization of endogenous gFmn2 to filamentous actin in filopodia and lamellipodia indicating its likely role in the maintenance of these structures. This was further confirmed by studies in fixed spinal neurons treated with morpholino against gFmn2 which results in fewer and shortened filopodia along with other growth cone morphology defects such as reduced area (Sahasrabudhe et al., 2016).

Fmn2 is an actin nucleator that produces unbranched actin filaments (Higgs and Peterson, 2005), perturbations of which could affect filopodial formation. However, we show that Fmn2 is dispensable for the initiation or elongation of a filopodium but is crucial for the stability of an already formed filopodia. Loss of this stability could lead to short-lived

filopodia which could be the cause of growth cone morphology defects *in vitro* that can further lead to trajectory defects *in vivo* (Sahasrabudhe et al., 2016).

Stability of the filopodia is often attributed to point contacts that form at the tip of the filopodia due to interaction with the underlying extracellular matrix (ECM) which regulates filopodial contractility and generation of traction necessary for cell motility (Moore et al., 2009, 2012; Romero et al., 2013). Phospho-FAK (Y 397) labelling, which is a marker of the stability of adhesions, was reduced in gFmn2 deficient neurons which further emphasized the role of gFmn2 in the regulation of these tip adhesions and in turn filopodial stability (Sahasrabudhe et al., 2016). In addition, neurons cultured on compliant poly acrylamide gels with fluorescent tracer beads showed reduced bead pulling by the gFmn2 depleted filopodia which indicated weaker tip adhesions in growth cones (Sahasrabudhe et al., 2016).

Taken together, this study identifies Fmn2 as an important actin nucleator in developing chick nervous system, perturbation of which results in aberrant commissural interneuronal trajectories *in vivo* which could be attributed to the role of Fmn2 in regulating neuronal filopodia by stabilization of the filopodial tip adhesions.

2.4 Material and methods

Fertilized, white Leghorn chicken eggs (Gallus gallus) were obtained from Venkateshwara Hatchery Private Limited, Pune, India. All procedures were approved by the Institutional Animal Ethics Committee, IISER Pune, India.

2.4.1 Total RNA extraction and cDNA preparation

RNA extraction

Whole embryos (50 hrs post fertilization to 4th day i.e. HH14 – HH22) or dissected tissues (for 6th day i.e. HH 25/26) were harvested from the eggs in sterile, RNase free microfuge tubes and macerated in 1ml Trizol (Ambion) and 200µl chloroform followed by vigorous vortexing the mixture for 15 seconds and incubating for 2-3 min at room temperature. The tubes were centrifuged at 12,000 xg for 10 min at 4^{o}C in a fixed angle centrifuge. The aqueous phase was collected in fresh sterile, RNase free Eppendorf and the total RNA was precipitated by adding equal volumes of Isopropanol to the tube. This mixture was incubated at room temperature for 30 min followed by centrifugation under the conditions mentioned above. After precipitating the RNA, Isopropanol was removed and the pellet was washed with 70% ethanol followed by spinning at 7500 xg for 5 min at 4^{o}C. The RNA pellet was dried at room temperature after removing the ethanol and resuspended in nuclease-free water (Ambion). RQ1 DNase (Promega) was added to the total RNA and incubated at 37^{o}C for 30 – 40 min. Quality check for purity of RNA was performed by checking the RNA on 2% agarose gel and RNA without DNA contamination was precipitated using Isopropanol followed by 70% ethanol wash. Purified RNA was resuspended in nuclease-free water (Ambion) and stored at -40^{o}C.

cDNA preparation

2µg of total RNA extracted from the tissue was used as a template for *in vitro* reverse transcription. Following reaction mixture set was used for total cDNA preparation:

RNase inhibitor (Roche) - 0.5 µl

MMLV reverse transcriptase (Promega) - 1 µl

5X MMLVRT buffer (Promega) - 5 µl

OligodT (IDT) - 1 µl

dNTPs (Sigma) (2.5mM each) - 5 µl

After adding a calculated volume of 2µg RNA the reaction volume was made up to 25µl using nuclease-free water (Ambion). This entire reaction mixture without RNase inhibitor and reverse transcriptase were then denatured at 60^{o}C for 5 min to get rid of the secondary structures of RNA, followed by snap chilling on ice. At this point, the enzyme and inhibitor were added and the mixture was incubated at 40^{o}C for 2-3 hrs. The cDNA was stored afterward at -40^{o}C until further use.

2.4.2 Quantitative real-time PCR

The cDNA synthesized from total RNA using OligodT was utilised to perform quantitative real-time PCR. Two-fold serial dilutions of cDNA from 1:2 to 1:32 were used for standardizing primer pairs. The final analysis was one using 1:8 dilution of cDNA for all primers. SYBR green (KAPA Biosystems) enzyme mastermix was used to set up the PCR along with following primer pairs.

For housekeeping gene against which the relative abundance was calculated, chick β-actin primers (Forward: AGACATCAGGGTGTGATGGTTGGT;

Reverse: TCCCAGTTGGTGACAATACCGTGT) were used.

For actin nucleators, the following primer pairs were used –

Formin2 – Forward: TCAGCAGCGGATTCTGAGGCTAAA

Reverse: ATGCAAGTCCTCTTGACTGGCTGA

Diaph3 – Forward: CACAAAATCTCAGTCCAACCA

Reverse: AGCCTTGTTCCATGCCATAG

Spire1 – Forward: AGCCTTGGACTATGGCTTGAAGGA

Reverse: TCTGTGGTGTTGGTCATGTGGTCT

Spire2 – Forward: TGAAGAAGGTGCAGGAGAAGCAGT

Reverse: CATGACCTTGCGCAGCTTGTAGTT

Cobl – Forward: ATGGTGCAGAGACTTGCTCTGTGA

Reverse: GCTTAGCCGCAGCCATTTCTTCAT

Each reaction had each dilution in triplicates and each sample had three technical replicates every experiment was repeated three times. The pooled data were used for statistical analysis and graphical representations. All actin nucleators were normalized to β-actin and represented using brain expression as the reference.

2.4.3 Spinal neuronal culture and electroporation

Preparation of ECM coated plates

22 mm glass coverslips were glued on bottoms of drilled 35 mm plastic plates (Laxbro) using silicon glue (Dow Corning) and sterilized by 70% ethanol wash and UV treatment in the cell culture hood. These coverslip bottom plates were coated with 1mg/ml poly-L-lysine (Sigma) diluted in sterile phosphate buffered saline (137 mM NaCl, 2.7 mM KCl, 10 mM Na_2HPO_4, 1.8 mM KH_2PO_4) for 1 hour at 37^oC. After washing the PLL with sterile 1X PBS the plates were coated with 20µg/ml fibronectin (Sigma) in PBS for 1 hour at 37^oC. These plates were further used to culture the dissociated chick spinal neurons.

Dissection and culture

Six-day old eggs (HH25/HH26) were utilised to harvest entire spinal cords of embryos. The embryos were dissected in sterile phosphate buffered saline (mentioned above) on a Silgard coated plate under a dissecting microscope inside a horizontal laminar flow hood. The dissected tissue was collected in an Eppendorf with embryonic medium (Leibovitz's media (Gibco) with 1X penicillin-streptomycin (Gibco)). The spinal cord was spun at 3000 rpm for 3 min at room temperature after which the embryonic medium was replaced with 1X trypsin-EDTA (Lonza). The tissue was macerated in trypsin and incubated at 37^oC for 15-20 min. The further embryonic medium was added to the trypsin and the dissociated spinal cord was spun at 3000 rpm for 3 min. The cells were plated in 2 ml of basal culture medium (L-15 (Gibco), 1X PenStrep (Gibco), 10% heat-inactivated FBS (Gibco)) with 20ng/ml NGF (Invitrogen) supplement and incubated without CO_2 at 37^oC for 24-36 hrs.

For electroporation, cells were resuspended in 100µl OptiMEM (Gibco) with 10 µg of plasmid and 100 µM morpholino.

(Standard morpholino sequence that was used as a negative control: CCTCTTACCTCAGTTACAATTTATA, Fmn2 morpholino sequence that was used: CCATCTTGATTCCCCATGATTTTTC).

The cell suspension with plasmid and morpholino was transferred to the electroporation cuvette and current was delivered under following conditions using NepaGene electroporator (NEPA 21 *In-vitro* and *In-vivo* electroporator).

Poring pulse:	**Transfer pulse:**
Voltage (V) – 125	Voltage (V) - 20
Pulse length (msec) – 5	Pulse length (msec) - 50
Pulse interval (msec) – 50	Pulse interval (msec) - 50
Number of pulses – 2	Number of pulses - 5
Decay rate (%) – 10	Decay rate (%) - 40
Polarity - +	Polarity - +/-

After electroporation, the cell suspension was transferred to a microfuge tube with 400 µl OptiMEM (Gibco) and plated on ECM coated coverslip bottom plates with 2 ml of basal culture media (mentioned above).

2.4.4 Immunocytochemistry

Spinal neurons were cultured (as mentioned above) for 24 hrs and fixed using 4% PFA (Electron microscopy sciences) and 0.05% glutaraldehyde (Electron microscopy sciences) in PBS (mentioned earlier) for 10 min. After removing PBS, cells were washed with PBS 3 times for 10 min each. The cells were permeabilized using 0.1% Triton-X in PBS for 30 min. After permeabilization, 2 brief PBS washes were given and the cells were blocked in 3% BSA for 60 min. The blocking solution was replaced by an antibody against chick Fmn2 in 1:250 dilution in 3% BSA and incubated at 4^{o}C for 14-16 hrs. Subsequently, after removing primary antibody, the cells were washed 4 times with PBS+0.1% TritonX, 10 times each. Later the sample was incubated at room temperature for 60 min in secondary antibody (Invitrogen) diluted 1:1000 in 3% PBS. After removing the secondary antibody, the cells

were washed again in PBST 4 times, 10 min each. Further, the cells were labelled with phalloidin (Invitrogen) diluted 1:200 in blocking for 30-45 min at room temperature. Lastly, the cells were washed thrice in PBST, 10 min each and mounted in 80% glycerol.

2.4.5 Fmn2 antibody generation

Antibody specific against chick Fmn2 was generated with a unique peptide sequence CRQKKGKSLYNIRPK. This peptide was synthesized and injected in rabbits for the generation of antibody. Anti-gFmn2 antisera were collected intermittently after administration of booster doses. The second-last (6^{th}) bleed was used to stain growth cones for antibody validation and localization studies.

2.4.6 Imaging

For immunocytochemistry imaging, a PlanApo 60x/1.4 oil immersion objective was used on an Olympus IX81 system with Hamamatsu ORCA-R2 CCD camera.

For filopodial lifetimes the imaging was done using a PlanApo 60x/1.4 oil immersion objective on an Olympus IX81 system with Hamamatsu ORCA-R2 CCD camera. Growth cones were imaged for 30 min with 1 sec interval in DIC. The growth cones were co-transfected with pCAG-GFP (Addgene #11150) and morpholino thus only fluorescing growth cones were imaged.

2.4.7 Analysis

For real-time PCR quantification, ΔCt values were calculated by subtracting Ct values of β-actin from Ct values of respective genes. Relative abundance was calculated using formula $2^{-\Delta\Delta Ct}$ in Microsoft Excel 2007.

For the endogenous localization, a line of 2-pixel width was drawn on the demarcated filopodia in Fiji and mean grey values were obtained for both fluorescent channels. These values were plotted in GraphPad Prism 5.

For filopodial lifetime analysis, individual filopodial protrusions were followed in the DIC movie of the growth cone. A montage was made of consecutive time-points and a line of height 2 µm was drawn near filopodia to be analysed. The protrusion that crosses the 2 µm threshold was considered as filopodia and the parameters were manually calculated (every frame had 1 sec time interval) as described in results. The analysis was done in Fiji.

2.4.8 Data representation and statistics

Real-time data were plotted as bar graphs in Microsoft Excel 2007, the error bars represent SEM calculated across replicates. The line graph for mean grey values was plotted in GraphPad Prism 5 where the intensity values were imported from Fiji. Box and Whisker plots represent the spread of the data with the Tukey method. Outliers are represented outside the box as individual data points. All Box and Whisker plots were compared using the Mann-Whitney test. Statistical analysis was done in GraphPad Prism 5.

3. Fmn2 regulates the molecular clutch in growth cones

3.1 Introduction

3.1.1 Actin dynamics in neuronal motility

Neurons exhibit distal, highly dynamic and sensory structures known as growth cones whose motility is tightly regulated to accurately build neuronal circuits. Directed growth cone motility is a process that involves sensing of environmental cues and remodelling the underlying cytoskeleton for efficient translocation, thereby making the mechanical coupling of ECM to the cytoskeleton an important phenomenon to investigate. As described in an earlier chapter, growth cones are characterized by the presence of lamellipodia and filopodia that are main players in driving directional motility in neurons.

Importance of lamellipodial and filopodial size and dynamics has been long associated with growth cone translocation by microscopic observations in sympathetic neurons (Argiro et al., 1984, 1985). Quantitative studies performed thereafter further highlighted the dynamicity of filopodia and lamellipodia in axonal extension (Bray and Chapman, 1985). With improved microscopy techniques, studies in *Aplysia* growth cone indicated that growth cone goes

through certain defined stages repeatedly as they are growing to form axon segments (Goldberg and Burmeister, 1986). These morphological stages are namely protrusion, engorgement and consolidation. The protrusion is a phase dominated by polymerization of the actin cytoskeleton and is mediated via elongation of filopodia and lamellipodia, which also extend in between filopodia. Engorgement is characterised by the presence of vesicles and organelles in the veil which can occur via microtubule driven transport or Brownian motion. Final consolidation is observed where proximal part of growth cone acquired cylindrical shape adding a new axonal segment (Goldberg and Burmeister, 1986). These stages were also observed in growth cones *in vitro* and *in vivo* in various model systems further highlighting the importance of studying cytoskeletal dynamics in neuronal motility (Aletta and Greene, 1988; Kalil, 1996; Godement et al., 1994).

Further emphasis on the necessity of actin in growth cones was highlighted when chick sensory neurons were treated with Cytochalasin B, an actin depolymerizing drug (Yamada et al., 1970, 1971). However, subsequent experiments in dissociated neuronal cultures of other model organisms showed actin perturbation using Cytochalasin B actually affected directionality of outgrowth rather than axonal extension (Marsh and Letourneau, 1984; Lafont et al., 1993; Chien et al., 1993; Kaufmann et al., 1998). Similar experiments done on microtubule depolymerisation using colchicine did not affect filopodia initially but resulted in the ultimate retraction of axons (Yamada et al., 1971). These experiments indicated that filamentous actin is the major contributor for maintenance of growth cone shape and motility.

As mentioned in the previous chapter, actin is dynamic in nature and exhibits retrograde flow (Forscher and Smith, 1988) characterized by continuous movement of F-actin from growth cone periphery towards its centre (Lin and Forscher, 1995; Suter and Forscher, 2000). Both filopodia and lamellipodia exhibit retrograde actin flow (Lin and Forscher, 1993, 1995; Mallavarapu and Mitchison, 1999) and it is a combination of pulling of F-actin filaments caused by Myosin II motors in the transition zone and recoil from the pushing force by membrane against polymerizing actin (Medeiros et al., 2006). It is the balance between the actin polymerization rate and retrograde flow that governs growth cone extension or retraction (Fig. 3.1). The rate of actin polymerization dominating over that of the actin retrograde flow results in protrusion of the leading edge whereas equivalent rates of both these processes cause the growth cone to stall (Medeiros et al., 2006).

Data from various cell types identifies a number of formin family members to be involved in maintaining different aspects of actin dynamics in cell type specific manner. Formin DAAM has been identified in the *Drosophila* nervous system to act along with ENA/VASP, another actin regulatory protein to regulate filopodial dynamics (Matusek et al., 2008). Diaphanous has also been implicated in various cell types for nucleation and elongation of actin filaments that form the basis of filopodia and lamellipodia rendering the cell ability to move (Dent et al., 2011).

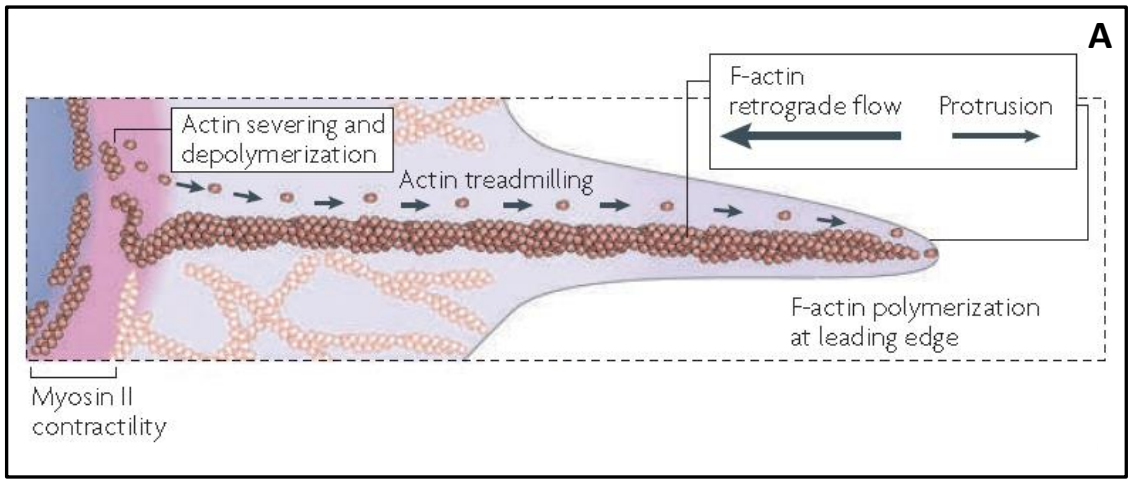

Figure 3.1: Schematic of filopodia depicting actin dynamics. (A) Polar nature of actin filaments causes actin tread-milling to occur where the monomers are added to the barbed end and are removed from the pointed end. Myosin II at the transition zone and pushing force from the leading edge gives rise to retrograde flow which when overcome by polymerization, the protrusion at the leading edge is observed (Reproduced from Lowery and Van Vactor, 2009).

3.1.2 Molecular clutch

Mitchison and Kirschner for the first time proposed the 'molecular clutch' hypothesis (Mitchison and Kirschner, 1988), which is also known as the substrate-cytoskeletal coupling model (Lin et al., 1994). This hypothesis suggested that as a growth cone receptor binds to its

underlying adhesive substrate, it forms a complex which acts as a molecular clutch that mechanically couples actin retrograde flow thus attenuating it and allowing the actin polymerization to take over for the resultant growth cone protrusion.

During protrusion, the molecular clutch engages, consequently fixing the actin filaments with respect to the substrate and reducing the actin retrograde flow whereas disengagement of the clutch releases the actin filaments from the substrate adhesions allowing the retrograde flow to dominate over the rate of actin polymerization causing retraction (Fig. 3.2). The molecular clutch is also modulated by substrate stiffness indicating its mechano-sensitive behaviour allowing it to generate traction in stiffness dependent manner. On stiffer substrates like glass, the clutch engages over short time resulting in frictional slippage whereas on compliant substrates the engagement is more long lasting with sudden intermittent detachments known as load and fail cycle (Chan and Odde, 2008).

Studies done on Aplysia growth cones on an adhesive substrate indeed demonstrated the 'molecular clutch' hypothesis in actin as the sites of adhesion was observed to have more actin and reduced retrograde flow resulting in overall growth cone protrusion (Suter and Forscher, 2000, 2001; Lee and Suter, 2008). Studies also show that for regulating growth cone motility by clutching the actin retrograde flow downstream of chemical, surface-bound or mechanical cues the neurons recruit several adaptor and signalling proteins to growth cone point contact that serve as link to the underlying substrate (Bard et al., 2008; Myers and Gomez, 2011; Toriyama et al., 2013). Molecular clutch model in neurons is further highlighted by the studies where point contacts in growth cones indeed modulate retrograde flow locally (Santiago-Medina et al., 2013) and higher density of these point contact has also observed to yield in decreased retrograde flow (Koch et al., 2012).

In order to balance the protrusive forces at the leading edge upon molecular clutch engagement, cell exerts traction forces on the substrate which can be measured by deformations in compliant matrices (Hyland et al., 2014). These traction forces are generated at the point contacts and their magnitude is observed to dominate the directionality of the growth cone migration (Lo et al., 2000; Plotnikov et al., 2012). As described earlier, in growth cones even though filopodia sense and explore the environment around the growth cone, lamellipodia by virtue of its area and numerous substrate adhesions dominates the motility and could be the major contributor in modulating molecular clutch and underlying traction forces.

These interactions and in turn the forces generated by them are key players in regulating the growth cone motility. Sensing of guidance cues, diffusible or substrate bound, trigger assembly of point contacts which reorganises the traction forces thus determining the direction of growth cone motility (Kerstein et al., 2015).

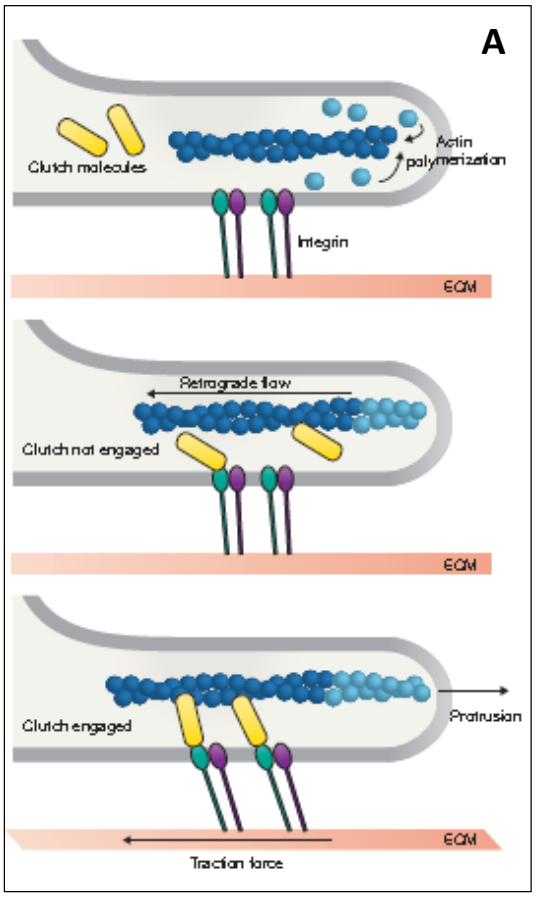

Figure 3.2: Molecular clutch. (A) Schematic representing molecular clutch. The model suggests that for a cell to move forward, a mechanical coupling between the actin retrograde flow and the underlying substrate exists which by reducing the retrograde flow favours leading edge protrusion due to actin polymerization. (Reproduced from Case and Waterman, 2015).

3.1.3 Growth cone point contacts

During development, adhesion molecules serve as guidance cues providing as a roadmap in laying down accurate connections (Kamiguchi, 2007; Kolodkin and Tessier-Lavigne, 2011; Maness and Schachner, 2007; Myers et al., 2011). During this process, neurons communicate by physical interactions with the surrounding viaintegrin-mediated adhesion whereas it exploits cadherins and immunoglobin superfamily receptors to interact with neighbouring tissue (Koldkin and Tessier-Lavigne, 2011). The attractive and repulsive cues during development have been found to have an effect on adhesion dynamics which results in overall neuronal migration or a directed guidance response making it essential to study these adhesions more carefully (Woo and Gomez, 2006; Myers and Gomez, 2011; Myers et al., 2011). Adhesions not only dynamically assemble and disassemble in motile growth cones (Thoumine, 2008; Myers and Gomez, 2011) but they also undergo spatiotemporal regulation by mechanical strain and substrate stiffness (Pelham and Wang, 1997; Schedin and Keely, 2011) indicating their role in maintaining tensional homeostasis.

The integrin-mediated transient connections that growth cones form with the underlying ECM substrate are known as point contacts (Fig. 3.3) that share certain similarities with the focal adhesions described in non-neuronal cells like fibroblasts (Gomez et al., 1996; Renaudin et al., 1999). Although not as systematically classified as the focal adhesions in non-neuronal cells, they share similar composition and have observed to form at filopodial and lamellipodial protrusions during growth cone motility (Gomez et al., 1996; Renaudin et al., 1999; Woo and Gomez, 2006; Robles and Gomez, 2006). These point contacts usually assemble in dynamic filopodia leading to receptor clustering and recruitment of scaffolding proteins such as talin, paxillin, and vinculin (Robles and Gomez, 2006). To regulate growth cone advance they remain anchored and stabilize filopodia and rapidly disassemble in fast-moving neurons (Robles and Gomez, 2006; Myers and Gomez, 2011). It has also been shown that a large population of point contacts enriched in β1 integrin, talin and vinculin accumulate in central region of growth cone which is a strongly anchored region of growth cone suggesting role of point contact adhesions in growth cone stabilization (Zheng et al, 1994; Renaudin et al., 1999). Furthermore, growth cone central region has a greater spread area that is rich in adhesions and is the place where the strongest traction forces are generated necessary for motility. Evidence for the importance of the growth cone central region also comes from studies that demonstrate that loss of filopodia does not completely abrogate

growth cone motility but mainly compromise directionality of the protrusion further highlighting the role of the central region in driving motility (Marsh and Letourneau, 1984).

Integrins have observed to be present at the tip of filopodia in growth cones (Jones, 1996; Pinkstaff et al., 1999) and their activation leads to recruitment of talin which also decorate the filopodial tips (Sydor et al.,1996; Gomez et al., 2001) indicating their role in filopodial extension. Following this, proteins like paxillin and vinculin are recruited that further provide structural support to point contacts (Myers et al., 2011). Talin disruption resulting in altered filopodial dynamics and growth cone motility highlights its role in assembly of point contacts (Sydor et al., 1996; Kerstein et al., 2013). Studies have also shown that stretching of talin facilitates vinculin recruitment to the point contacts which is an actin-binding protein (del Rio et al., 2009; Margadant et al., 2011) and thus directly coupling actin cytoskeleton to the underlying substrate. Along with the structural and scaffolding proteins such talin, paxillin and vinculin, clustering of integrin also recruits non-receptor tyrosine kinase such as focal adhesion kinase (FAK) that together with Src group of kinases regulates phosphorylation of other point contact proteins allowing further stability and turnover of point contacts (Robles and Gomez, 2006; Bechara et al., 2008; Myers et al., 2011). Furthermore, phosphorylation of FAK at Y 397 residue is shown to play an important role in force-dependent stabilization of the focal contacts in growth cone and other cell types (Chacón et al., 2012; Moore et al., 2012) which is central to recruitment of additional focal contacts proteins and traction force generation.

Association of point contacts with actin cytoskeleton was indicated by observation of these clusters along actin filament bundles (Robles and Gomez, 2006) indicating their role in traction force generation. Importance of the actin and point contact interaction that highlights the ‘molecular clutch’ hypothesis is further demonstrated by studies where neurons grown on adhesive substrates that cause integrin or non-integrin mediated point contact assembly namely laminin and poly-D-lysine, exhibit differential retrograde flow (Short et al., 2016). These experiments indicate that point contacts that are assembled in response to adhesive substrate indeed communicate with actin cytoskeleton modulating its dynamics resulting in growth cone motility (Robles and Gomez, 2006).

Guidance cues such as BDNF, netrin which are previously known to affect growth cone motility have found to have downstream effectors which are components of point contacts such as FAK (Robles and Gomez, 2006; Woo et al., 2009; Myers and Gomez, 2011)

suggesting role of point contacts in regulating signalling in growth cone that drives neuronal pathfinding. Importance of physical interaction between the guidance cue and downstream regulation of point contact stabilization that underlies growth cone expansion and axon extension is studied in mammalian spinal neurons subjected to classical attractive cue netrin-1 (Moore et al., 2012). This study demonstrates the physical association of dynamic actin with immobilized netrin-1 is essential for the generation of traction forces necessary for growth cone translocation via phosphorylation of point contact protein FAK (Moore et al., 2012).

Taken together, these studies suggest that mechanical coupling between actomyosin network and substrate contacts form a mechanical clutch which allows the cell to translocate. Failure of this coupling or slippage of the molecular clutch would result in defective growth cone – substrate attachments resulting in affected growth cone motility.

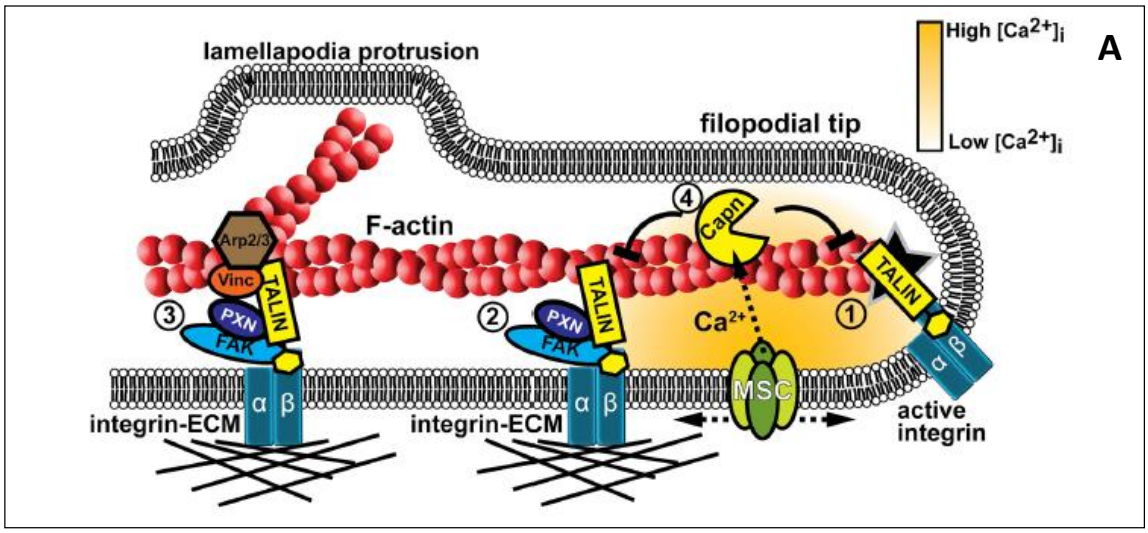

Figure 3.3: Growth cone point contacts in the protrusion. (A) Schematic representing actin and point contact interaction underlying the motility. Adhesion to ECM substrate inducesintegrin-mediated point contact assembly. Talin is recruited earliest to point contacts among other proteins, followed by paxillin and FAK. These proteins relay further intracellular signalling causing recruitment of proteins such as vinculin which due to their interaction with actin cause polymerization of F-actin resulting in membrane protrusion (Reproduced from Kerstein et al., 2015).

3.2 Results

3.2.1 Fmn2 is important for optimal motility of growth cone

In vivo guidance defect caused by gFmn2 knockdown (Sahasrabudhe et al., 2016) and filopodial instability observed in *in vitro* cultures prompts to exploring the role of Fmn2 in neuronal motility. To understand whether the *in vivo* phenotype is a result of compromised neuronal motility, we followed growth cone dynamics on fibronectin-coated glass.

Dissociated spinal neurons electroporated with either control morpholino or morpholino against chick Fmn2 along with pCAG-GFP reporter plasmid were cultured on fibronectin-coated glass and imaged after 24 hrs by epifluorescence microscopy (Fig. 3.4). The GFP expressing growth cones were followed for 30 min at 10 sec time interval. In order to analyse motility parameters of the growth cones, the images were exported to Fiji and the centre of the growth cone was manually tracked within each time frame. The resultant coordinates from the software were exported to Chemotaxis and Migration tool developed by Ibidi (http://ibidi.com/xtproducts/en/Software-and-Image-Analysis/Manual-Image-Analysis/Chemotaxis-and-Migration-Tool) from where the growth cone velocity, displacement, and directionality parameters were calculated.

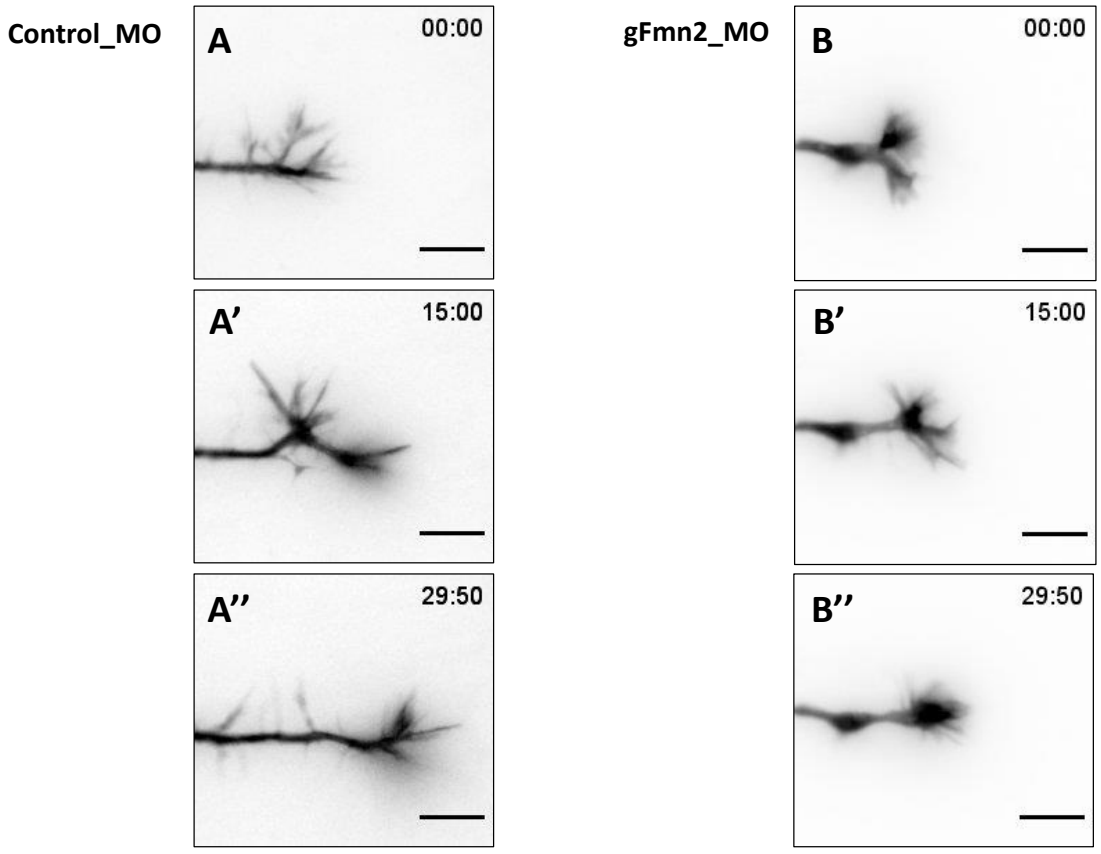

Figure 3.4: Fmn2 depletion results in slow-moving spinal neurons. Images showing snapshots of representative growth cones tracked for 30 min in epifluorescence. (A - A'') Control morpholino treated growth cones moving on fibronectin-coated glass faster as compared to (B - B'') growth cones with morpholino against gFmn2 over the similar time frame (Scale bar = 5 µm).

The results of this study show that neurons that lack gFmn2 move slowly and cover less distance as compared to the control neurons (Fig. 3.5 A, B). Directionality which is calculated by the ratio of displacement to the distance covered is also lost in neurons with gFmn2 morpholino (Fig. 3.5 C). Taken together, these results indicate the importance of gFmn2 in neuronal motility.

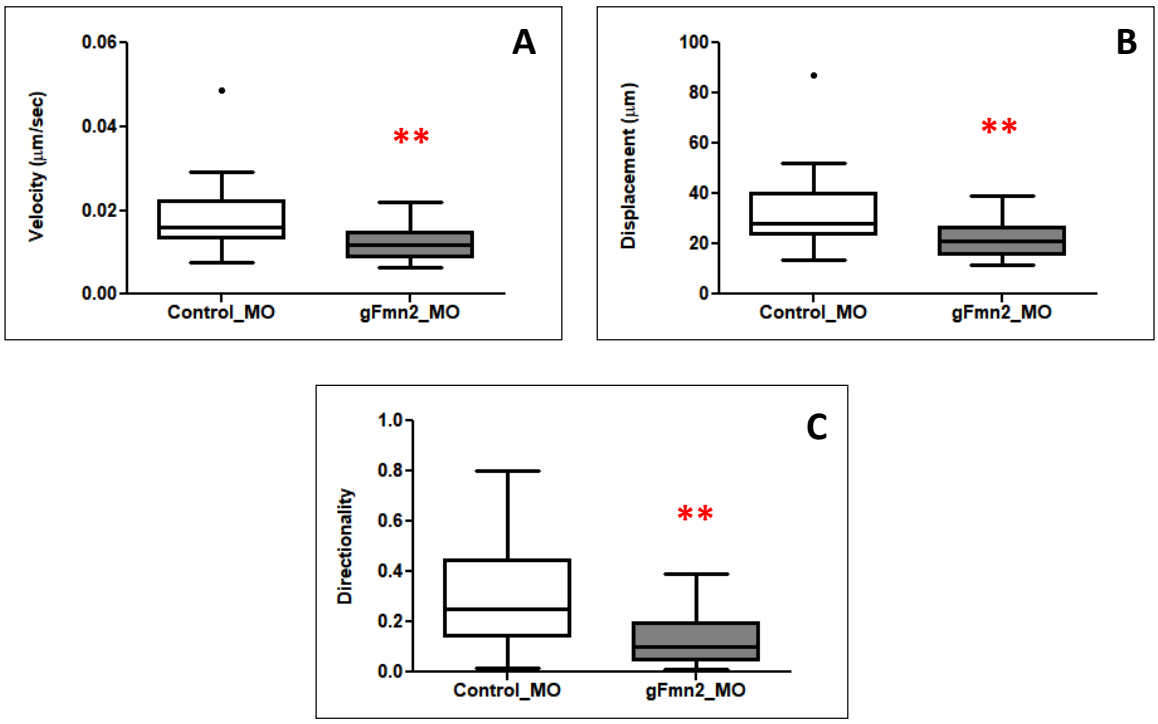

Figure 3.5: Fmn2 is necessary for maintaining persistent motility of growth cones. Neurons deficient in Fmn2 show (A) reduced velocity, (B) lesser accumulated distance and (C) loss in directionality during migration (** $P \leq 0.01$) (Graphs represent quantification of 20 control growth cones and 23 gFmn2 knockdown growth cones analysed across 6 independent replicates).

3.2.2 Fmn2 is essential for maintenance of point contacts in growth cone

Cellular motility is a complex process achieved by a combination of regulated actin dynamics and adhesions to the substrate. Apart from the importance of Fmn2 in regulating actin structures in neuronal growth cones, our lab has also suggested a role of gFmn2 in regulating focal contact stability as loss of gFmn2 reduces overall pFAK (Y 397) immunostaining in growth cones (Sahasrabudhe et al., 2016). These studies raise the intriguing question of gFmn2 function in modulating growth cone – substrate adhesion to regulate neuronal cell motility. In order to study this possible crosstalk, we decided to explore the assembly of growth cone point contacts more carefully using various point contact markers.

Spinal neurons transfected with morpholino and pCAG-GFP reporter plasmid were cultured on fibronectin-coated glass for 24 hrs after which the neurons were fixed using Kreb's fixative (Dent and Meiri, 1992) and stained for antibodies against Paxillin, phospho Paxillin (Y 31), Focal adhesion kinase (FAK), phospho FAK (Y 397) and Vinculin. The samples were imaged using confocal microscopy and the point contacts evaluated using multiple parameters. For analysis, the images were manually processed in Fiji. The growth cone area outlines were marked manually using the pCAG-GFP signal (Fig. 3.6 A) and processed (see materials and methods and Fig. 3.6 C, D). These processed images were thresholded using the Otsu algorithm in Fiji and (Fig. 3.6 E) later processed through the particle analyser with 1.5 pixels as a baseline threshold (Fig. 3.6 F). The results generated a number of point contacts observed within the area of the growth cone and also generated a mask demarcating the outlines around point contacts. This mask could be overlayed on the raw image of point contact staining to extract the original signal intensity of the point contacts (Fig. 3.6 G). These parameters allowed us to observe fluctuations in the endogenous levels of the point contact proteins.

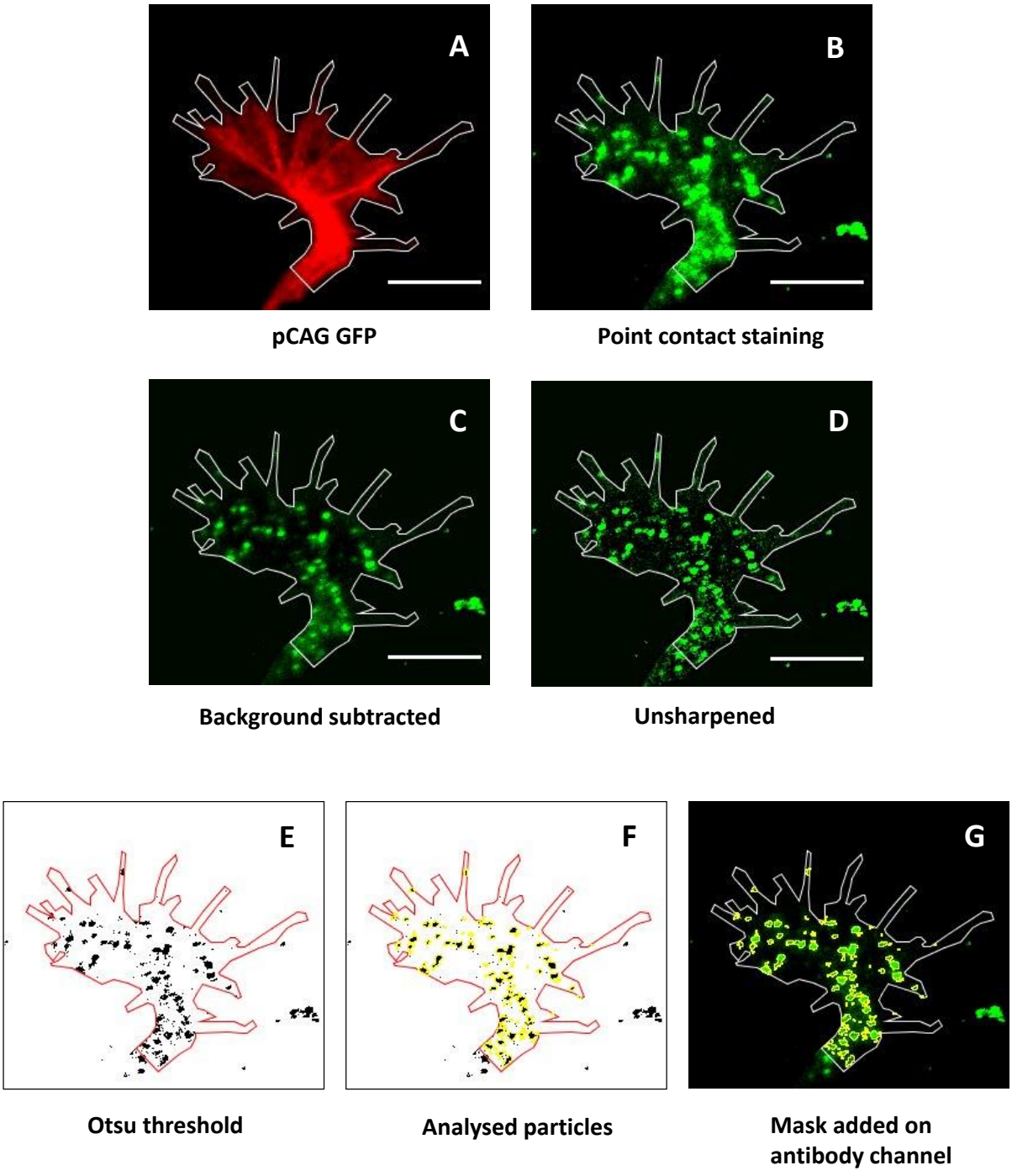

Figure 3.6: Workflow of point contact analysis. (A) Cytoplasmic marker for transfected neurons, pCAG-GFP (here pseudo coloured as red) was used to mark area outline of the growth cone. (B) Unprocessed antibody channel labelling respective point contact protein. Image after background subtraction (C) and unsharp mask (D) to extract the point contacts. Next, thresholding (Otsu method) (E) and particle analysis (F) was used to obtain point contact number and a point contact area mask (G) that could be applied on the original antibody channel to obtain the signal intensity at individual point contact (Scale bar = 5 µm).

Upon integrin engagement, paxillin is one of the early recruited proteins. Paxillin is thought to interact with vinculin which further facilitates actin crosstalk to focal points. Paxillin is known to be present in filopodia similar to what we observed in our growth cones. It also labels the central region which significantly reduced upon gFmn2 knockdown (Fig. 3.7).

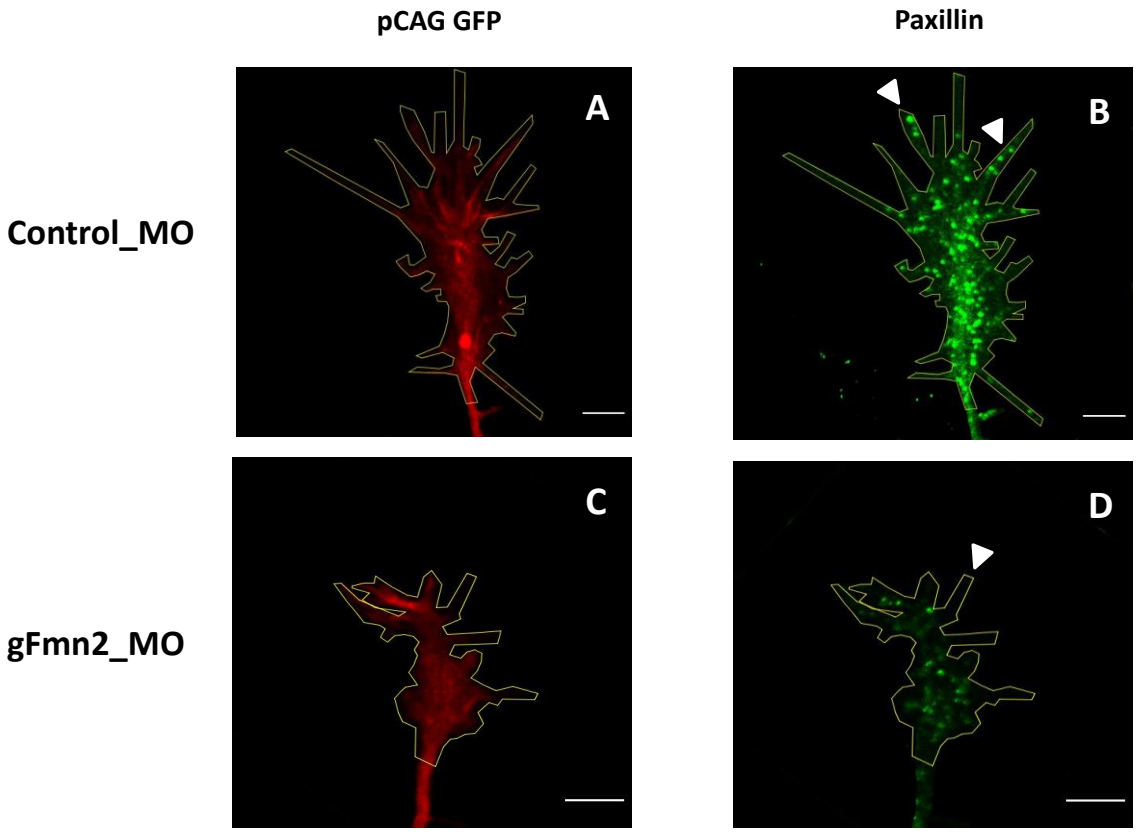

Figure 3.7: Paxillin staining in growth cones. (A) and (C) Cytoplasmic marker to label the electroporated growth cones (here pseudo coloured in red). (B) Paxillin labelling in control growth cones at filopodial tips (arrowheads) and in the central region. (D) Reduced paxillin labelling in gFmn2 knockdown neurons indicating loss of staining at the filopodial tips (arrowhead) along with overall reduced staining in the growth cone (Scale bar = 5 µm).

Analysis of paxillin staining of growth cones after gFmn2 knockdown did not affect a number of point contacts (Fig. 3.8 A). However, showed us a significant reduction in the area

of paxillin labelled point contacts (Fig. 3.8 B) and signal intensity of paxillin at each point contact upon loss of gFmn2 (Fig. 3.8 C).

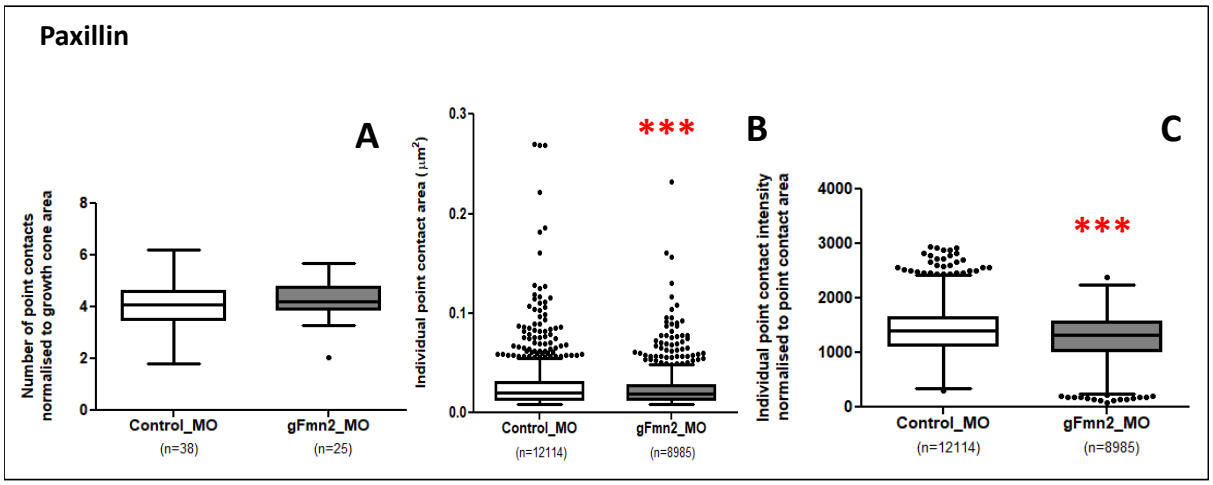

Figure 3.8: Loss of Fmn2 results in smaller point contacts and reduced paxillin staining. (A) Numbers of the point contacts detected remain unchanged across treatments. (B) and (C) show a significant reduction in intensity and area of individual point contacts (***P ≤ 0.001). (Numbers in bracket indicate the number of growth cones (A) and individual point contacts detected (B, C) over 4 independent experiments).

Phosphorylation of paxillin at tyrosine 31 is thought to be mediated by FAK at focal points in non-neuronal cells which is essential for focal point assembly and perhaps lamellipodial extension (Zaidel-Bar et al., 2006). We studied whether this marker is of adhesion assembly is affected in neurons upon loss of gFmn2. Our observations revealed that perturbation of gFmn2 leads to loss of point contacts labelled with pPax (Y 31) at the central growth cone as well as filopodial tips (Fig. 3.9).

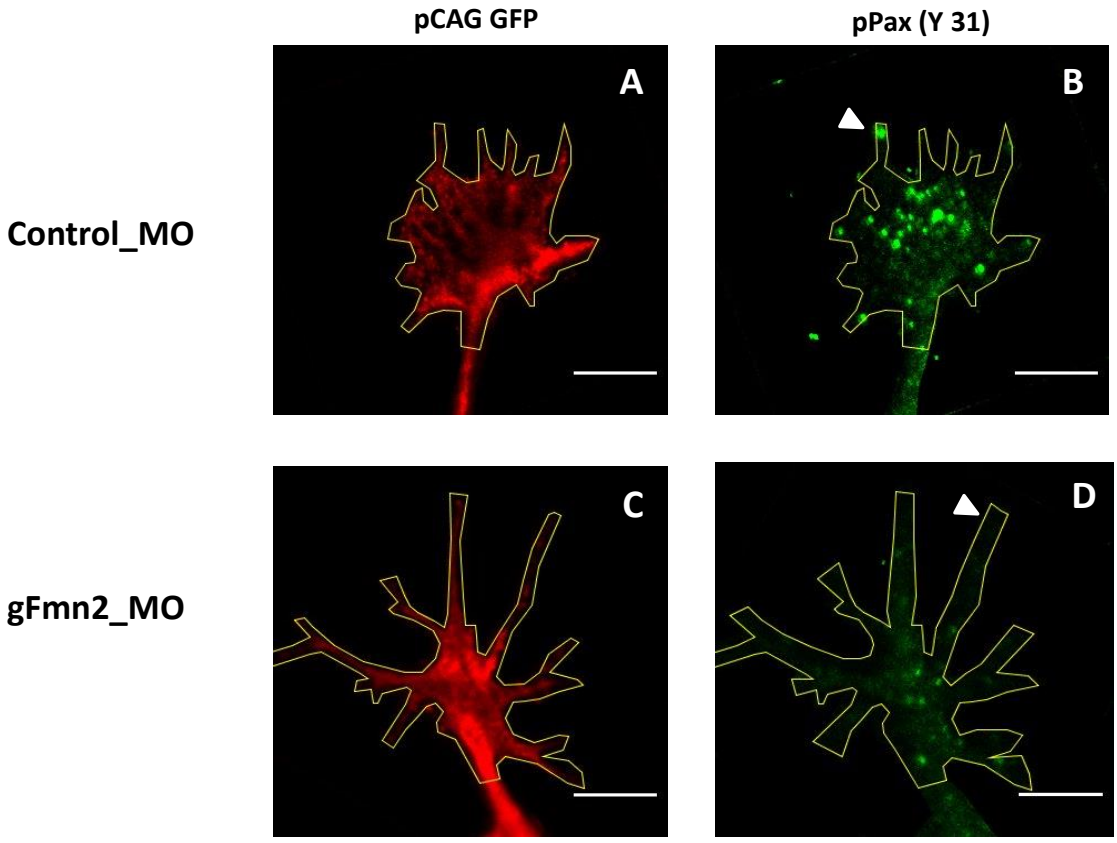

Figure 3.9: pPax (Y 31) staining in growth cones. (A) and (C) Cytoplasmic marker to label the electroporated growth cones (here pseudo coloured in red). (B) pPax labels at filopodial tips (arrowheads) and also as puncta all over the central region. (D) Reduced pPax puncta observed in gFmn2 depleted neurons indicating loss of staining at the filopodial tips (arrowhead) along with overall reduced staining in the growth cone (Scale bar = 5 µm).

Quantification of pPax (Y 31) further confirmed that even though the point contact number normalised to growth cone area remains unchanged (Fig. 3.10 A), the individual point contact area and intensity reduce after gFmn2 knockdown (Fig. 3.10 B, C).

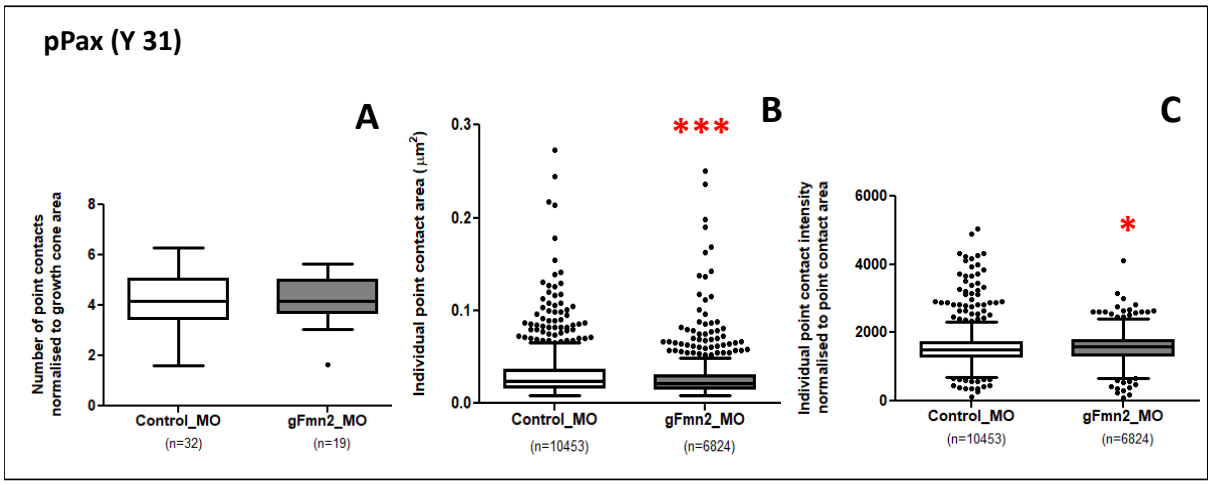

Figure 3.10: Loss of Fmn2 results in smaller point contacts and reduced pPax (Y 31) staining. (A) A slight reduction in intensity of individual point contacts (*P ≤ 0.05). (B) Significant reduction in the area of individual point contacts (***P ≤ 0.001) and (C) Numbers of the point contacts detected remain unchanged across treatments (Numbers in bracket indicate the number of growth cones (A) and individual point contacts detected (B, C) over 4 independent experiments).

As mentioned earlier, paxillin is thought to recruit vinculin at focal points which facilitates binding to F-actin enabling crosstalk between point contacts and the actin cytoskeleton. Loss of gFmn2 results in an overall reduction of vinculin rich point contact puncta in the growth cone compared to the control (Fig. 3.11).

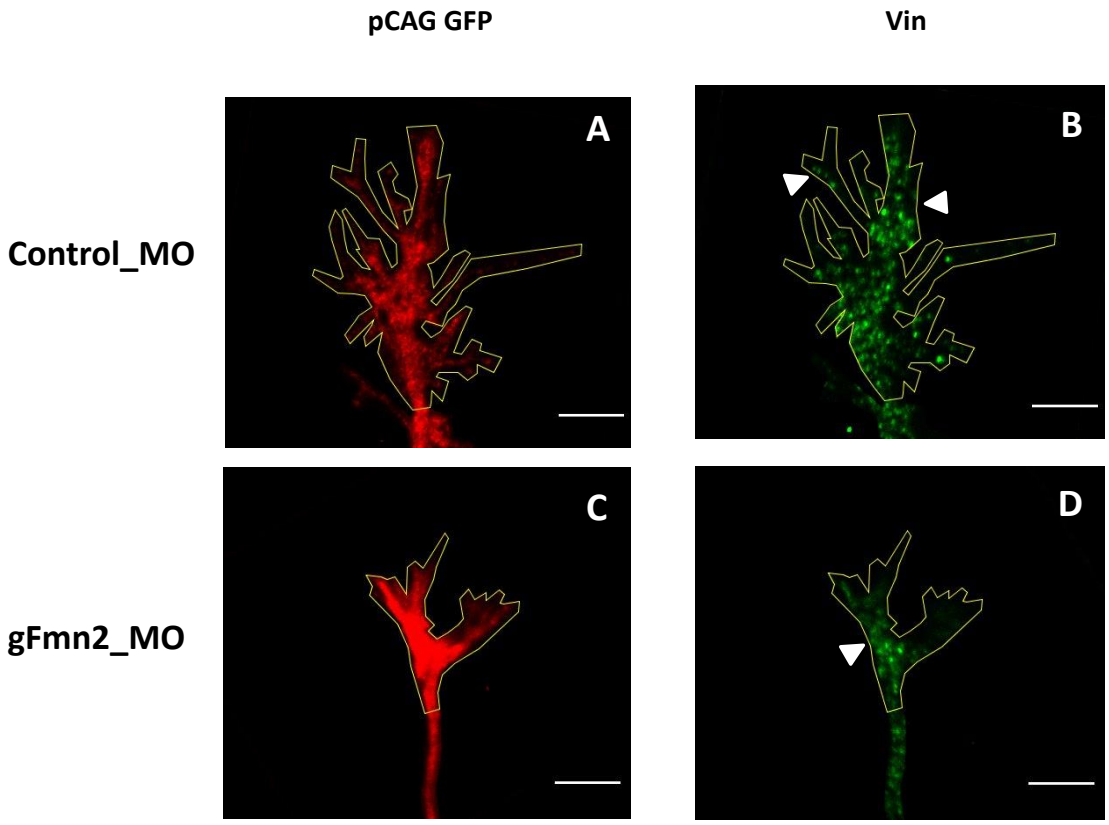

Figure 3.11: Vinculin staining in growth cones. (A) and (C) Cytoplasmic marker to label the electroporated growth cones (here pseudo coloured in red). (B) Vinculin is present in the entire growth cone and along the filopodia (arrowheads). (D) Loss of gFmn2 reduced the puncta labelled by vinculin in entire growth cone (Scale bar = 5 µm).

Also, like the paxillin and pPax, vinculin staining in gFmn2 knockdown neurons does not affect a number of point contacts (Fig. 3.12 A). But dramatically reduced point contact area and the signal intensity at individual point contacts (Fig. 3.12 B, C).

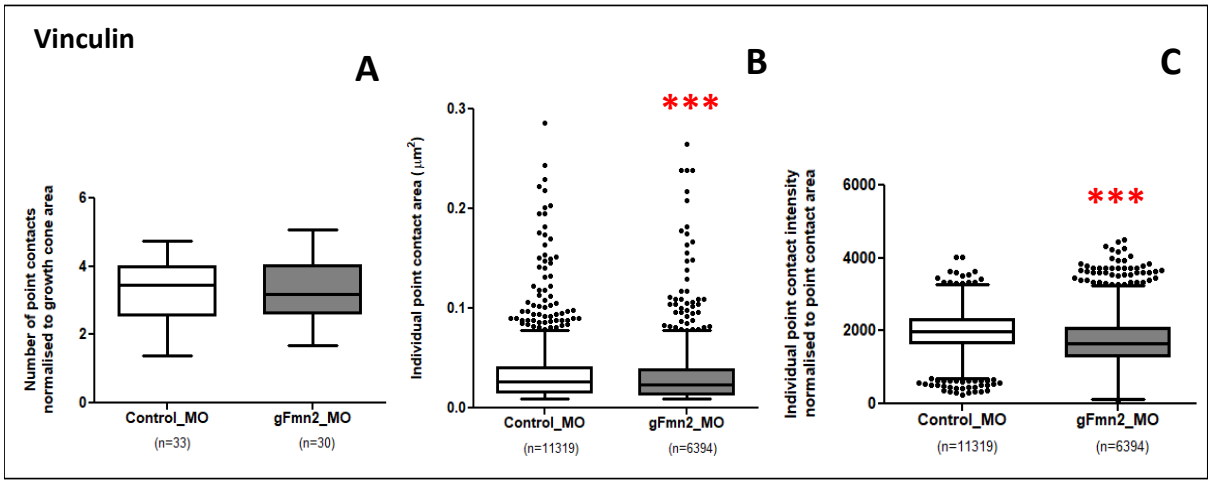

Figure 3.12: Fmn2 depletion results in smaller point contacts and reduced vinculin staining. (A) and (B) Show significant reduction in intensity of individual point contacts and area of individual point contacts (***P ≤ 0.001). (C) Numbers of the point contacts detected remain unchanged across treatments (Numbers in bracket indicate a number of growth cones (A) and individual point contacts detected (B, C) over 4 independent experiments).

Focal adhesion kinase (FAK), a non-receptor tyrosine kinase, that is activated downstream of integrin clustering, and is known to be enriched in neurons is one of the signalling proteins recruited upon initial point contact assembly. Our staining in growth cones shows labelling of the protein at filopodia tips and all over the growth cone area, however loss of gFmn2 reduced this staining pattern dramatically in neurons (Fig. 3.13).

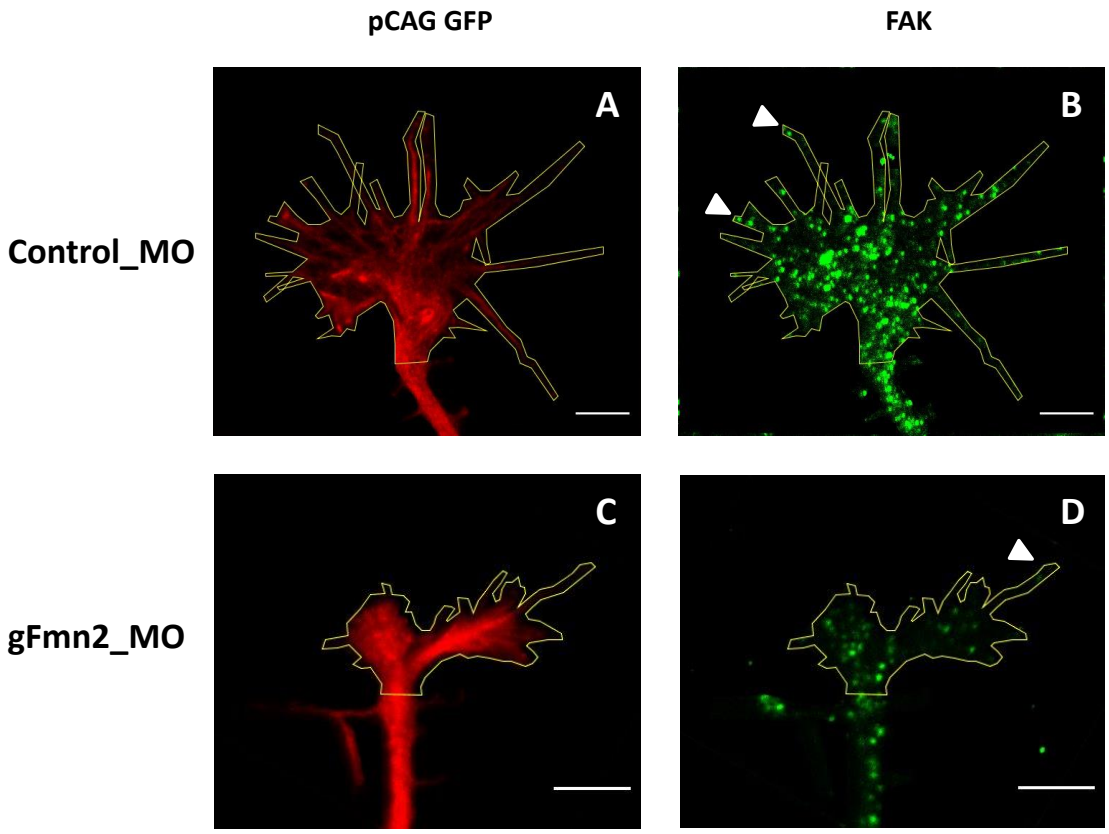

Figure 3.13: FAK staining in growth cones. (A) and (C) Cytoplasmic marker to label the electroporated growth cones (here pseudo coloured in red). (B) FAK labels filopodial tips (arrowheads) and also as distinct puncta all over the central region. (D) Reduced FAK observed in gFmn2 depleted neurons indicating loss of staining at the filopodial tips (arrowhead) along with overall reduced staining in the growth cone (Scale bar = 5 µm).

Quantitation of the neurons further showed the unaffected number of FAK labelled point contacts (Fig. 3.14 A) but indicated smaller point contacts with FAK label with reduced signal intensity upon gFmn2 knockdown (Fig. 3.14 B, C).

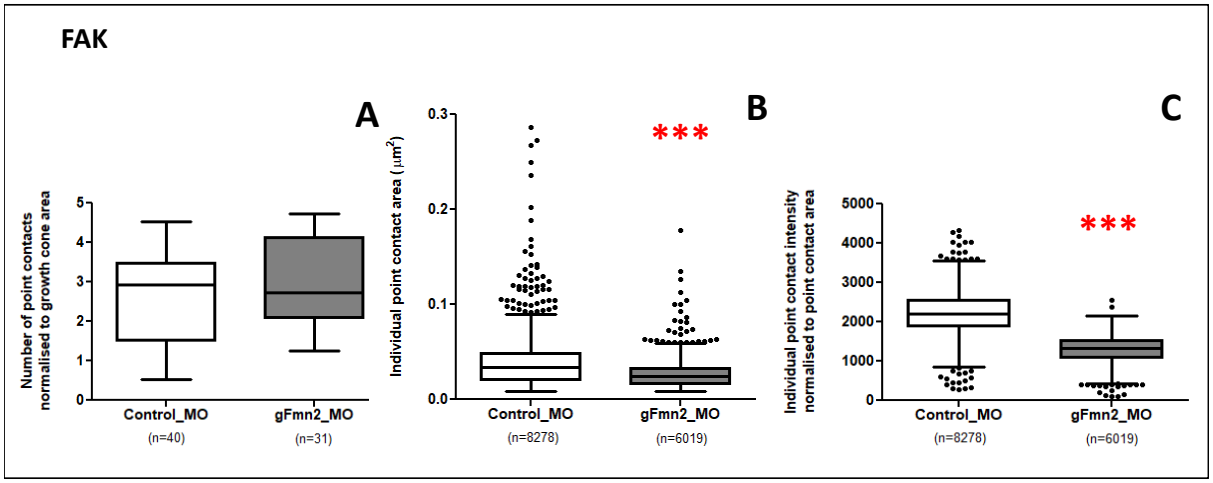

Figure 3.14: Loss of Fmn2 results in smaller point contacts and reduced FAK staining. (A) and (B) show a significant reduction in intensity and area of individual point contacts (***P ≤ 0.001). (C) Numbers of the point contacts detected remain unchanged across treatments (Numbers in bracket indicate a number of growth cones (A) and individual point contacts detected (B, C) over 4 independent experiments).

As mentioned earlier, autophosphorylation of FAK at Y 397 residue is an indicator of point contact stability and is central to force dependent maturation of the point contacts. We immunostained neurons with pFAK (Y 397) antibody to access the effect of gFmn2 depletion on point contact stability. We observed loss of tip adhesions labelled by pFAK (Y 397) along with an overall loss of signal intensity from the central region of the growth cone. These results are consistent with the previous report from our lab (Sahasrabudhe et al., 2016).

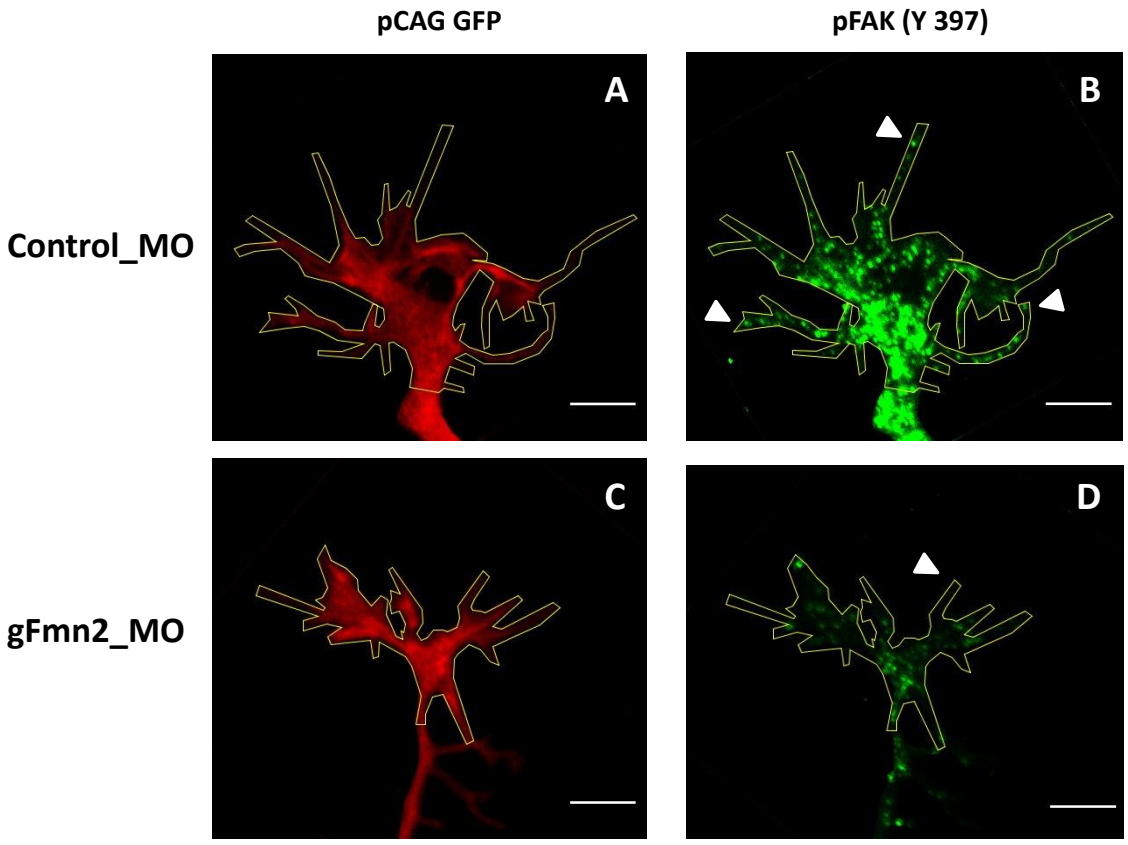

Figure 3.15: pFAK (Y 397) staining in growth cones. (A) and (C) Cytoplasmic marker to label the electroporated growth cones (here pseudo coloured in red). (B) pFAK labels along filopodia and tips (arrowheads) and also as puncta all over the central region. (D) Reduced pFAK intensity observed in gFmn2 depleted neurons indicating loss of staining at the filopodial tips (arrowhead) along with overall reduced staining in the growth cone (Scale bar = 5 µm).

Quantification of these growth cones demonstrated an unaffected number of point contacts and their individual area (Fig. 3.16 A, B) but showed a significant reduction in individual point contact intensity upon loss of gFmn2 (Fig. 3.16 C).

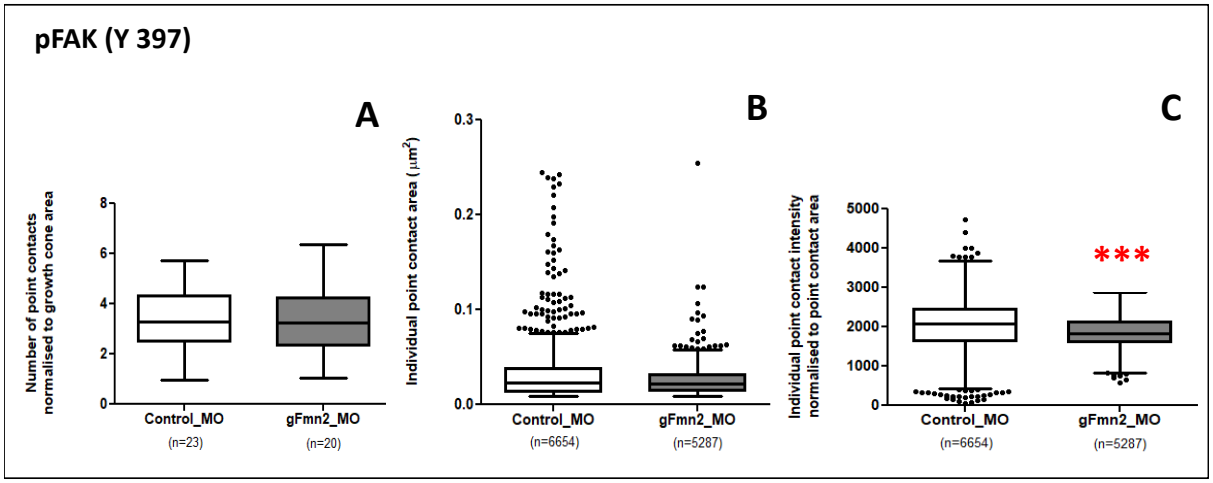

Figure 3.16: Fmn2 depletion results in smaller point contacts and reduced pFAK (Y 397) staining. (A) Significant reduction in intensity of individual point contacts (***P ≤ 0.001). However, (B) area of individual point contacts and (C) Numbers of the point contacts detected remain unchanged across treatments (Numbers in bracket indicate a number of growth cones (A) and individual point contacts detected (B, C) over 4 independent experiments).

Quantification of various point contact markers revealed a common trend demonstrating that loss of gFmn2 does not affect a number of point contacts formed suggesting their initial assembly is unaffected. Further, the similar trend where point contact intensity is reduced upon gFmn2 depletion suggests defects in stability or maturation of these point contacts (Table 3.1).

	Paxillin	pPax (Y 31)	Vinculin	FAK	pFAK (Y 397)
PC number/GC area	NC	NC	NC	NC	NC
PC area	↓	↓	↓	↓	NC
PC intensity	↓	▼	↓	↓	↓

Table 3.1: Fmn2 is necessary for regulating point contact stability but is perhaps dispensable for the initial assembly. This table summarizes, qualitatively, the results obtained for all the point contact markers analysed in gFmn2 knockdown growth cones compared to control growth cones. (NC: no change, arrowhead: slight decrease and bold arrow: strong decrease).

Previous studies from our lab involving the live imaging of focal adhesions in mouse fibroblasts have demonstrated that loss of mFmn2 increases rate of focal adhesion disassembly but their assembly is unaffected (Sahasrabudhe et al., 2016). Even though our current observation from immunostaining studies in neurons suggests that the initial assembly of point contacts is fine and it is the later dynamics of these complexes that might be affected it is necessary to perform live imaging of point contacts to conclusively determine the role of Fmn2.

3.2.3 Fmn2 regulates actin retrograde flow

Slower growth cone translocation rates and compromised ECM substrate attachment, as indicated by the point contact markers in gFmn2 deficient neurons point to a weak molecular clutch in absence of gFmn2. Apart from ECM attachments, modulation of dynamic actin retrograde flow is also an essential component of this mechanical coupling. Reduction in retrograde flow indicates stronger engagement of molecular clutch whereas an increase in the clutch suggests weakly engaged molecular clutch.

To study the effect of loss of gFmn2 on actin dynamics, we cultured spinal neurons on glass transfected with either morpholino. To observe actin dynamics we co-transfected these neurons with pCAG-actin-GFP and imaged the actin expressing neurons by epifluorescence microscopy. Time-lapse movies of the growth cones were captured for 30 min with 10 sec time interval.

To obtain actin retrograde velocities, we created kymographs of different regions of the growth cone, filopodial protrusions and veil-like actin network extending into growth cone central region. Retrograde flow velocities were determined from these kymographs using flow tracker code acquired from Dr. David Odde (University of Minnesota).

Our experiments demonstrate that gFmn2 is important for regulating actin dynamics and perturbation of it increases actin retrograde flow particularly in the lamellipodial and central region. As suggested by the molecular clutch model, increased actin retrograde flow indicates weakly engaged clutch which further highlights the role of gFmn2 in the modulation of the molecular clutch underlying growth cone motility.

Our results also indicate filopodial retrograde flow unaffected upon gFmn2 knockdown; however, this could be due to the dynamic nature of filopodia as compared to the other regions of the growth cone. It is also possible that the limited space of filopodia and differential attachment states of filopodia pose a technical limitation to assess its retrograde flow accurately.

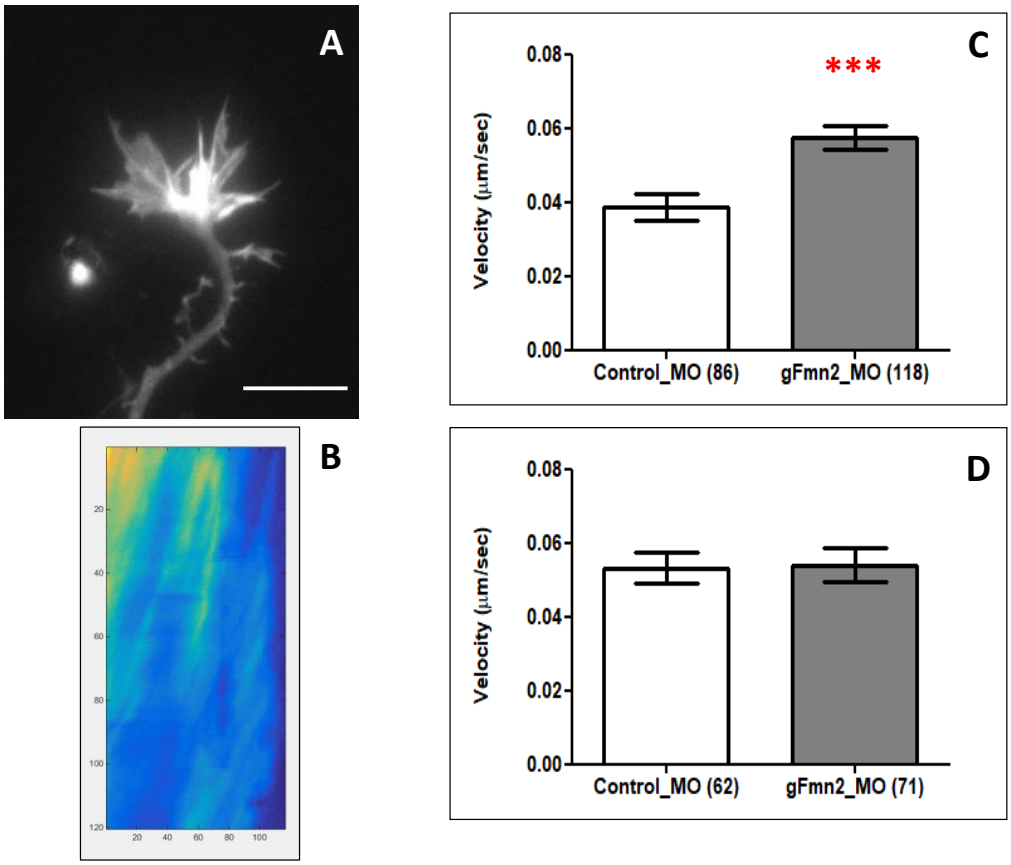

Figure 3.17: Fmn2 knockdown increases actin retrograde flow in growth cone central region and lamellipodia but not in filopodia. (A) Representative growth cone labelled with Actin-GFP to assess actin retrograde flow (Scale bar = 5 µm). (B) Heat map of a representative kymograph generated using flow tracker code. (C) Quantitation for retrograde flow in lamellipodia and central region increases in absence of gFmn2 (***P ≤ 0.001) (D) Quantitation of retrograde flow in filopodia which does not get affected upon gFmn2 knockdown. (Numbers in bracket indicate a number of regions over which the retrograde flow velocity is calculated. Total growth cones analysed were 25 -28 over 7 independent experiments).

3.2.4 Traction forces exerted by growth cone are impaired upon Fmn2 knockdown

The mechanical coupling between the actin cytoskeleton and the ECM attachment form molecular clutch that can modulate cell motility and generate traction forces necessary for the cell to move in a particular direction. As our earlier studies indicate the importance of gFmn2 in neuronal cell motility by modulating growth cone point contacts and actin retrograde flow, we further studied the role of gFmn2 in the traction forces that are generated by the neuron on the substrate during their movement. Previous studies indicate that the magnitude of the overall traction is dominated by traction forces generated in the central region of growth cone (Koch et al., 2012; Polackwich et al., 2015). Our studies also demonstrate that Fmn2 affects point contacts and actin retrograde flow mainly in the growth cone centre making it essential to assess traction forces in this region.

To address this, morpholino and pCAG-GFP co-transfected neurons were cultured on compliant poly-acrylamide gels with embedded fluorescent beads the stiffness of which was measured using atomic force microscopy (AFM) by Kavitha Sthanam from Dr. Shamik Sen's lab at IIT Bombay. To assess traction forces, neurons were grown on the gels and after 48 hrs of the culture they were imaged before and after de-adhesion by trypsin treatment. Images of growth cone and beads acquired pre and post trypsin treatment were used to quantify traction generated using the Fourier Transform Traction Cytometry (FTTC) method (Butler et al., 2002).

In spite of intrinsic variations in the traction forces exerted by growth cones, our experiments revealed that gFmn2 depletion caused generation of weaker traction forces compared to control morpholino treated growth cones (Fig. 3.18) further highlighting the role of gFmn2 in modulating the molecular clutch necessary for neuronal growth cone motility.

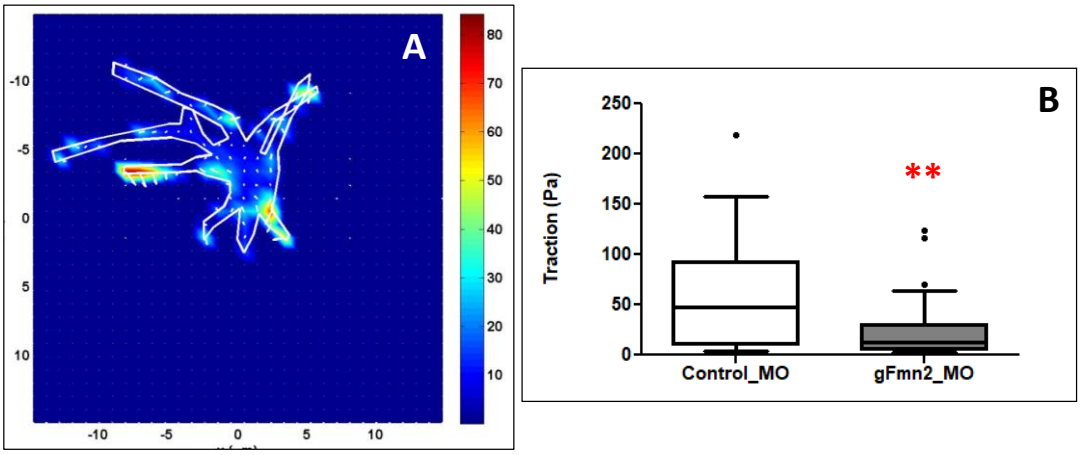

Figure 3.18: Fmn2 regulates traction forces generation in neuronal growth cones. (A) Distribution of traction forces under the constrained growth cone area as output from the code. Heat map showing traction in Pa. (B) Quantitation of traction indicates significant reduction upon gFmn2 knockdown (**P ≤ 0.01) (n = 40).

3.3 Discussion

Growth cone motility is primarily driven by actin in response to diffusible or surface bound cues. However, over the years it has been observed that these cues are immobilized to engage the receptors in order to translocate the growth cone (Bard et al., 2008; Myers and Gomez, 2011; Toriyama et al., 2013). These cues trigger intracellular signalling that causes remodelling of the cytoskeleton and thus its inherent dynamics is translated into motility. An important hypothesis which models this notion is the 'molecular clutch' which suggest that upon binding of a growth cone receptor to its underlying adhesive substrate, a complex is formed which serves as a molecular clutch that mechanically couples retrograde actin flow thereby attenuating it and in turn allowing the actin polymerization to take over for the resultant growth cone protrusion (Mitchison and Kirschner, 1988).

Our study of actin nucleator Fmn2 in neuronal growth cones of chick embryo suggest that this actin regulatory protein might be regulating growth cone motility by behaving as a molecular clutch.

Our previous observations of *in vivo* trajectory defects upon gFmn2 knockdown indicated the role of gFmn2 not only in filopodial stability but also overall compromised motility. The current study further emphasized the role of gFmn2 in persistent motility of neurons in culture. Loss of gFmn2 compromises overall growth cone motility by affecting the growth cone speed which can be attributed to affected actin remodelling probably due to diminished substrate interaction.

Important aspect underlying cell motility is substrate adhesions which in neurons are described as point contacts. Point contacts somewhat resemble focal adhesions in non-neuronal cells in term of their molecular composition and are known to get rapidly remodelled downstream of a number of guidance cues (Myers et al., 2012; Moore et al., 2012; Kerstein et al., 2015). In order for a cell to move, not only assembly, but signalling, maturation, and turnover of substrate adhesions are equally important in the entire growth cone. This study indicates that Fmn2 is necessary for stabilization of growth cone point contacts. Reduction in several of point contact markers upon loss of gFmn2 suggests defected formation of point contacts which probably further cannot mature since that depends on efficient force transmission across actin network.

This study also demonstrated the importance of gFmn2 in regulating actin dynamics. Fmn2 deficiency caused increased actin retrograde flow at the dynamic lamellipodia and in the central region of the growth cone. It has been shown that myosin II at the base of filopodia and lamellipodia is causes of retrograde actin flow in neurons by pulling onto actin filaments; however, clutching F-actin at the leading edge can lower this retrograde flow allowing the polymerization driven protrusion to occur. Our study further highlights defect in such an attenuation of actin retrograde flow at the lamellipodia upon reduction of gFmn2.

Therefore, apart from regulation of compaction of actin architecture as described earlier (Sahasrabudhe et al., 2016), Fmn2 is also necessary for maintaining actin dynamics by regulation actin retrograde flow and relaying substrate cues by acting as a molecular clutch.

During cell motility, the contractile actin network is engaged to the substrate adhesions, thereby exerting a force on them which is known to cause mature these adhesions into a more stable complex (Gardel et al., 2010). However, to balance this tension cell exerts traction forces on the underlying substrate. Our studies of traction forces exerted by growth cones showed the important role of gFmn2 in generating traction forces underlying growth cones further supporting the role of Fmn2 in interaction with actin and the underlying ECM.

Taken together, our data support the molecular clutch model identifying Fmn2 as an actin regulatory protein that not only governs actin dynamics but also plays a role in modulating ECM interactions which are the basis of traction generation and the resultant growth cone motility.

However, in addition to these studies, as mentioned earlier, it is necessary to look at the dynamics of growth cone point contacts by live imaging to be able to conclusively define the role of gFmn2 in their turnover. To address this, point contact proteins like paxillin, vinculin can be overexpressed and followed to study their dynamics. In addition, photoactivatable point contact proteins could be expressed in the growth cones along with morpholinos which will allow us to differentially visualize the point contact dynamics in the selected region of the growth cone.

Nonetheless, growth cones are highly dynamic structures and even though important, it can be challenging to study these dynamics in them. As our data indicate, Fmn2 modulates actin dynamics as well as focal contacts. Also, our immunostaining studies in neurons indicate localization of gFmn2 to actin but due to the size of point contacts, it is difficult to address

where Fmn2 localizes with respect to them. In order to address this question, parallel studied in mouse fibroblast were performed which allowed us better visualization of localization of Fmn2 with respect to both actin and focal adhesions. Following chapter discusses our findings in mouse fibroblasts further highlighting the role of Fmn2 in mediating actin and focal contact crosstalk.

3.4 Material and methods

3.4.1 Spinal neuronal culture and electroporation

Preparation of ECM coated plates

22 mm glass coverslips were glued on bottoms of drilled 35 mm plastic plates (Laxbro) using silicon glue (Dow Corning) and sterilized by 70% ethanol wash and UV treatment in the cell culture hood. These coverslip bottom plates were coated with 1mg/ml poly-L-lysine (Sigma) diluted in sterile phosphate buffered saline (137 mM NaCl, 2.7 mM KCl, 10 mM Na2HPO4, 1.8 mM KH2PO4) for 1 hour at 37oC. After washing the PLL with sterile 1X PBS the plates were coated with 20µg/ml fibronectin (Sigma) in PBS for 1 hour at 37oC. These plates were further used to culture the dissociated chick spinal neurons.

Dissection and culture

Six-day old eggs (HH25/HH26) were utilised to harvest entire spinal cords of embryos. The embryos were dissected in sterile phosphate buffered saline (mentioned above) on a Silgard coated plate under a dissecting microscope inside a horizontal laminar flow hood. The dissected tissue was collected in an Eppendorf with embryonic medium (Leibovitz's media (Gibco) with 1X penicillin-streptomycin (Gibco)). The spinal cord was spun at 3000 rpm for 3 min at room temperature after which the embryonic medium was replaced with 1X trypsin-EDTA (Lonza). The tissue was macerated in trypsin and incubated at 37oC for 15-20 min. The further embryonic medium was added to the trypsin and the dissociated spinal cord was spun at 3000 rpm for 3 min. The cells were plated in 2 ml of basal culture medium (L-15 (Gibco), 1X PenStrep (Gibco), 10% heat-inactivated FBS (Gibco)) with 20ng/ml NGF (Invitrogen) supplement and incubated without CO2 at 37oC for 24-36 hrs.

For electroporation, cells were resuspended in 100µl OptiMEM (Gibco) with 10 µg of plasmid and 100 µM morpholino.

(Standard morpholino sequence that was used as a negative control: CCTCTTACCTCAGTTACAATTTATA, Fmn2 morpholino sequence that was used: CCATCTTGATTCCCCATGATTTTTC).

The cell suspension with plasmid and morpholino was transferred to the electroporation cuvette and current was delivered under following conditions using NepaGene electroporator (NEPA 21 *In-vitro* and *In-vivo* electroporator).

Poring pulse:	Transfer pulse:
Voltage (V) – 125	Voltage (V) - 20
Pulse length (msec) – 5	Pulse length (msec) - 50
Pulse interval (msec) – 50	Pulse interval (msec) - 50
Number of pulses – 2	Number of pulses - 5
Decay rate (%) – 10	Decay rate (%) - 40
Polarity - +	Polarity - +/-

After electroporation, the cell suspension was transferred to a microfuge tube with 400 µl OptiMEM (Gibco) and plated on ECM coated coverslip bottom plates with 2 ml of basal culture media (mentioned above).

3.4.2 Growth cone motility imaging

Neurons with both morpholino and pCAG-GFP were cultured on fibronectin-coated glass and imaged after 24 hrs in epifluorescence for 30 min with 10 sec time interval.

3.4.3 Growth cone point contact immunostaining

Spinal neurons were electroporated and cultured with morpholino and pCAG-GFP (Addgene) as described earlier. After 24 – 30 hrs the cells were fixed using modified Kreb's fixative (Dent and Meiri 1992).

50% Kreb's buffer (145mM NaCl, 5mM KCl, 1.2mM $CaCl_2$, 1.3mM $MgCl_2$, 1.2mM NaH_2PO_4, 10mM glucose, 20mM HEPES) with 0.4M sucrose was mixed with 50% Bouin's fixative and cells were fixed in this buffer for 15 min at room temperature. Cells were further permeabilized for 20 min in 0.01% saponin in 10% heat-inactivated normal goat serum in PBS. Following permeabilization, the samples were washed in 0.5% BSA in Kreb's buffer twice for 10 min each. Further cells were blocked in 3% BSA in PBS for 1 hr. Antibodies

against total FAK (Abcam ab33141), phosphor-FAK-Y397 (Abcam ab4803), Vinculin (Abcam ab11194-200), total Pax (Abcam ab2264), phosphor-Pax-Y31 (Abcam ab4832) were added in blocking in 1:600 dilution and the cells were incubated with them overnight at 4^{o}C.

After removing primary antibodies, the cells were washed twice in 0.5% BSA in Kreb's buffer for 10 min each. The samples were blocked with 10% normal goat serum in PBS for 45-60 min and then 1:300 dilution of secondary antibody (Invitrogen) was added and incubated for 60 min at room temperature. After the secondary antibody, the cells were washed thrice in 0.5% BSA in Kreb's buffer for 10 min each. Samples were finally mounted in 80% glycerol.

3.4.4 Actin retrograde flow imaging

Neurons with either morpholino and pCAG actin-mGFP (Addgene #21948) were cultured on the fibronectin-coated glass and imaged after 24 hrs in epifluorescence for 30 min with 1 sec time interval. Kymographs were generated in MetaMorph software using a segmented line tool (width: 5 pixels). Velocities were calculated from kymographs using flow-tracker code (Obtained from Dr. D. Odde, University of Minnesota), in the Matlab 2007. Retrogradely moving regions from the heat map generated of the kymograph were selected using a rectangular selection. The analysis was restricted to parts of time lapse with non-dynamic and detached filopodia to reduced fluctuations due to the membrane.

3.4.5 Traction force microscopy

A. Activation of coverslips

For a better attachment of compliant poly-acrylamide gel to the glass coverslip, the coverslips are chemically activated. This allows the gel to covalently attach to the coverslip. 28 mm clean coverslips were treated with 0.5% APMS-3-aminopropyltrimethoxysilane (APMS) (Sigma) in water for 15-20 min followed by 4-5 washes with distilled water. These coverslips were baked at 160^{o}C for 1-2 hrs. 35mm culture plates were drilled at the bottom beforehand and the APMS treated coverslips were glued on it using silicone glue with the APMS treated side facing inside the plate. The glue was allowed to dry overnight, after which 0.5% glutaraldehyde (Sigma) (~ 200 µl) diluted in water was added on the coverslips and incubated for 1 hr at room temperature. Further, the coverslips were washed with water 3-4 times and allowed to dry completely.

B. Bead coating on top of coverslips

The required number of 18 mm clean coverslips was taken and incubated with 50 µg/ml fibronectin (Sigma) coating in PBS (~20 µl) at 37^{o}C for 30 min. After removing the fibronectin, the coverslips were dried completely. 100 µl of 1:20 diluted Fluorosphere carboxylate modified beads (Thermo) (200 nm) from 1:1 working stock was spin coated on these coverslips at 1500 rpm for 5 min.

C. Gel preparation

Gel stiffness was measured using atomic force microscopy (AFM). This work was done by Kavitha Sthanam from Dr. Shamik Sen's lab at IIT Bombay. Two technical replicates, each with minimum 30 readings were performed using a pyramidal cantilever. Data analysis was done using Hertz fitting (MacKay and Kumar, 2012).

Poly-acrylamide gel mixture for stiffness 0.438 ± 0.064 kPa was made using 3% acrylamide and 0.1% bisacrylamide as described previously in (Tse and Engler, 2010) and 15 µl of the gel mixture was added onto each coverslip bottom culture plate. Immediately the smaller bead coated coverslip was inverted on the gel facing with the beads facing the gel mixture. Once the gel was solidified, MiliQ water was filled in the plates to prevent the gels from drying and the top coverslips were removed carefully using a razor blade.

D. ECM cross-linking

After removing the MiliQ from the gels, 200 µl of 2 mg/ml sulfo-SANPAH (Covachem) was added on the gels and allowed to coat the gels for 1 hr at 5 to 8 cm distance under a hand-held UV lamp (365 nm) in the cell culture hood. The plates were later washed with sterile distilled water 3 times and incubated with 250 µl of 50 µg/ml fibronectin (Sigma) overnight at 4^{o}C until further neuronal culturing.

3.4.6 Imaging

For motility assay imaging a PlanApo 60x/1.4 oil immersion objective was used on an Olympus IX81 system with Hamamatsu ORCA-R2 CCD camera.

For imaging point contacts a PlanApo 63 x/1.40 oil immersion objectives were used on Zeiss 710 inverted microscope. The images were acquired with 2X zoom and all the conditions were kept constant across treatments so that intensity can be analysed.

For retrograde flow and traction force imaging a PlanApo 60x/1.4 oil immersion objective on an Olympus IX81 system with Hamamatsu ORCA-R2, CCD camera was used.

The growth cones were co-transfected with pCAG-GFP and morpholino thus only fluorescing growth cones were imaged.

3.4.7 Analysis

For motility analysis, the centre of growth cone was tracked manually in Fiji and the coordinates were exported to Chemotaxis and Migration tool developed by Ibidi (http://ibidi.com/xtproducts/en/Software-and-Image-Analysis/Manual-Image-Analysis/Chemotaxis-and-Migration-Tool). New co-ordinates generated in this software were used to calculate the growth cone velocity, displacement, and directionality.

For analysing point contacts, the images were manually processed in Fiji manually. After demarcating the growth cone area outlines manually from the pCAG-GFP image signal, the growth cone area was selected in the antibody immunostaining channel. The antibody image was subjected to background subtraction to reduce the noise followed by application of unsharp mask which sharpened the boundaries of the point contact staining observed. These images were thresholded using Otsu algorithm available in Fiji and the resultant binary image was processed through the particle analyser with 1.5 pixels as a baseline threshold to get a mask demarcating the outlines around point contacts in the selected growth cone area. This mask could be overlayed on the raw image of point contact staining to get extract the original signal intensity of the point contacts.

The particle analysis tool in Fiji generated number and area of point contacts detected and the addition of the mask on the antibody channel yielded the intensity at each detected point contacts. These outputs from Fiji were exported to Microsoft Excel 2007 and GraphPad Prism 5 for further analysis.

The retrograde flow was analysed using Fiji to make substacks of the original movie followed by MetaMorph software for the generation of kymographs. Matlab 2007 was used to run the flow tracker code to get a heat map of kymographs for velocity analysis.

For traction force analysis, the images of beads pre and post trypsin treatment, stressed and relaxed respectively, were stabilized using template matching plugin in Fiji. The images were analysed using code based on Fourier Transform Traction Cytometry (FTTC) method established by Butler and colleagues (Butler et al., 2002). The stressed and relaxed bead images along with the growth cone images were imported in the code followed by gel stiffness (0.438 kPa), Poisson ratio for the gel (0.48) and gel thickness (60 µm) parameters.

The code creates displacement fields by employing the cross-correlation between stressed and relaxed images after regularization and further generates the traction force values.

3.4.8 Data representation and statistics

All data were plotted in GraphPad Prism 5 by either Box and Whisker plots represent the spread of the data with the Tukey method or a bar graph with SEM as the error bars. Outliers are represented outside the box as individual data points in the Box and Whisker Plots. All plots were compared using Mann-Whitney test in GraphPad Prism 5.

4. Fmn2 localizes to ventral stress fibres of mouse fibroblasts and plays a role in leading edge dynamics during their spreading

4.1 Introduction

4.1.1 Actin structures in mesenchymal cell motility

Cell motility is a complex process that requires dynamic remodelling of cell shape and cell-matrix adhesion. This process is essential not only during development of an organism but also later during physiological processes such as wound healing and tissue regeneration. Defects in cell motility and migration can lead to cancer metastasis and immunological diseases. During motility, a cell explores its surrounding by extending the lamellipodium followed by formation of new points of contacts with the substrate at the leading edge while the cell body contracts and moves forward, retracting and disengaging the substrate attachments at the trailing edge (Ridley 2011; Moissoglu and Schwartz 2006). The actin cytoskeleton that provides force for these events is constantly reorganised during these processes in order to maintain the cell shape, sense the substrate and transmit the forces that the cell requires during its motility.

During adhesion-dependent migration, mainly 3 distinct actin structures can be observed (Fig. 4.1), finger-like thin filopodia, flat sheet-like lamellipodia and myosin II containing contractile stress fibres. Filopodia are thin membrane protrusions present at the leading edge if a cell which has parallel bundles of actin with the barbed end facing the leading edge. Lamellipodia are veil like region of leading edge which are characterised by branched actin network. Stress fibres are contractile structures present in the cells that are often composed of shorter actin filaments and have mixed polarity of actin bundles unlike filopodia (Sanger et al., 1983; Cramer et al., 1997; Svitkina et al., 1997).

Cell protrusion is achieved by flat, broad lamellipodial and/or thin, cylindrical filopodial structures which are regulated by Arp2/3 complex and formins respectively (Small 1988; Pollard and Borisy 2003). Arp2/3 complex generates array of branched actin filaments whereas formins like mDia or VASP family proteins nucleate and elongate unbranched actin filaments (Svitkina et al., 2003; Faix and Rottner 2006; Gupton and Gertler 2007) which are bundled in filopodia by Fascin (Abercrombie et al., 1971; Mallavarapu and Mitchison 1999). Addition of g-actin monomers to the barbed ends of actin filaments in these structures generate a pushing force that not only drives the leading edge forward, but also cause the actin network to move backward resulting in actin retrograde flow (Forscher and Smith 1988; Symons and Mitchison 1991; Lin and Forscher 1995; Pollard & Borisy 2003; Ponti et al., 2004). The pool of actin monomers is restored at the base of lamellipodial and filopodial structures by proteins that sever actin filaments such as Cofilin (Miyoshi et al., 2006; Iwasa and Mullins 2007) or Myosin II motors that move along actin filament and also generate contractile forces (Medeiros et al., 2006). These severed actin filaments could also be utilised by the cell to assemble contractile stress fibres at lamella, a flat structure behind the leading edge rich in F-actin and Myosin II (Abercrombie et al., 1971; Hotulainen and Lappalainen 2006).

Actin stress fibres are contractile bundles of actin consisting of unipolar or bipolar actin filaments. They exhibit Myosin II dependent retrograde flow which is much slower compared to the retrograde flow observed at the leading edge (Ponti et al., 2004; Hotulainen and Lappalainen 2006; Schaub et al., 2007). Stress fibres are known to form in response to the physical properties of the extracellular matrix and are known to have a role in regulating cell polarity (Lehtimäki et al., 2016). They are often observed to be associated with focal adhesion complexes allowing the actin cytoskeleton to communicate with the extracellular matrix as the cell migrates (Geiger et al., 2009). Depending on the composition and

localization of stress fibres in the cell, they perform a variety of functions and are characterised as dorsal stress fibres, transverse arcs and ventral stress fibres (Heath 1983; Small et al., 1998).

Dorsal stress fibres lack Myosin II and hence are not contractile. They are characterised by the presence of focal adhesions on a distal end through which they are polymerized till the cell centre. This subtype of stress fibres exhibits uniform polarity of actin bundles near the focal adhesions (Cramer et al., 1997) and is important for cell migration (Hotulainen and Lappalainen 2006). Dorsal stress fibres also connect other subtypes of stress fibres such as transverse arcs to focal adhesions which are contractile actin structures shown to move to cell centre during migration (Hotulainen and Lappalainen 2006; Tee et al., 2015). Second subtypes are the transverse actin arcs which unlike the dorsal stress fibres do not interact with focal adhesions (Hotulainen and Lappalainen 2006; Kovac et al., 2013). These fibres are parallel to the leading edge and they move toward the nucleus as the cell migrate (Vallenius 2013). The third subtype of stress fibres, the ventral stress fibres are thought to emerge from dorsal stress fibres and transverse arcs at least in part and are observed to assemble perpendicular to the direction of migration. The arrangement of the array of actin filaments in ventral stress fibres resembles muscle sarcomeres with the presence of bipolar actin filaments. Ventral stress fibres and transverse arcs exhibit a periodic pattern of α-actinin and Myosin II which make these structures contractile (Sanger et al., 1983; Hotulainen and Lappalainen 2006). This subtype of stress fibres communicates with the extracellular matrix (ECM) and exerts traction forces via characteristic focal adhesions present on either end of them (Small et al., 1998; Tojkander et al., 2012). They are usually present underneath the nucleus and their presence is usually associated with stabilization of the cell (Hotulainen and Lappalainen 2006; Kovac et al., 2013). Functional relevance of ventral stress fibres is associated with cell adhesion, morphogenesis, and mechanosensing (Tojkander et al., 2015).

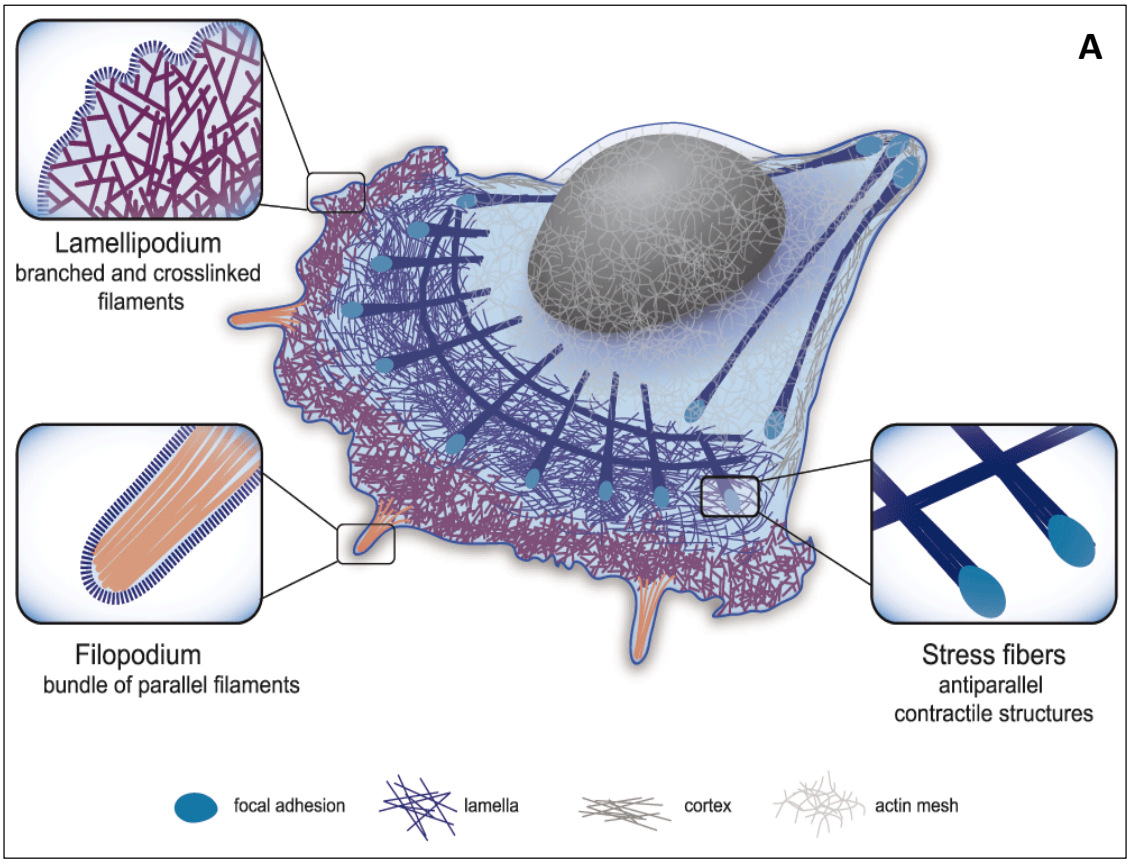

Figure 4.1: Actin structures in mesenchymal cells. (A) Schematic depicting actin structures such as filopodia containing parallel, unbranched actin bundles. Lamellipodia with branched actin meshwork is present at the leading edge. Contractile bundles of stress fibres that maintain cell shape are distributed in the cell.

4.1.1.a Actin architecture comparison in neuronal growth cones and mesenchymal cells

Neuronal growth cones are highly specialized extensions of the neuronal cell. They extend over a longer distance from the soma and exhibit an intricate network of actin and microtubules which impart the growth cone its unique structure and function. As described earlier, growth cones have distinct actin-rich regions which surround the central microtubule region, whereas, mesenchymal cells exhibit concentrated actin structures at the motile leading edge and microtubules are splayed quite uniformly. The sensory and dynamic actin-rich filopodia are much more abundant and long in neurons as compared to the ones in the mesenchymal cells. Well spread mesenchymal cells exhibit unique, contractile actin stress fibres which impart structural integrity to these cells in contrast to neuronal growth cones that

do not show the presence of actin stress fibres. Additionally, as described earlier, the stress fibres in mesenchymal cells often exhibit the presence of focal adhesion complexes at either end which are distinctive structures as compared to small, circular growth cone point contacts.

4.1.2 Focal adhesion dynamics in fibroblasts

As described earlier, during cell motility, not only lamellipodial or filopodial membrane protrusions are essential, but also dynamic formation and turnover of focal adhesion complexes is very important (Fig. 4.2). As the cell moves ahead, new contacts must be formed with the ECM at the leading edge and mature preformed contacts must be disassembled at the rear end of the cell resulting in retraction of the trailing edge. It has been observed that as the lamellipodial edge progresses, nascent adhesions (smaller than ~ 0.25 μm), also known as focal complexes (Bershadsky et al., 1985; Nobes and Hall, 1995) formed at the leading edge of the cell and as the cell moves ahead, subpopulation of these focal complexes matures into elongated focal adhesions or focal contacts (3 – 10 μm) (Heath and Dunn, 1978; Geiger et al., 2001). Focal adhesions are associated with actomyosin rich stress fibres and can further be matured into fibrillary adhesions that remodel the ECM substrate (Zamir et al., 2000; Webb et al., 2004).

Focal adhesions initiate by the formation of integrin microclusters (Wiseman et al., 2004) however further activation of the integrin dimer happens upon binding of talin to β subunit of the dimer. Talin further facilitates binding to actin and vinculin during maturation of the focal complexes (Tadokoro et al., 2003). Shortly after integrin activation, paxillin is recruited to the nascent focal complexes which further promote recruitment and clustering of integrin molecules (Webb et al., 2004; Wiseman et al., 2004). Nascent adhesions can be rapidly disassembled if further proteins that aid focal adhesion maturation are not recruited, although their growth is accompanied by the association of α-actinin which is an actin bundling protein (Choi et al., 2008). Mechanical tension exerted by Rho-mediated Myosin II activity or external forces is thought to stimulate maturation of nascent focal complexes to mature focal adhesions (Chrzanowska-Wodnicka and Burridge 1996; Balaban et al., 2001; Choi et al., 2008). During cell motility the nascent adhesion complexes, along with Myosin II driven actin retrograde flow convey pulling forces from lamellar actin to the ECM- integrin linkage, promoting assembly of actomyosin bundles that are associated with these nascent adhesions. These actomyosin bundles further promote binding of adapter proteins namely vinculin and

zyxin (Choi et al., 2008). These small actin bundles further undergo force dependent elongation which is mediated by formins such as mDia (Riveline et al., 2001; Hotulainen and Lappalainen 2006; Gupton et al., 2007).

Tension mediated secondary ECM-integrin binding induces recruitment of focal adhesion kinase (FAK) and its phosphorylation (Shi & Boettiger 2003; Friedland et al., 2009) which consequently phosphorylates paxillin and p130 cas (Ballestrem et al., 2006) and creates a scaffold for SH-2 domain proteins to bind which in turn promote growth of focal adhesion.

As much important is the assembly of focal adhesions, their turnover and disassembly is also crucial for the cell to move forward. FAK is also associated in turnover of focal adhesions possibly by reducing local Myosin II contractility (Arthur and Burridge 2001; Holinstat et al., 2006; Schober et al., 2007) or upregulation of Rho antagonist Rac1 (Sander et al., 1999; Arthur and Burridge 2001).

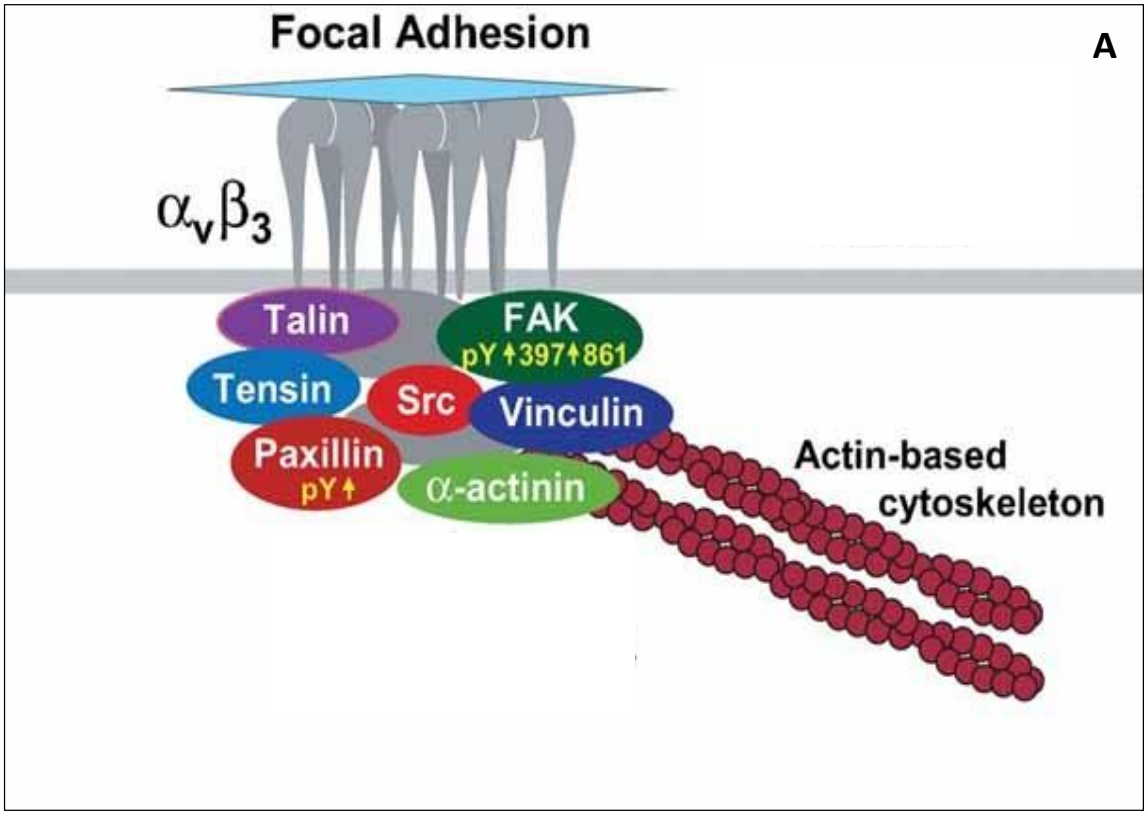

Figure 4.2: Schematic of focal adhesion complex. (A) The typical structure of a focal adhesion complex. It is characterized by the assembly of numerous scaffolding and signalling proteins that associate ECM substrate to the actin cytoskeleton.

4.1.3 Cell spreading

Over the years cell spreading has been studied to improve our understating of cellular physiology of cell and ECM interaction. Cell spreading serves as a quantitative approach to investigate molecular changes underlying chemical and mechanosensing (Wolfenson et al., 2014).

Studies show that when cells are plated on fibronectin-coated glass, cells undergo three major morphological changes, initial attachment with the substrate leading to rapid increase in cell spread area followed by a slow spreading phase characterised by periodic membrane dynamics (Dubin-Thaler et al., 2004; Giannone et al., 2004) (Fig. 4.3).

Integrin attachment is critical during cell spreading, as when the cell membrane protrudes; it engages talin and kindlin to the nascent adhesions that form underneath the leading edge (Jiang et al., 2003; Moser et al., 2009; Bachir et al., 2014). Some of these initially assembled focal contacts are stabilised by Myosin II to form stable focal adhesions (Choi et al., 2008; Stricker et al., 2013) which on their further association with formins like FHOD1 can assemble actin fibres which in turn help mature the focal adhesions (Yu et al., 2011; Iskratsch et al., 2013). Once activated by initial integrin attachment, cell rapidly progresses in the second phase of rapid cell spreading where it does not need further integrin activation (Gauthier et al., 2011). During this phase rate of polymerization at the leading edge is significantly higher than that of the cell centre (Wolfenson et al., 2014). After reaching the maximum cell area, at the end of this phase, myosin contraction is activated that leads to periodic contraction of lamellipodia of cells on rigid substrates (Giannone et al., 2004; 48). These periodic contractions are thought to be involved in sensing rigidity of the substrate as they are absent on cells cultured on softer substrates (Giannone et al., 2004). Over time, these protrusion – retraction cycles result in the organization of adhesions that stabilize and mature over time (Saez et al 2005).

Once the cells stabilize, focal adhesion formation and maturation occurs by interaction with actin cytoskeleton via a molecular clutch which can further act as a force transducer that exerts traction forces on the substrate.

Taken together, by observing cell spreading early events of actin and ECM interaction can be studied which can further give insights into adhesion mediated mechanosensing.

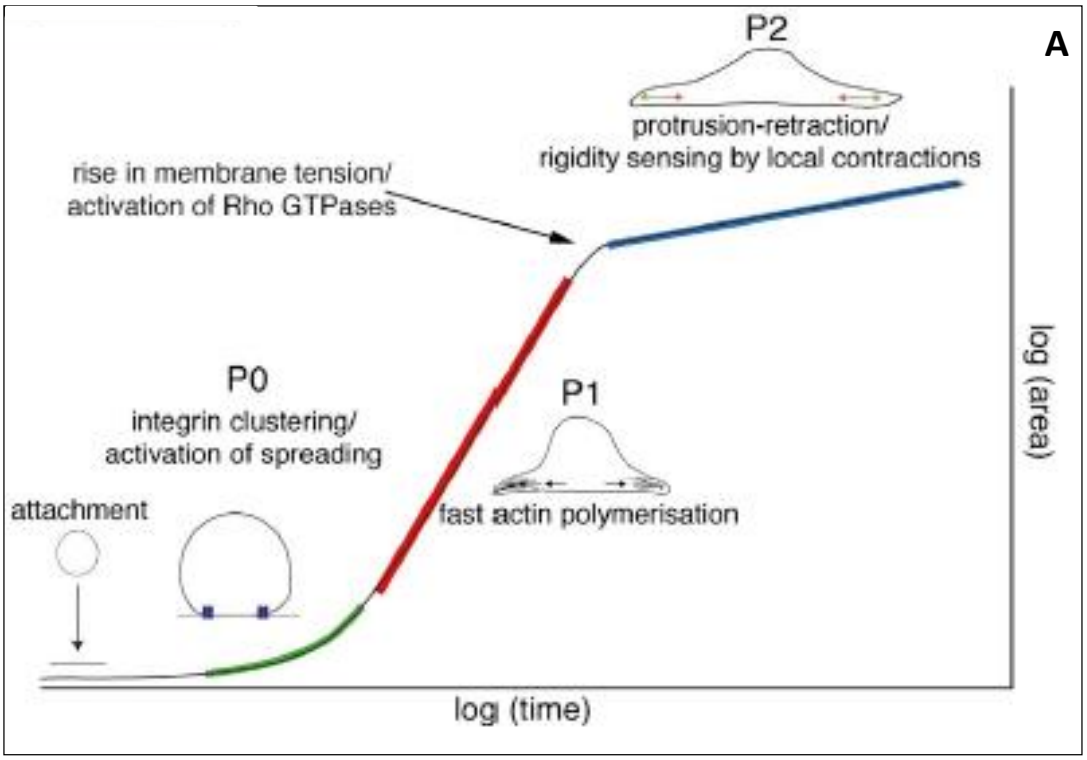

Figure 4.3: Schematic of phases of cell spreading. (A) Representation of various phases that cell undergoes during cell spreading, initial attachment, rapid cell spread followed by protrusion – retraction cycles for rigidity sensing. (Reproduced from Wolfenson et al., 2014).

4.2 Results

4.2.1 mFmn2 localizes to actin-rich ventral stress fibres and is juxtaposed to focal adhesion complexes

Studies done in spinal neuronal growth cones reveal the unique function of Fmn2 in remodelling actin architecture and possibly, in turn, the point contact dynamics resulting in overall defects in growth cone traction generation and hence motility. Although, we showed localization of Fmn2 with actin we wanted to investigate the interaction of Fmn2 with focal contacts as we. To have a better understanding of Fmn2 localization with respect to actin as well as focal adhesions, we utilised NIH3T3.

From studies in growth cones, we confirmed the recruitment of gFmn2 to actin structures. To study the localization of mFmn2 to actin structures in NIH3T3 we overexpressed full-length mFmn2 construct along with Actin-mRFP (Fig. 4.4 C). Line scan intensity analysis indicated mFmn2 localization was concentrated mainly at the cell centre caging the nucleus furthermore discontinuously decorating the ventral stress fibres present below the nucleus (Fig. 4.4 E, F).

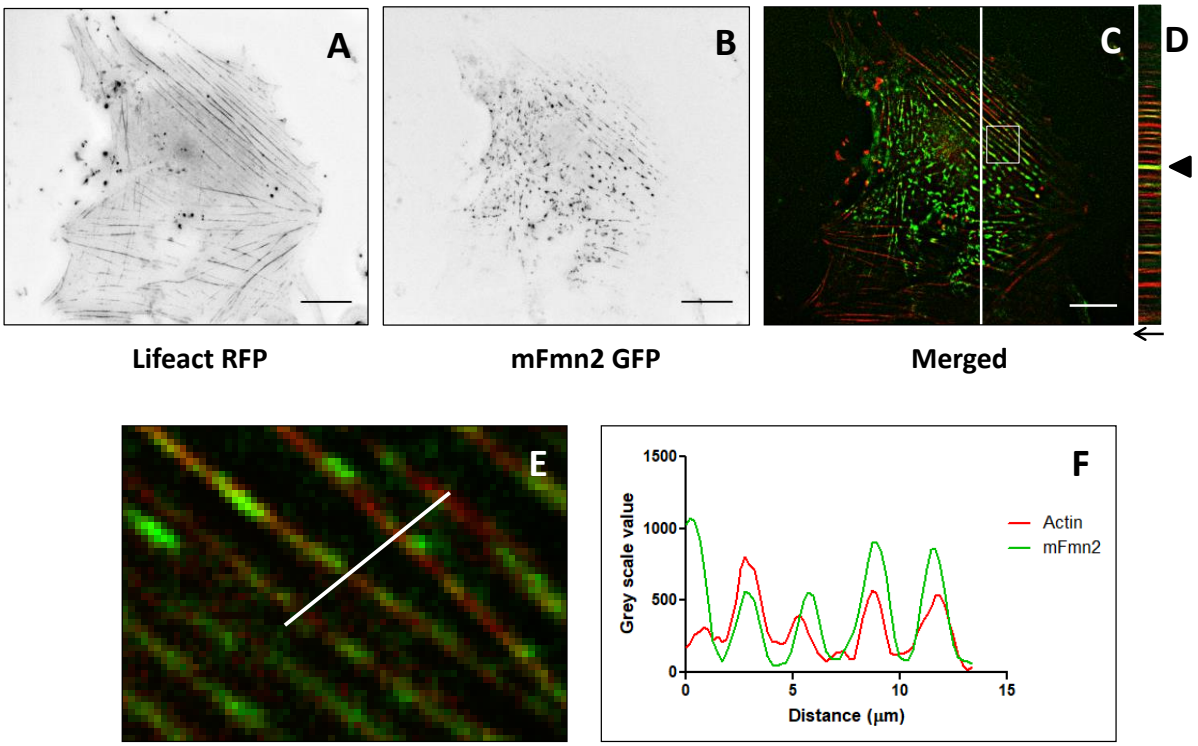

Figure 4.4: mFmn2 localizes to ventral stress fibres in mouse fibroblasts. (A) Maximum intensity projection of actin structures labelled by overexpression of Lifeact RFP. (B) Maximum intensity projection of overexpression of full-length mFmn2 GFP. (C) Maximum intensity projection merged to show mFmn2 localization to stress fibres. (D) Orthogonal view along the vertical line in (C) showing the colocalization of mFmn2 with ventral stress fibres (arrowhead). The black arrow represents the direction of ventral planes. (E) Enlarged inset in (C) showing region where the mFmn2 colocalization is observed and quantified by line scan in (F). (F) intensity along the line drawn in (E) shows that mFmn2 colocalizes with actin (Scale bar = 10 µm).

To further detect localization of mFmn2 in context with focal adhesions, we overexpressed the full-length mFmn2 with focal adhesion marker paxillin tagged with mCherry. The cells were immunolabelled after 48 hrs with phalloidin to label actin stress fibres. Line scan drawn along the stress fibre to analyse the intensity of each channel indicated mFmn2 localization to

ventral stress fibres, caging the nucleus as observed earlier but interestingly mFmn2 also seemed to be present right next to the focal adhesions which are present on either side of these ventral stress fibres (Fig. 4.5).

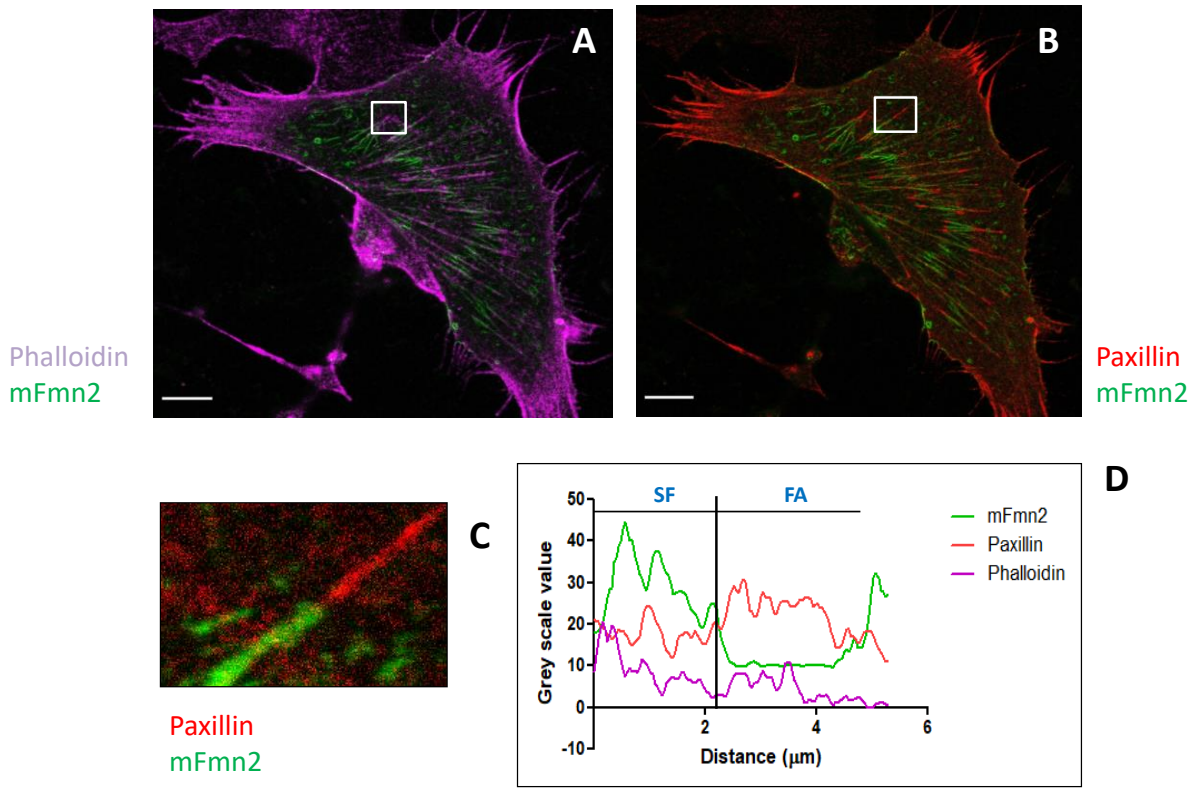

Figure 4.5: mFmn2 localization juxta-posed the focal adhesion complexes of ventral stress fibres. (A) mFmn2 colocalization with actin stained with phalloidin conjugated with Alexa 633. (B) Paxillin mCherry and full-length mFmn2 overexpression. (C) Zoomed inset from (B) showing green signal from mFmn2 just next to a red signal from paxillin. (D) Intensity along a line drawn along the region in (C) confirmed mFmn2 localization juxtaposed to paxillin.

The distinct localization of mFmn2 to contractile actin stress fibres suggested its role in their assembly and maintenance which was confirmed by our group with fluorescence recovery after photobleaching (FRAP) experiments (Sahasrabudhe et al., 2016). In addition, the

localization of mFmn2 right next to the focal adhesion complex at the end of these ventral stress fibres suggests its role in a complex that facilitates actin bundles crosstalk to the focal adhesions.

4.2.2 mFmn2 is essential for the stability of focal adhesions on ECM substrate

After studying the mFmn2 localization in NIH3T3, to understand its potential role in these cells we employed siRNA mediated knockdown approach for our further studies. To estimate the level of knockdown achieved during our studies by siRNAs against LacZ and mFmn2, we resorted to quantitative real-time PCR analysis. The cells were transfected with either siRNAs and incubated for 24 or 48 hrs, followed by RNA extraction and *in vitro* cDNA synthesis. Similar to qRT PCR in neurons, the transcript level changes were estimated by comparing the relative abundance of the housekeeping gene GAPDH and mFmn2 at each time points. This assay showed 70% knockdown in the transcript levels upon treatment at 24 and 48 hrs (Fig. 4.6).

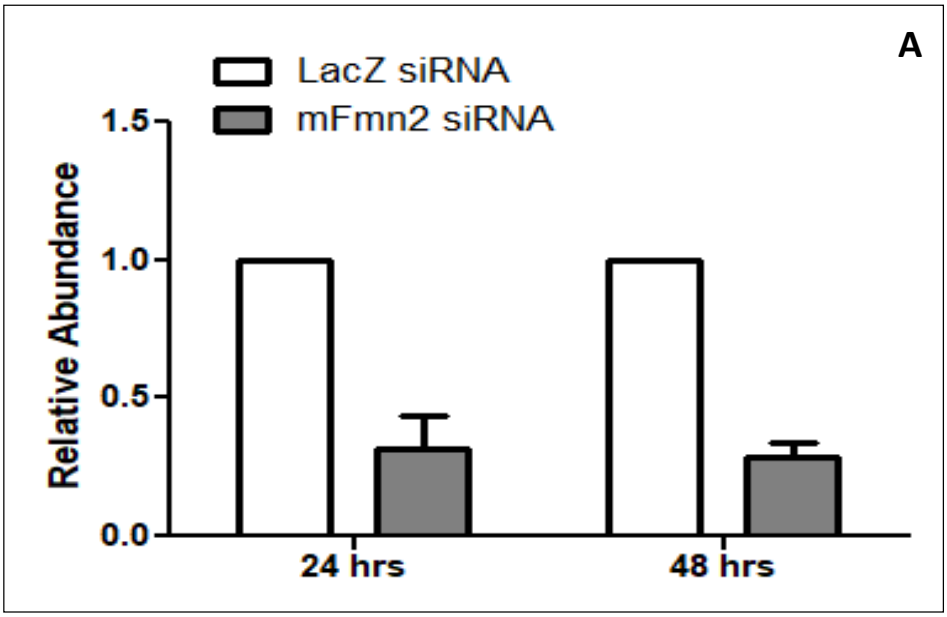

Figure 4.6: Depletion of endogenous mFmn2 was achieved by siRNA mediated knockdown. (A) Quantification of real-time PCR studies after siRNA mediated knockdown of mFmn2 in NIH3T3. Relative abundance of the transcript is based on normalisation with GAPDH transcript levels (The graph represents the average relative abundance of 9 technical replicates. Each replicate utilised RNA from independent experiments).

As described in the earlier chapter Fmn2 plays a role in regulating growth cone point contacts. To assess the similar role of Fmn2 in mouse fibroblasts, we cultured NIH3T3 overnight on glass coated with or without fibronectin followed by transfection with siRNA against LacZ or mFmn2 and a reporter focal adhesion plasmid, paxillin - EGFP (obtained from Rick Horwitz, University of Virginia; Addgene plasmid #15233). After 24 hrs of siRNA treatment, the cells were fixed and stained with phosphor-FAK (Y 397) antibody to visualise stable focal adhesions. To analyse this data, the fluorescent channel of paxillin EGFP was processed through focal adhesion analysis server (FAAS) (Berginski and Gomez 2013) from which a mask encircling the labelled focal adhesions was obtained. This mask was added onto the pFAK (Y 397) channel of the same image and the underlying intensities were measured (Fig. 4.7).

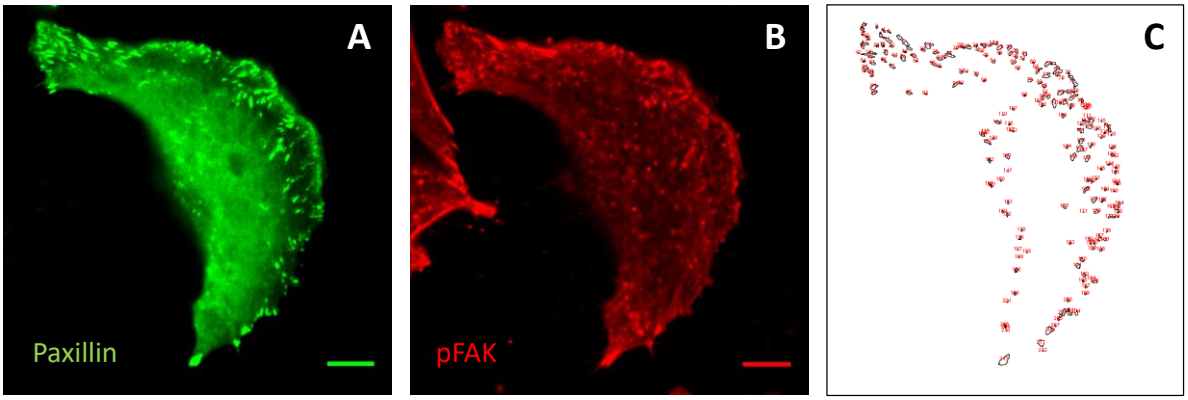

Figure 4.7: Flow of analysis of pFAK (Y 397) stained images. (A) Paxillin overexpression channel was used to generate mask through focal adhesion analysis server (FAAS) (Berginski and Gomez 2013). (B) pFAK immunolabelled channel onto which mask obtained added to measure intensities of specific focal adhesion signal. (C) Mask generated by FAAS server from paxillin channel.

When cells were plated on glass without fibronectin coating, knockdown of mFmn2 did not affect the stable focal adhesions as observed from the unaltered levels of pFAK (Y 397) in these cells (Fig. 4.8).

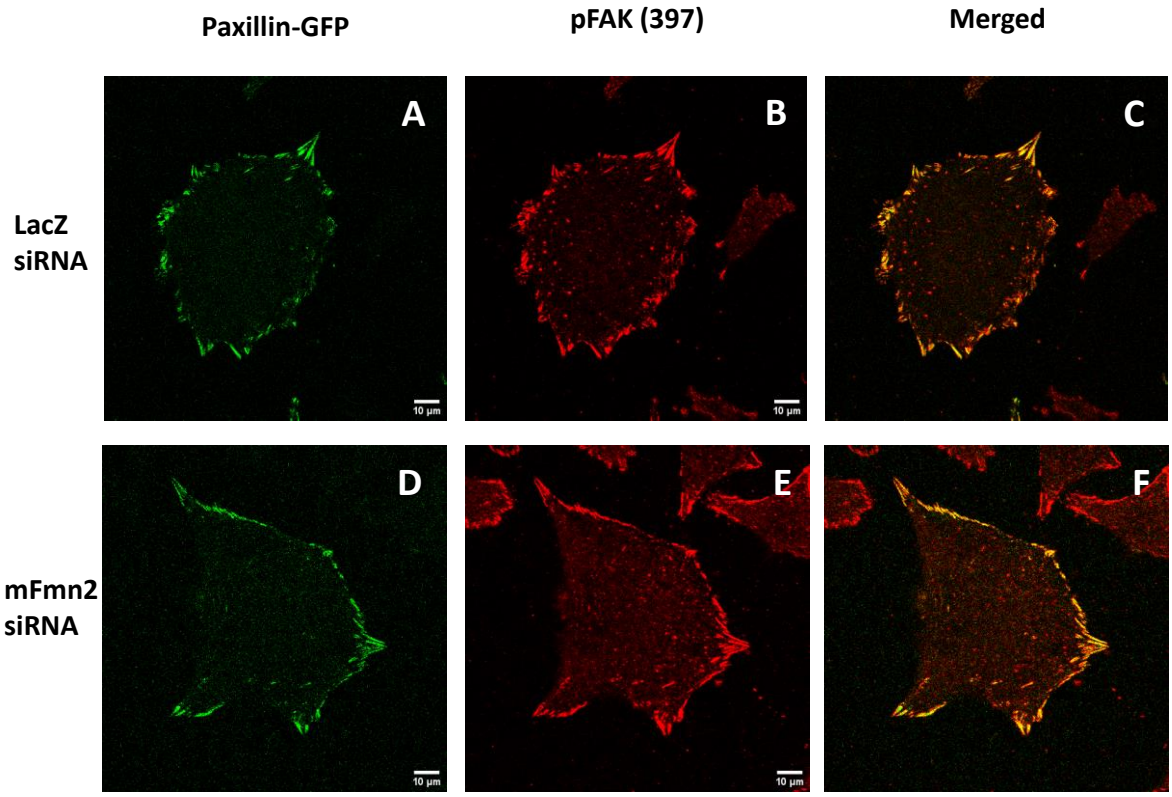

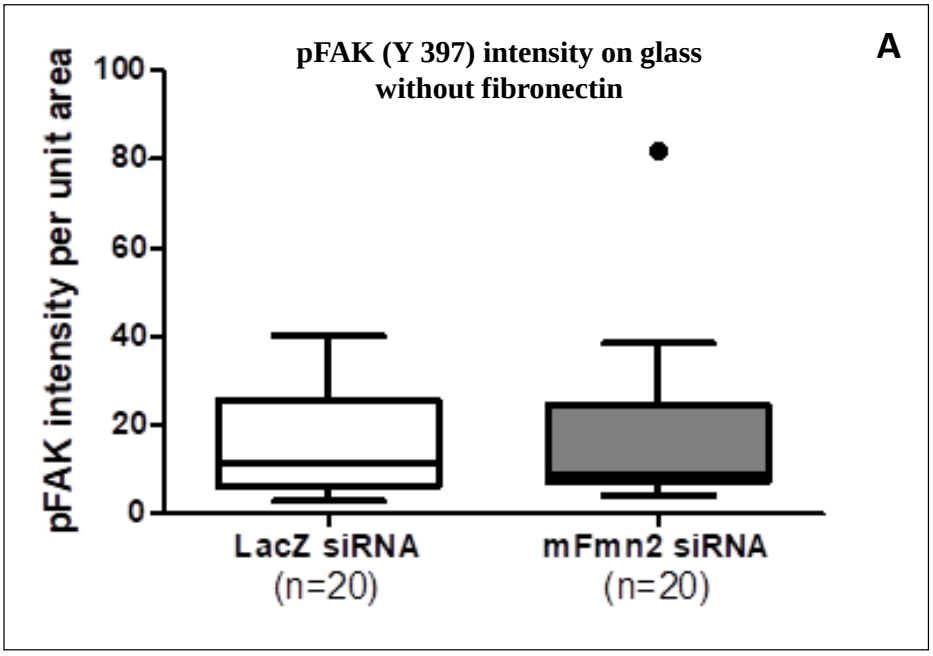

Figure 4.8: Fmn2 is dispensable for focal adhesion stability in fibroblast cultured on glass. Representative images fibroblasts showing of (A) Paxillin GFP along with control siRNA, (B) pFAK staining and (C) merged. Representative images of (D) paxillin GFP with siRNA

against mFmn2, (E) pFAK staining and (F) merged. (G) Quantitation of pFAK intensity does not show any change upon loss of mFmn2 (Scale bar = 10 µm) (N = 3; n = 20).

This experiment suggested that mFmn2 might not be stabilizing focal adhesions on non ECM substrates that lack integrin-mediated signalling.

However, coating the glass with ECM substrate, fibronectin significantly reduced the population of stable focal adhesions labelled by pFAK (Y 397) upon loss of mFmn2 (Fig. 4.9). These results are consistent with our observation of stable point contacts in growth cones as mentioned earlier, further supporting the role of Fmn2 in stabilizing the focal adhesions on ECM substrates.

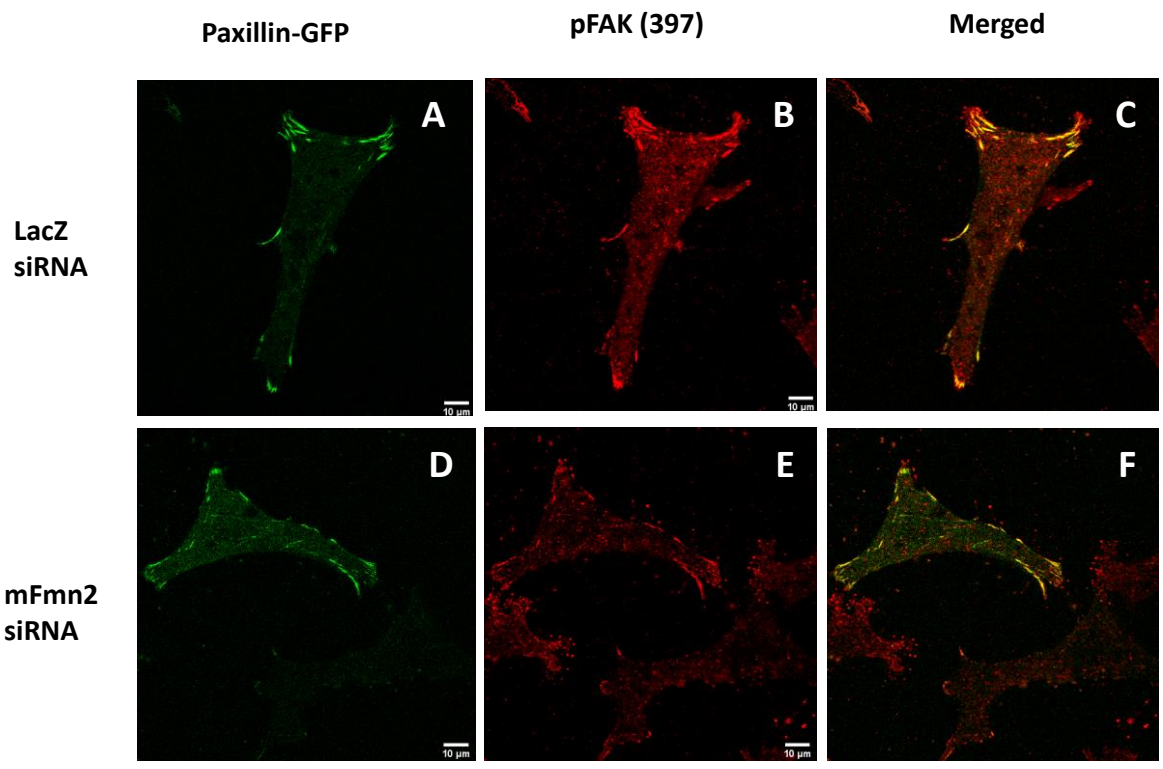

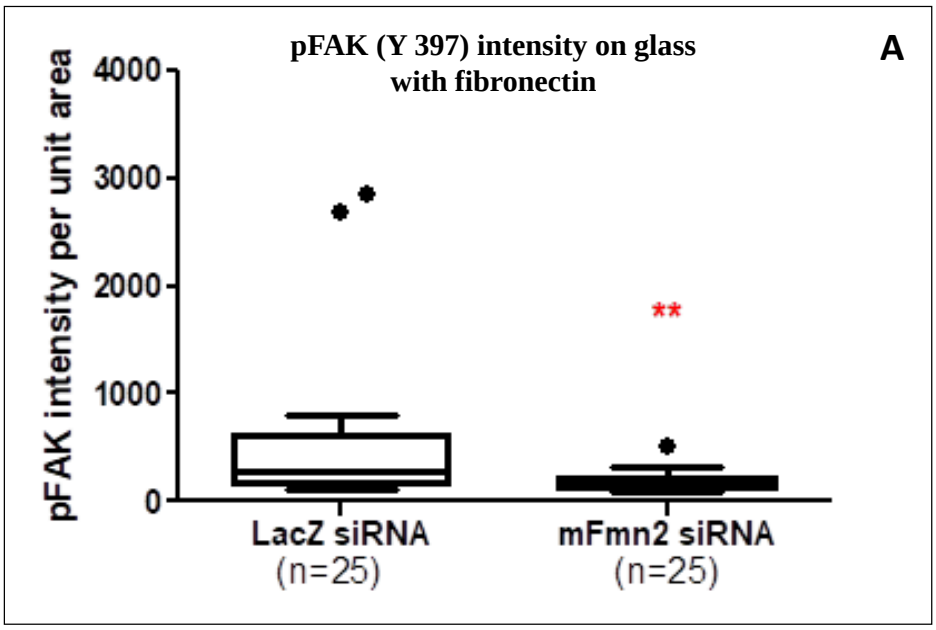

Figure 4.9: Fmn2 regulates focal adhesion stability in cells cultured on the ECM substrate. Representative images of fibroblasts showing (A) Paxillin GFP along with control siRNA (B) pFAK staining and (C) merged. Representative images of (D) paxillin GFP with siRNA against mFmn2, (E) pFAK staining and (F) merged. (G) Quantitation of pFAK intensity shows reduction upon loss of mFmn2 (Scale bar = 10 μm) (**P ≤ 0.01) (N = 3; n = 25).

4.2.3 mFmn2 stabilizes leading edge dynamics during cell spreading and aids in uniform cell spreading

As demonstrated in an earlier chapter, in neurons Fmn2 indicated a role in modulating actin cytoskeleton as well as growth cone point contacts. In fibroblasts, mFmn2 regulates the stability of focal adhesions on ECM substrates and additionally as reported by our group earlier depletion of mFmn2 results in defected assembly of stress fibres in mouse fibroblasts along with smaller and rapidly disassembling focal adhesions (Sahasrabudhe et al., 2016).

In order to understand the importance of mFmn2 in events where actin cytoskeleton is rapidly remodelled at the leading edge along with ECM substrate attachments in form of nascent adhesions, we performed cell spreading assay in NIH3T3.

The cells were initially plated on glass and transfected with both siRNA and lifeact reporter plasmid. After 24 hrs of knockdown, the cells were trypsinized and suspended in Ringer's buffer for 30 min. Following this, the cells were replated on fibronectin-coated glass and the cell spreading was followed for around 90 min at 10 sec time interval (Fig. 4.10).

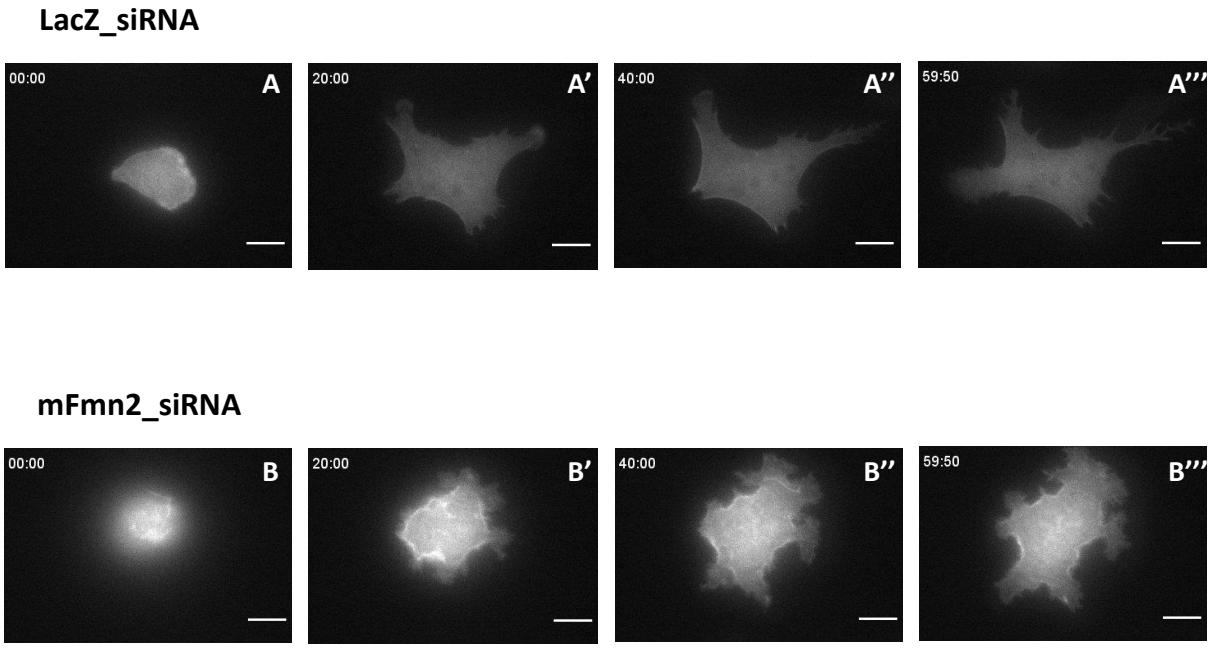

Figure 4.10: Representative images for cell spreading assay. (A-A''') Control siRNA and lifeact mCherry treated cell spreading quickly and more or less uniformly. (B – B''') Cells with siRNA against mFmn2 and lifeact mCherry eventually catch up with control cells in the area, however, they exhibit much more membrane dynamics.

To analyse the overall activity of the leading edge during cell spreading, an automated CellGeo shape analysis platform (Tsygankov et al., 2014) which revealed an overall increase in the retraction activity in mFmn2 knockdown fibroblasts (Fig. 4.11).

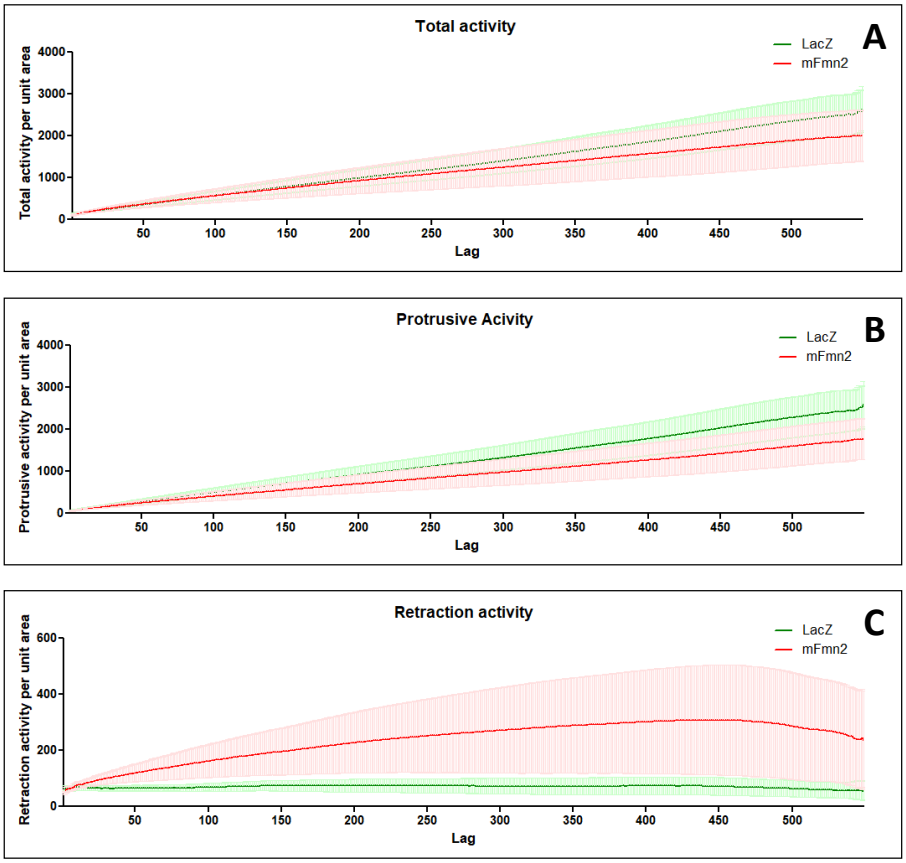

Figure 4.11: Loss of Fmn2 alters leading edge activity during cell spreading. Quantification of overall membrane activity done using the CellGeo shape analysis platform (Tsygankov et al.,, 2014). (A) Overall membrane activity during the cell spread. (B) Only protrusive activity and (C) only retraction activity during the ell spread assay shows more retraction activity in mFmn2 deficient cells (n = 15).

It was also observed that in spite of an increase in the overall retraction activity, the mFmn2 depleted cells eventually exhibit comparable cell area as the control cells (Fig. 4.12).

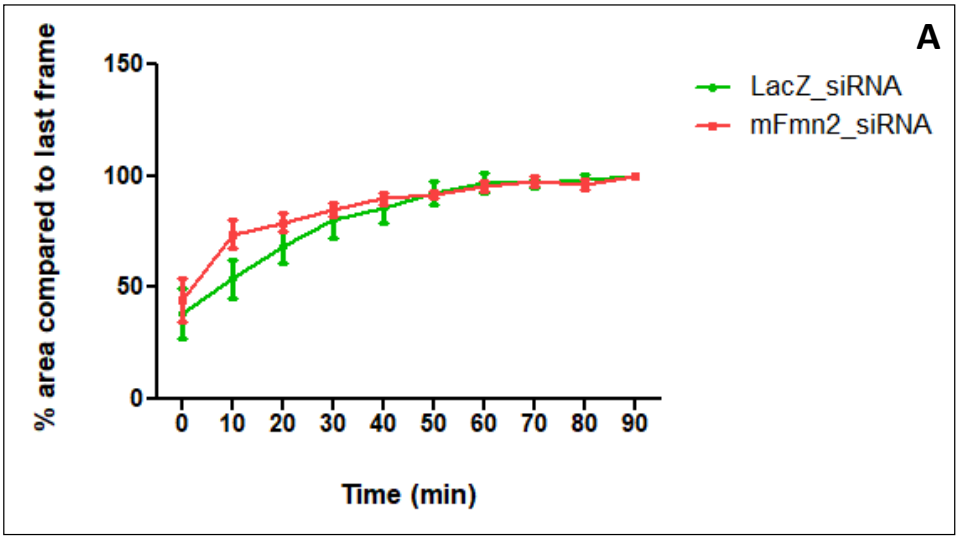

Figure 4.12: Despite affected leading edge dynamics, Fmn2 depletion does not affect cell spread area. (A) Cell area was manually calculated and plotted as a percentage of area compared to the last frame. Even though cells exhibit initial fluctuations in the area, eventually the cells attain a similar area as the control cells (n = 15).

However, to understand the leading edge dynamics more in detail in terms of protrusion or retraction events, we further manually analysed the cells using Fiji. Random lines were drawn from the cell centre to cell periphery in 4 – 5 directions on each cell and kymographs were generated which revealed the leading edge activity across the entire assay (Fig. 4.13). The membrane protrusion and retraction events were counted manually and the velocity was calculated by their slope. These results demonstrated elevated events of membrane activity in mFmn2 depleted cells (Fig. 4.14 A, C) as well as the increased velocity of protrusive events (Fig. 4.14 B).

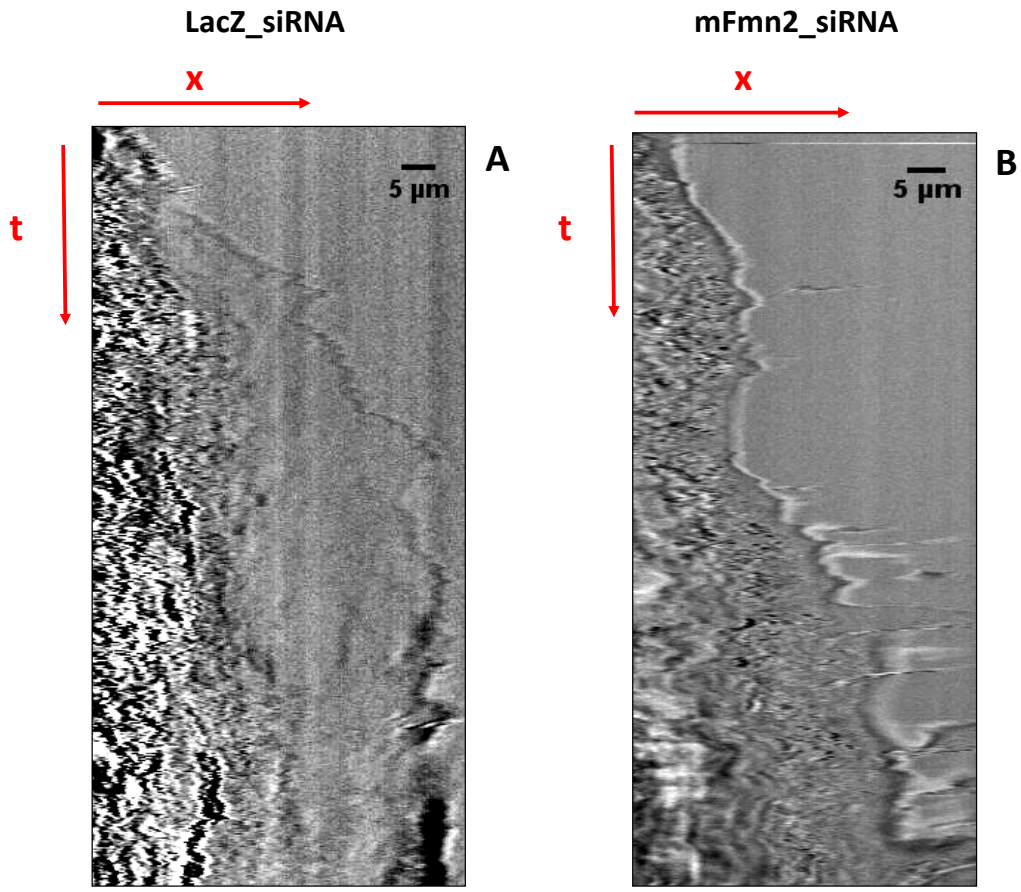

Figure 4.13: Fmn2 stabilizes leading edge dynamics during cell spreading. Representative graphs of (A) control cell spreading and (B) cell deficient in mFmn2. mFmn2 depleted cells exhibit more leading edge dynamics as compared to control.

As observed by these experiments, even though the overall membrane change during spreading does not affect the final cell spread area, mFmn2 knockdown significantly affects the dynamics at the leading edge. The observation suggests an increase in instability at the leading edge which could arise from weakly formed nascent focal contacts.

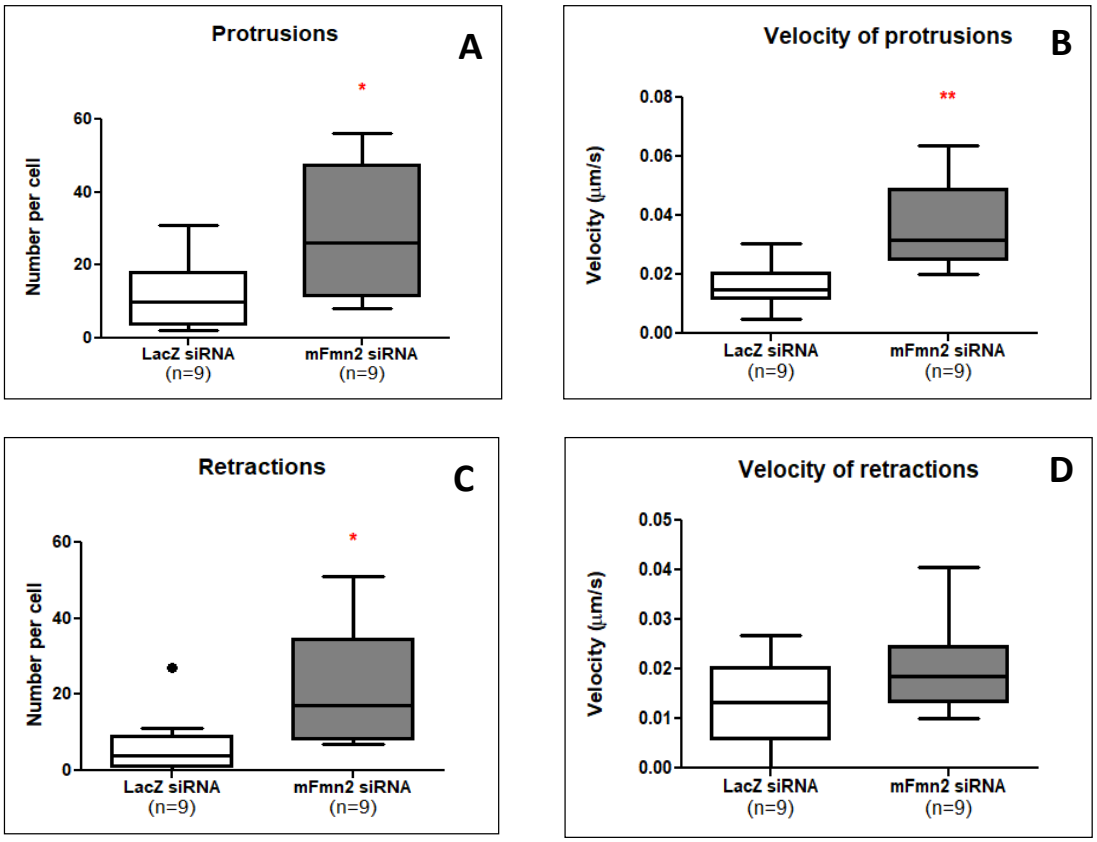

Figure 4.14: Loss of fmn2 regulates membrane activity in spreading fibroblasts. (A) and (C) showed number of protrusions and retractions noted and (B) and (D) show their velocity (n = 10) (*P ≤ 0.05, **P ≤ 0.01).

This assay further indicates the role of mFmn2 in regulating leading edge stabilization during cell spreading. The defects observed could be due to compromised focal adhesion formation and defective actin structures together resulting in poor ECM recognition. Taken together, the studies from NIH3T3 further highlight the role of Fmn2 in actin and focal adhesion interaction.

4.3 Discussion

Our studies from neuronal growth cones identified Fmn2 as a novel regulator of growth cone motility by behaving as a molecular clutch. Fmn2 regulates persistent motility in neuronal growth cones by controlling actin retrograde flow along with modulating growth cone point contact dynamics and regulating resultant traction forces. However, due to the dynamics of growth cones and point contacts, it was challenging to understand the precise localization of Fmn2 which allows it to function as a molecular clutch. In order to gain more insight into Fmn2 localization and function, we chose to study cultured mouse fibroblasts.

Cell motility in fibroblasts is also achieved by the orchestration of cellular cytoskeleton and attachment to the substrate via integrin based contacts. For efficient interaction among these two different aspects, repertoires of proteins work together. Various actin structures impart structural support and cell polarity during cell migration in response to substrate derived cues making it essential to understand the regulation of their interaction. Formins have been implied in generation and maintenance of various actin structures in the cultured cells such as mDia functions in stress fibre assembly (Hotulainen and Lappalainen 2006) and filopodia development (Svitkina et al., 2003; Faix and Rottner 2006; Gupton and Gertler 2007). FHOD1 regulated the formation of stress fibres by differentially regulating precursors namely, dorsal stress fibres and transverse arcs (Schulz et al., 2014). Role of FHOD has also been explored in cell migration by regulating adhesion maturation (Iskratsch et al., 2013). Formins FMNL2 and FMNL3 have been identified to function for lamellipodial force generation during cell migration (Kage et al., 2017). Work from our lab has provided us with insights about the involvement of mFmn2 in stress fibre maintenance and regulation of focal adhesion dynamics (Sahasrabudhe et al., 2016).

The current study identifies less explored actin nucleator mFmn2 as a promising candidate which can regulate actin cytoskeleton and focal adhesion dynamics underlying cell motility. Heterogeneous localization of mFmn2 along ventral stress fibres, especially around the nuclear region of fibroblasts, indicate a possible role of mFmn2 in nuclear compaction and maintenance of stress fibres that generate contractile forces, this is further confirmed by FRAP studies performed on stress fibres (Sahasrabudhe et al., 2016). Study of myosin II dependent focal adhesion maturation has previously identified Fmn2 in biochemical proteome analysis predicting its role in focal adhesion dynamics (Kuo et al., 2011). Localization of mFmn2 juxtaposed to focal adhesions at the end of ventral stress fibres, as

shown in this study, is indicative of its possible role in force dependent adhesion stabilization which was further confirmed by the altered pFAK levels upon mFmn2 knockdown. FAK is an important protein in the focal adhesion complex and self-phosphorylation of it, especially at Y397 residue is thought to be an indicator of tension based maturation of the focal adhesion complex (Oakes et al., 2012). Findings of this study indicate that mFmn2 is necessary for tension dependent focal adhesion maturation especially on ECM substrates such as fibronectin. Importance of mFmn2 in adhesion turnover, especially in disassembly of focal adhesions is already demonstrated by our lab further emphasizing this function (Sahasrabudhe et al., 2016).

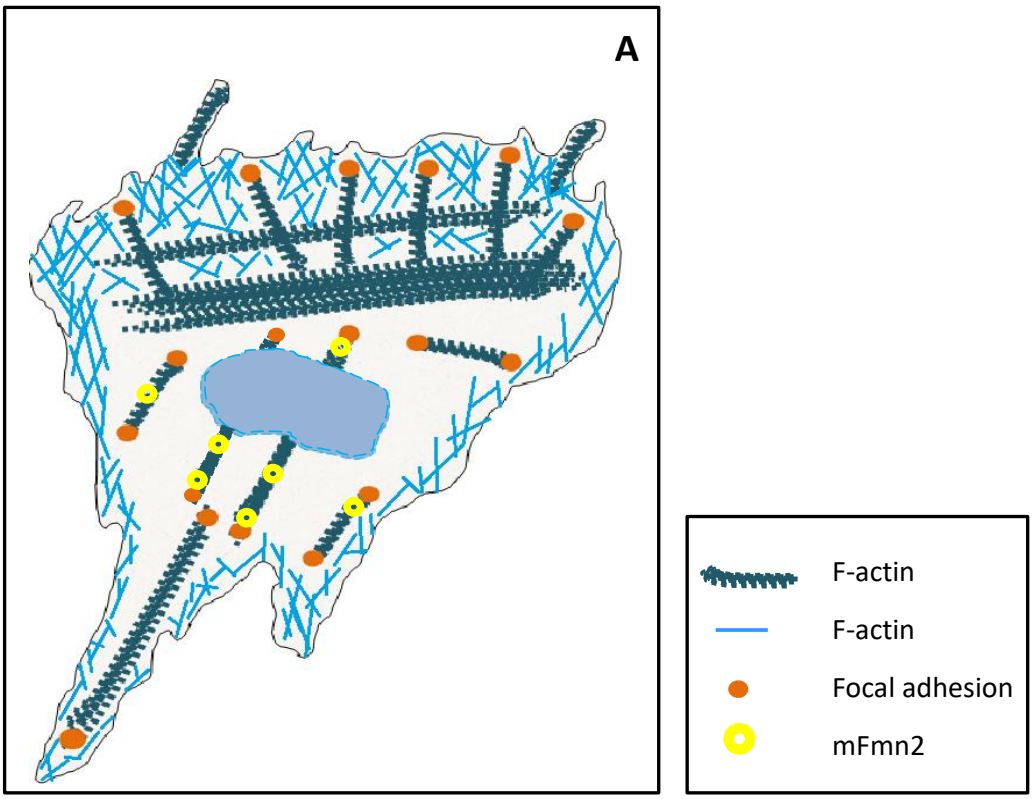

Figure 4.15: Model of fibroblasts showing mFmn2 localization. (A) Schematic depicting cytoskeletal organization in NIH3T3. As per our observations, mFmn2 is present along the contractile ventral stress fibres, juxtaposed to the focal adhesions which are present on either ends of the stress fibres.

In order to understand the role of Fmn2 in regulating both actin remodelling and focal adhesion dynamics simultaneously, this study explores the role of mFmn2 in early cell

spreading. Observations in this study reveal that mFmn2 is necessary to stabilize leading edge dynamic necessary during spreading and even though the loss of mFmn2 increases membrane instability during spreading, the cell area catches up as compared to the control cells as the spreading progresses. Instability of the leading edge could be attributed to unstable focal adhesions as also suggested by earlier observation where mFmn2 depletion affects pFAK (Y 397) immunostaining. A plausible way this might be achieved is by sensing the substrate and relaying the signals to remodel the dynamic actin underlying leading edge. A possible role of Fmn2 in sensing ECM and generation of cellular responses can be deduced not only from the cell spreading assay but also from the observation that Fmn2 stabilizes focal adhesions on ECM substrates and not otherwise (result 4.2.2).

Taken together, the studies from neurons and fibroblasts indicate the role of Fmn2 in the regulation of actin cytoskeleton and stabilization focal contacts that in turn regulate cellular translocation.

4.4 Methods and materials

4.4.1 NIH3T3 culture

NIH3T3 mouse embryo fibroblast cell line was procured from Dr. N. Balasubramanian (IISER, Pune) and checked for contamination prior to use. Cells around passage no. 25 to 40 were used for experiments. Cells frozen previously in liquid nitrogen were thawed and cultured in complete DMEM (Lonza) with 1X PenStrep (Gibco), 1X sodium pyruvate (Invitrogen) and 10% heat-inactivated FBS at 37^{o}C with 5% CO_2. After the cells were 80-90% confluent, the media was removed and cells were washed with DPBS without Ca^{2+} and Mg^{2+} (Lonza), thereafter 1-2 ml of 1X trypsin-EDTA was added (Lonza). Cells with trypsin were incubated at 37^{o}C for 3-5 min. 4 ml DMEM was added to trypsin and cells were collected in a 15 ml falcon and then centrifuged at 100xg for 3 min. After aspirating the trypsin with DMEM the cell pellet was resuspended in 1 ml complete DMEM. Cells were seeded in 10 ml complete DMEM with approximately $3*10^5$ density.

4.4.2 Transfection

NIH3T3 were seeded with approx. $2*10^4$ density on glass bottom chambers (Labtek) directly or upon 20µg/ml fibronectin (Sigma) in PBS for 1 hour at 37^{o}C. The cells were allowed to adhere for 14-16 hrs and further transfected using Lipofectamine 2000 (Invitrogen). After cells were about 60-70% confluent, the cell culture media was replaced by OptiMEM (Gibco) and cells were incubated at 37^{o}C for 20 min. Parallely the transfection mix was prepared with OptiMEM, 1-5ug plasmid DNA, 3-5µl lipofectamine and control LacZ siRNA (sense strand: CGUCGACGGAAUACUUCGAUU) or mFmn2 siRNA (sense strand: UGGUUAGACUUGUGGGUAAUU) and incubated in the hood at room temperature for 20 min. Subsequently, the transfection mix was added onto the cells and they are incubated for 4 hours at 37^{o}C after which the media was supplemented by complete DMEM and 30% FBS.

The original clone of full-length mFmn2 was obtained from Prof. Philip Leder, Harvard Medical School. Actin-mRFP was a generous gift from obtained from Bidisha Sinha, IISER Kolkata. The paxillin-mCherry construct was obtained from Martin Schwartz, Yale University.

4.4.3 Total RNA extraction and cDNA preparation

RNA extraction

Cultured NIH3T3 were utilised to study the mFmn2 enrichment baseline. After initial primer standardization, the cells were transfected with LacZ or mFmn2 siRNA (as described above) and after 24 and 48 hrs of knockdown, the cells were utilised to extract RNA. Cells were scraped and macerated in 1ml Trizol (Ambion) and 200µl chloroform followed by vigorous vortexing the mixture for 15 seconds and incubating for 2-3 min at room temperature. The tubes were centrifuged at 12,000 xg for 10 min at 4^{o}C in a fixed angle centrifuge. The aqueous phase was collected in fresh sterile, RNase free Eppendorf and the total RNA was precipitated by adding equal volumes of Isopropanol to the tube. This mixture was incubated at room temperature for 30 min followed by centrifugation under the conditions mentioned above. After precipitating the RNA, Isopropanol was removed and the pellet was washed with 70% ethanol followed by spinning at 7500 xg for 5 min at 4^{o}C. The RNA pellet was dried at room temperature after removing the ethanol and resuspended in nuclease-free water (Ambion). RQ1 DNase (Promega) was added to the total RNA and incubated at 37^{o}C for 30 – 40 min. Quality check for purity of RNA was performed by checking the RNA on 2% agarose gel and RNA without DNA contamination was precipitated using Isopropanol followed by 70% ethanol wash. Purified RNA was resuspended in nuclease-free water (Ambion) and stored at -40^{o}C.

cDNA preparation

1µg of total RNA extracted from the tissue was used as a template for *in vitro* reverse transcription. Following reaction mixture set was used for total cDNA preparation:

RNase inhibitor (Roche) - 0.5 µl

MMLV reverse transcriptase (Promega) - 1 µl

5X MMLVRT buffer (Promega) - 5 µl

OligodT (IDT) - 1 µl

dNTPs (Sigma) (2.5mM each) - 5 µl

After adding a calculated volume of 1µg RNA the reaction volume was made up to 25µl using nuclease-free water (Ambion). This entire reaction mixture without RNase inhibitor

and reverse transcriptase were then denatured at 60^{o}C for 5 min to get rid of the secondary structures of RNA, followed by snap chilling on ice. At this point, the enzyme and inhibitor were added and the mixture was incubated at 40^{o}C for 2-3 hrs. The cDNA was stored afterward at -40^{o}C until further use.

4.4.4 Quantitative real-time PCR

The cDNA synthesized from total RNA using OligodT was utilised to perform quantitative real-time PCR. Two-fold serial dilutions of cDNA from 1:2 to 1:32 were used for standardizing primer pairs. The final analysis was one using 1:8 dilution of cDNA for all primers. SYBR green (KAPA Biosystems) enzyme mastermix was used to set up the PCR along with following primer pairs.

For housekeeping gene against which the relative abundance was calculated, GAPDH (Forward: GCCTTCCGTGTTCCTACC; Reverse: CCTCAGTGTAGCCCAAGATG) were used. For mFmn2 following primers were used (Forward: TCCTCTATTTTGGAAAGCCCG; Reverse: TTTGTGCGTAGATCCTCGATG)

Each reaction had each dilution in triplicates and each sample had three technical replicates Every experiment was repeated three times. The pooled data were used for statistical analysis and graphical representations. The mFmn2 Ct values were normalised to GAPDH.

4.4.5 Immunocytochemistry

NIH3T3 cells were cultured overnight (as mentioned above) and fixed using 4% PFA (Electron microscopy sciences) and 0.05% glutaraldehyde (Electron microscopy sciences) in PBS for 10 min. After removing PBS, cells were washed with PBS 3 times for 10 min each. The cells were permeabilized using 0.1% Triton-X in PBS for 30 min. After permeabilization, 2 brief PBS washes were given and the cells were blocked in 3% BSA for 60 min. The blocking solution was replaced by an antibody against phosphor-FAK (Y 397) (Abcam) in 1:1000 dilution in 3% BSA and incubated at 4^{o}C for 14-16 hrs. Subsequently, after removing primary antibody, the cells were washed 4 times with PBS+0.1% TritonX, 10 times each. Later the sample was incubated at room temperature for 60 min in secondary antibody (Invitrogen) diluted 1:1000 in 3% PBS. After removing the secondary antibody, the cells

were washed again in PBST 4 times, 10 min each. Further, the cells were labelled with phalloidin (Invitrogen) diluted 1:200 in blocking for 30-45 min at room temperature. Lastly, the cells were washed thrice in PBST, 10 min each and mounted in 80% glycerol.

4.4.6 Cell spreading assay

NIH3T3 cells were transfected with LacZ or mFmn2 siRNA and lifeact-mCherry. After 24 hrs of knockdown, these cells were trypsinized as mentioned above and resuspended in 1X Ringers solution (150 mM NaCl, 5 mM KCl, 1 mM $CaCl_2$, 1 mM $MgCl_2$, 20 mM HEPES, 2 g/l D-glucose, pH 7.4) and incubated at 37^{o}C for 30 min. After incubation, the cells were plated on fibronectin (20µg/ml) (Invitrogen) coated coverslip bottom chambers (Labtek) and immediately imaged for cell spreading.

4.4.7 Imaging

For mFmn2 overexpression imaging, a PlanApo 60x/1.4 oil immersion objective was used on an Olympus IX81 system with Hamamatsu ORCA-R2 CCD camera (ventral stress fibre and mFmn2). For imaging focal adhesion marker along with mFmn2 overexpression, a PlanApo 63x/1.40 oil immersion objective was used on Zeiss LSM 800 with Airyscan system.

For immunocytochemistry imaging of pFAK PlanApo 63x/1.40 oil immersion objective was used on Zeiss 710 inverted microscope.

Imaging of cell spreading assay was performed a PlanApo 60x/1.4 oil immersion objective on an Olympus IX81 system with Hamamatsu ORCA-R2 CCD camera. Cells were imaged for about 90 min with 10 sec interval in DIC or in fluorescence.

4.4.8 Analysis

For colocalization analysis, a line was drawn on selected region in Fiji and mean grey values were obtained which were plotted in GraphPad Prism 5.

For real-time PCR quantification, deltaCt values were calculated by subtracting Ct values of GAPDH from Ct values of mFmn2. Relative abundance was calculated using formula $2^{-\Delta\Delta Ct}$.

For analysing pFAK labelled cells, the paxillin expression images were uploaded on Focal adhesion analysis server (FAAS) (Berginski and Gomez, 2013) to get masks based on focal adhesions marked by paxillin. This mask was further added to the imaged pFAK channel to

measure intensities only at the demarcated focal adhesions. The intensity per unit area was plotted and analysed in GraphPad Prism 5.

The analysis of leading edge dynamics was performed manually on DIC images every 10 min. Lines were drawn in Fiji to obtain kymographs of the leading edge and the number of protrusion or retraction events were counted manually. Analysis of cell spreading assay with cells transfected with Lifeact-mCherry was done with a Matlab code CellGeo (Tsygankov et al., 2014). The values were exported, plotted and analysed in GraphPad Prism 5.

4.4.9 Data representation and statistics

Real-time data were plotted as bar graphs in Microsoft Excel 2007, the error bars represent SEM calculated across replicates. The line graph for mean grey values was plotted in GraphPad Prism where the intensity values were imported from Fiji. Box and Whisker plots represent the spread of the data with the Tukey method. Outliers are represented outside the box as individual data points. All Box and Whisker plots were compared using the Mann-Whitney test. Statistical analysis was done in GraphPad Prism 5.

5. Future directions

During development, specialized cells of the nervous system, neurons need to make accurate connections with their targets so that the neuronal circuits function properly in adult organisms. An important aspect of this process is precise guidance of neurons to their targets which is guided by a distally present dynamic structure of the neuronal cell known as the growth cone. The growth cone is known to be guided by a combination of several surface bound and chemically diffusible cues. These cues are known to interact with specific receptors on the growth cone causing changes in the growth cone cytoskeleton which impart the directional motility of the neuron. In this study we investigated the function of an actin nucleator, Formin-2 (Fmn2) pertaining growth cone motility and we found that loss of Fmn2 reduces the stability of growth cone point contacts possibly due to the failure of efficient clutch engagement consequently reducing the traction generated by neurons in turn leading to reduced translocation rates.

5.1 Investigating effect of gFmn2 knockdown on the dynamics of point contacts

As described previously, directional neuronal motility is a basic yet complex aspect of neuronal circuit formation which combines not only the remodelling of growth cone cytoskeleton and substrate adhesion events to achieve proper guidance but also incorporates temporally expressed guidance cues upstream to these morphological changes. Our group has

previously described *in vivo* trajectory defects in commissural neurons upon Fmn2 depletion (Sahasrabudhe et al., 2016) which could be the result of a combination of motility defects and affected guidance sensing of the neurons.

In the current thesis, we have shown the role of Fmn2 in modulating growth cone motility by regulating the molecular clutch. Fmn2 regulates point contact assembly and stability while also controlling actin dynamics underlying the directional motility of neuron. We have also demonstrated that Fmn2 is responsible for the generation of traction forces by growth cones that aid in successful neuronal movement.

Even though several markers that we tested point to a general role of Fmn2 in assembly and regulation of point contacts, it would be interesting to investigate which phase of the assembly, stabilization or disassembly of point contacts is affected upon Fmn2 knockdown.

As reported previously by our group, knockdown of Fmn2 in mouse fibroblasts increases disassembly rates of focal adhesions suggesting unstable substrate attachments in these cells, however, similar studies have not been performed in neuronal growth cones.

This dynamics of point contacts can be addressed by dynamic imaging of expressing tagged point contact proteins such as paxillin or vinculin along with morpholinos in neuronal growth cones. However, these experiments should be done with the minimum amount of tagged proteins to avoid artefacts arising due to overexpression. To assess this, the point contact dynamics could be also studied by expressing photoactivatable constructs of these proteins along with the morpholino. Photoactivatable constructs will allow us activation of the point contact proteins in different regions of growth cones allowing us to study differences in their dynamics which could be specific to the growth cone region. This could further explain their role in the regulation of neuronal translocation.

To assess dynamics of point contacts we transfected spinal neurons with pCAG-paxillin mCherry and we tracked them using total internal reflection microscopy (TIRF). This allows us to visualize the population of point contacts that is adhered to the culture plates (Fig. 5.1).

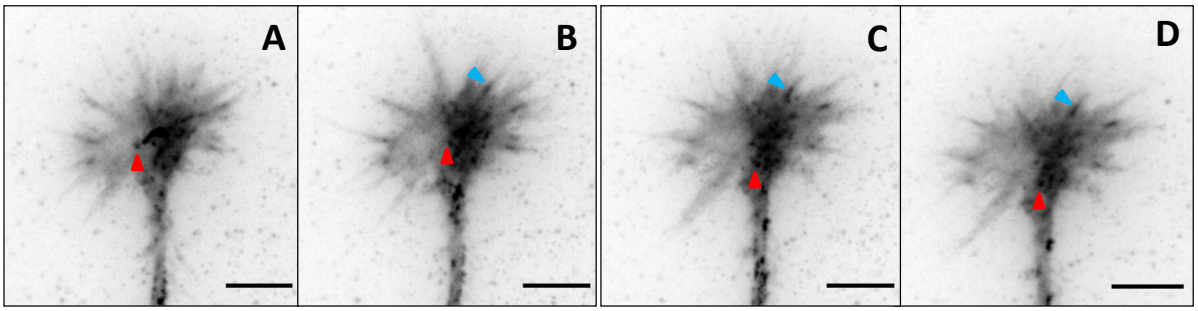

Figure 5.1: Paxillin expression in spinal neurons. pCAG-paxillin mCherry imaged in TIRF showed punctate expression similar to immunostaining observed (Chapter 3). Paxillin dynamically labels growth cone point contacts (A-D). The red arrowhead points to paxillin labelled puncta at the central region of the growth cone and blue arrowhead shows paxillin expression at the base of filopodia (Scale bar = 5 µm).

5.2. Exploring motility defects downstream of guidance cue

Several studies have shown regulation of point contacts downstream of a number of guidance cues such as BDNF, netrin, ephrins (Woo et al., 2009; Myers and Gomez, 2011; Moore et al., 2012). Our study indicates compromised point contacts upon Fmn2 depletion, however, the possible role of upstream chemoattractants still remain to be explored. An interesting study would be to observe the role of Fmn2 in regulating point contact dynamics and in turn cell motility downstream of a characterized growth factor that is known to have a distinct effect on growth cone morphology.

We have performed preliminary studies which can be further utilized to address the role of chemoattractant on Fmn2 mediated point contact dynamics. To study this we utilised chick dorsal root ganglia (DRG) neurons which are known to respond to nerve growth factor (NGF) induction.

Several studies show that upon treatment with NGF, chick sensory neurons exhibit elevated axonal outgrowth and axonal branching which involves actin cytoskeletal remodelling (Loudon et al., 2006; Ketschek and Gallo, 2010; Spillane et al., 2012). We examined the role of Fmn2 in regulating growth cone morphology of cultured chick sensory neurons upon NGF

induction. Cultured chick dorsal root ganglia (DRG) neurons were electroporated with morpholino control or against gFmn2 along with reporter pCAG-GFP plasmid for 24 hrs after which they were treated with 50 ng/ml NGF for every 15 min interval up to 1 hr. These neurons were fixed using paraformaldehyde and imaged in epifluorescence. Morphological parameters such as growth cone area, growth cone filopodia length along with axonal filopodia length and density were calculated manually using Fiji.

NGF induction shows an increase in growth cone area in control neurons after 45 minutes of treatment whereas in gFmn2 depleted neurons a slight increase in area is observed after 60 minutes of NGF treatment. Increase in filopodial length also seems to appear as a delayed response in neurons lacking gFmn2. Well, known arborisation that occurs along axons upon NGF treatment (Ketschek et al., 2015) was severely affected in gFmn2 depleted neurons, however, the lengths of axonal filopodia calculated were not dramatically different in gFmn2 knockdown neurons (Fig. 5.2).

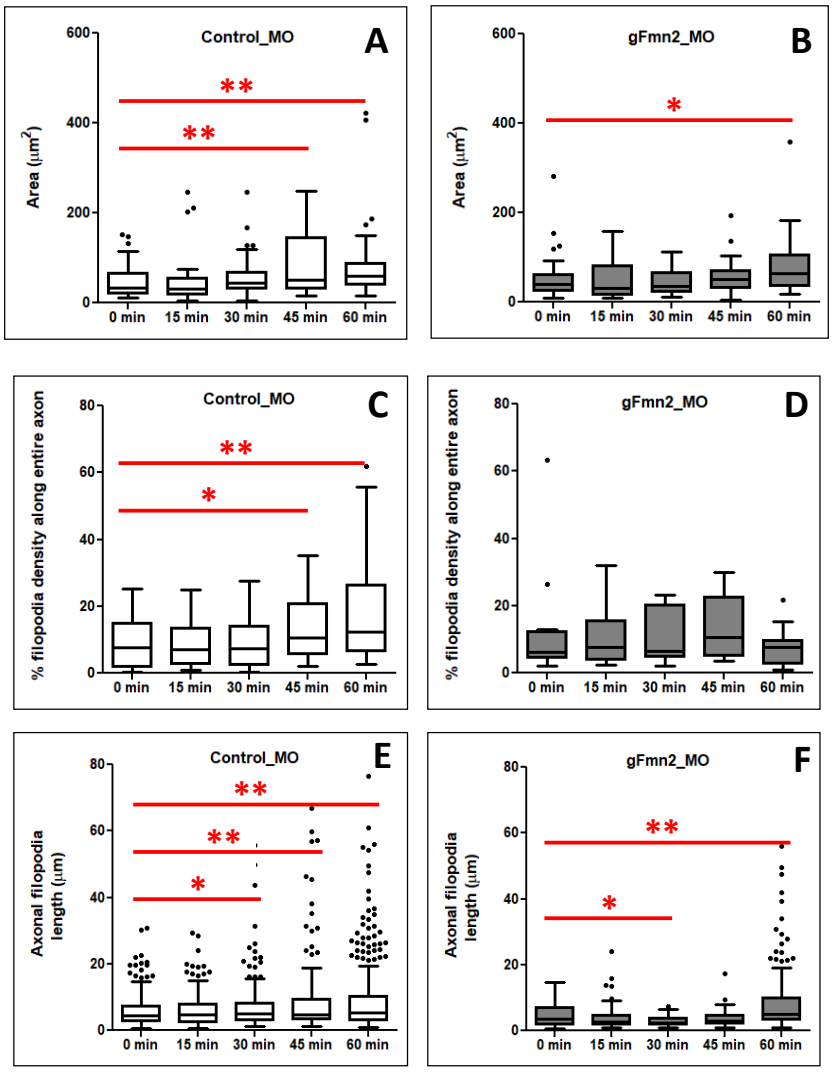

Figure 5.2: gFmn2 affects morphology changes driven by NGF induction in chick DRG neurons. (A) Growth cone area increases in control neurons at 45 min of NGF treatment whereas this response time is delayed in gFmn2 depleted neurons (B). (C) The density of axonal branches emerged along the length of the axon increases upon NGF treatment. (D) Neurons lacking gFmn2 do not show a significant change in arborisation arising along axon upon NGF induction. (E) Axonal filopodia lengths increase as the neurons are exposed to NGF for longer time periods in control growth cones. (F) Loss of gFmn2 does not seem to affect the elongation of the axonal filopodia upon NGF induction (This analysis was done on 20 control neurons and 23 neurons with gFmn2 knockdown imaged over 4 independent experiments) (**P ≤ 0.01, *P ≤ 0.05).

Analysis of these preliminary study shows that lack of Fmn2 in DRG neurons might not be completely unresponsive to growth factor exposure albeit they might exhibit a rather delayed response to the cue as observed by morphological changes across a number of morphology parameters. However, we can utilise this system to investigate whether depletion of Fmn2 actually affects growth cone motility first and then look at point contact dynamics upon NGF induction.

5.3 Exploring the role of Fmn2 interactors in developing spinal cord.

We demonstrate in this study by quantifying the relative transcript levels that spinal cord of stage HH25/HH26 is enriched in Fmn2. As we study the relative transcript levels in developing spinal cord of chick embryo, we also showed that Fmn2 expression is sustained as the spinal cord develops coinciding with the commissural neurons development time window. Strikingly apart from the Fmn2 levels, expression levels of another nucleator from WH2 family of proteins, Spire-2 (Spir2) also shows a similar sustained level of expression in the developing spinal cord (Fig. 5.3).

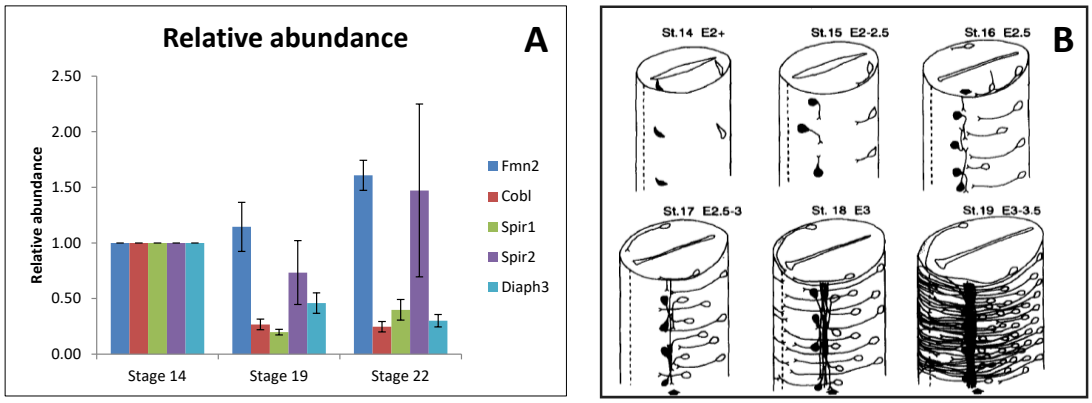

Figure 5.3: Spir2 shows persistent expression in developing chick spinal cord. (A) Represents sustained enrichment of gFmn2 transcript as discussed in chapter 2, along with similar expression pattern of Spir2 transcript (N = 9). (B) Schematic representing the commissural interneuron development time window (Reproduced from Yaginuma et al., 1990).

Previous reports from *Drosophila* embryos and mammalian oocytes indicate a co-operative interaction between Spir2 and Fmn2 (Schumacher et al., 2004; Rosales-Nieves et al., 2006; Pfender et al., 2011; Montaville et al., 2014). As our observations indicate, the similar expression pattern of Fmn2 and Spir2 in chick spinal neurons could also play a co-operative role in remodelling growth cone actin cytoskeleton.

To address this question, Spir2 can be depleted in spinal neurons and the morphological defects can be studied in a similar fashion. If indeed the two proteins are working together to modulate the actin dynamics, a double knockdown of them in neurons can yield us severe morphological defects further confirming the functional interaction between the two proteins.

5.3.1 Knockdown of Spir2 affects commissural trajectories *in vivo*

To understand the role of Spir2 in spinal neurons, we started by employing morpholino-based approach similar to Fmn2 to analyse commissural interneuron trajectories. In these experiments, we delivered the morpholino in the developing spinal cord using *in ovo* injection and electroporation (Fig. 5.4) which allows the morpholino to affect one side of the spinal cord whereas the other half serves as internal control.

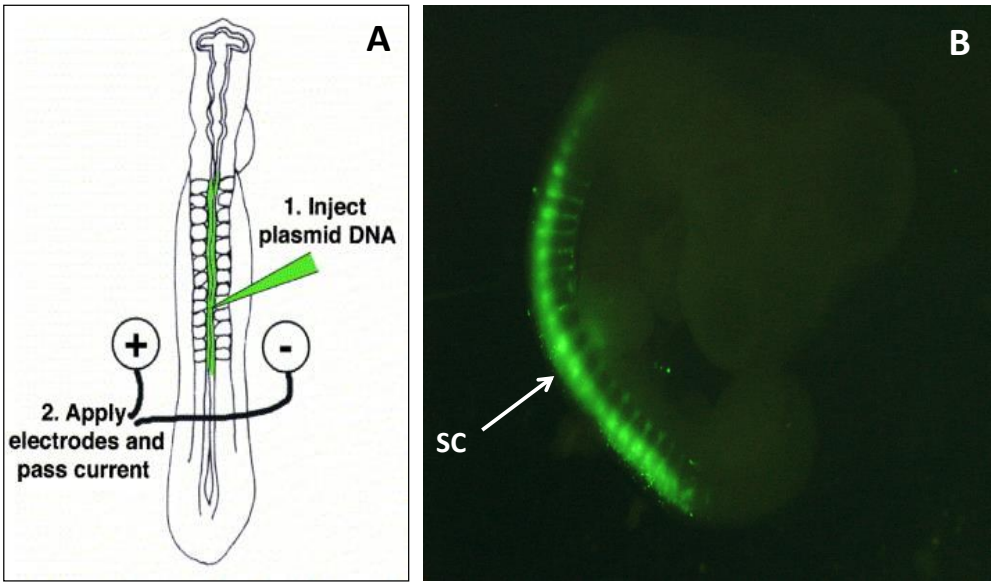

Figure 5.4: *In ovo* electroporation to observe neuronal trajectories. (A) Schematic of the procedure of injection of the plasmid into developing spinal cord (Courtesy Google images). Note the DNA being negatively charged will only be delivered to one half of the spinal cord. (B) Chick embryo of stage HH26 injected with pCAG-GFP in the spinal cord.

These treated spinal cords were later dissected, cryosectioned and immunostained with Axonin-I antibody which labels a cell surface marker expressed in a subpopulation of commissural neurons that move towards the midline (Fitzli et al., 2000). It is speculated that upon reaching the midline, Axonin-I is downregulated on the cells and thus can be used as a marker to examine proper guidance at the midline (Fig. 5.5).

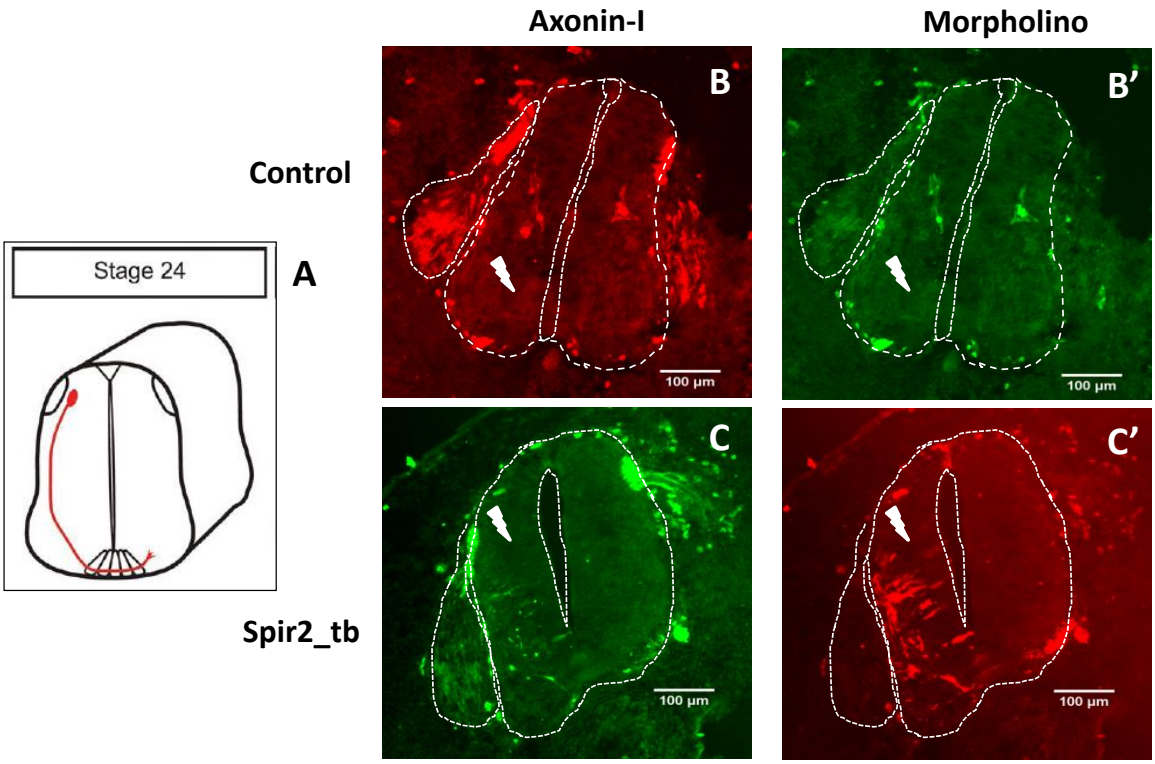

Figure 5.5: Loss of Spir2 impairs commissural trajectories in the chick spinal cord. (A) Schematic of a cross-section of the spinal cord. The labelled interneurons trajectory can be traced by co-labelling withthe appropriate antibody. (B, B') Sections of spinal cord injected with control morpholino and stained with Axonin-I antibody. Note the lack of staining in the sections indicating proper development of commissural neurons. (C, C') Sections of spinal cord injected with morpholino against Spir2 and stained with Axonin-I antibody. The staining is observed in the injected half of spinal cord suggesting disturbed commissural trajectories (N = 2).

As observed in the Spir2 knockdown spinal cord sections, Axonin-I labelling is retained in Spir2 deficient half of the spinal cord indicating defected commissural trajectories. Another approach for observing the trajectories is to dissect the entire spinal cord and mount in like an open book to image complete ipsilateral and contralateral trajectories. To perform this experiment, a promoter specific to commissural neurons Atoh1-tau-mCherry was co-transfected with the morpholinos and the open book preparations of spinal cords were imaged (Fig. 5.6).

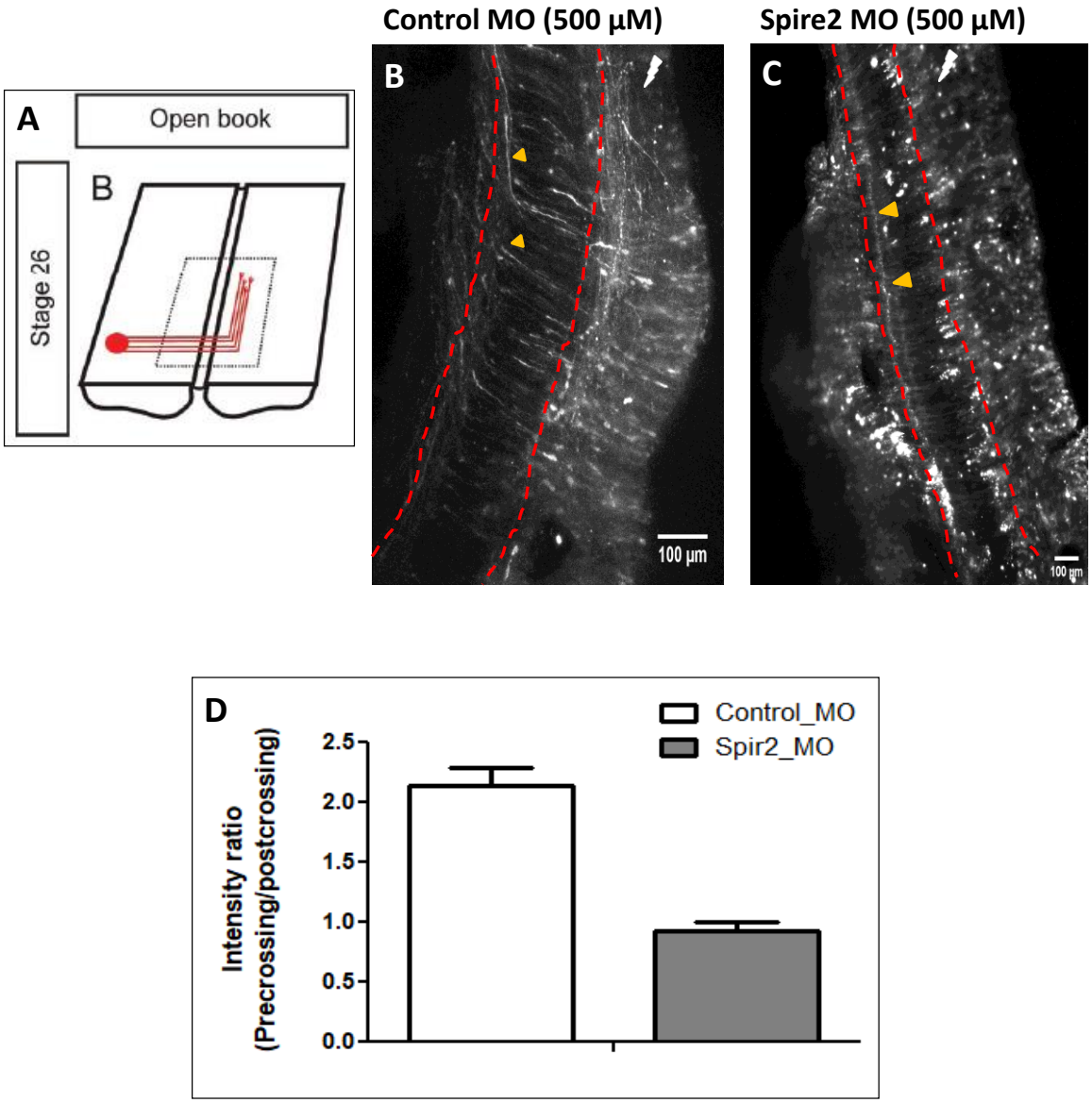

Figure 5.6: Knockdown of Spir2 affects commissural trajectories in the chick spinal cord. (A) Schematic showing visualization of labelled interneurons population upon open book preparation of the spinal cord. (B) Spinal cord with control morpholino and tracks of

commissural neurons. Atoh1 promoter labels the interneuron population ipsilaterally (on the side of injection) as well as contralaterally (opposite side of the injection). (C) Affected trajectories of commissural neurons upon loss of Spir2. Note the aberrant halt of the tracks post crossing the midline (arrowheads) (N = 2). (D) Quantification of intensity estimated by the ratio of pre-crossing and post-crossing regions.

Similar to the ones observed in Fmn2 knockdown (Sahasrabudhe et al., 2016), the open book preparation also shows defective commissural trajectories upon Spir2 knockdown. Even though similar *in vitro* studies and detailed analysis of the *in vivo* phenotype needs to be performed to confirm exact role of Spir2 in neuronal growth cones, this preliminary study indicates a possible role of Spir2 in neuronal motility similar to Fmn2. The co-operative role of these two nucleators could further be tested by a double knockdown study in neuronal cultures as well biochemical approach to pinpoint their role in neuronal motility.

(Materials and methods for this chapter can be found as an appendix at the end of the thesis.)

6. Proposed model of Fmn2 function in neuronal motility.

Cell motility is a complex process that arises due to the remodelling of the cellular cytoskeleton along with interactions with the underlying substrate. During this process, the inherently dynamic actin cytoskeleton is rapidly remodelled to generate forward motion of the leading edge. The underlying extracellular matrix provides a substrate for integrin-based attachments that by anchoring on to the actin filaments in the cell redirect actin dynamics into leading edge protrusion.

In this thesis, we have identified Formin-2 as a key regulator that regulates persistent motility of chick spinal neurons. As our observations indicate, Fmn2 decorates actin structures in chick spinal neurons and is essential for maintenance of growth cone morphology; knockdown of this protein results in smaller growth cones with short filopodia (Fig. 6.1). Fmn2 is essential for maintaining long-lived filopodia by stabilizing tip adhesions suggesting their role in filopodial contractility (Sahasrabudhe et al., 2016).

Depletion of filopodia also affects the persistent motility of cultured neurons and results in loss of directionality. As mentioned earlier, motility is achieved due to the orchestrated interaction between actin remodelling and substrate adhesion. Loss of Fmn2 not only affects growth cone point contacts but also increases actin retrograde flow in the central region of the growth cone indicating weakly formed adhesions (Fig. 6.1). As postulated by the molecular

clutch hypothesis, the mechanical coupling of actin retrograde flow to underlying adhesion substrate via a molecular complex attenuates actin retrograde flow allowing the actin polymerization to take over and exerts rearward traction forces on the substrate resulting in growth cone protrusion (Mitchison and Kirschner, 1988). Our observed phenotypes of Fmn2 depletion support this hypothesis and indicate the role of Fmn2 in modulating neuronal motility as a molecular clutch. This function of Fmn2 is further supported by the observation that traction forces are reduced in neuronal growth cones upon depletion of Fmn2 (Fig. 6.1).

Parallel studies in mouse fibroblasts contributed to our understanding of Fmn2 localization with respect to actin and focal adhesions that might enable it to modulate the molecular clutch. Fmn2 in fibroblasts decorates ventral stress fibres, contractile actin structures which have characteristic focal adhesions present on their either ends. Fmn2 situates itself juxtaposed to these focal adhesions at the end of ventral stress fibres giving it perfect access to modulate the two. Importance of Fmn2 is further emphasized in these cells, similar to neurons by modulating stability of focal adhesions as determined by pFAK (Y 397), a marker of focal adhesion stability. In a dynamic assay such as cell spreading, we determined the role of Fmn2 in sensing the substrate and forming initial adhesions that are necessary for stabilizing the leading edge dynamics. Taken together the studies from neurons and the insights from fibroblast studies we put together a possible model of Fmn2 function underlying growth cone advance (Fig. 6.1).

Model

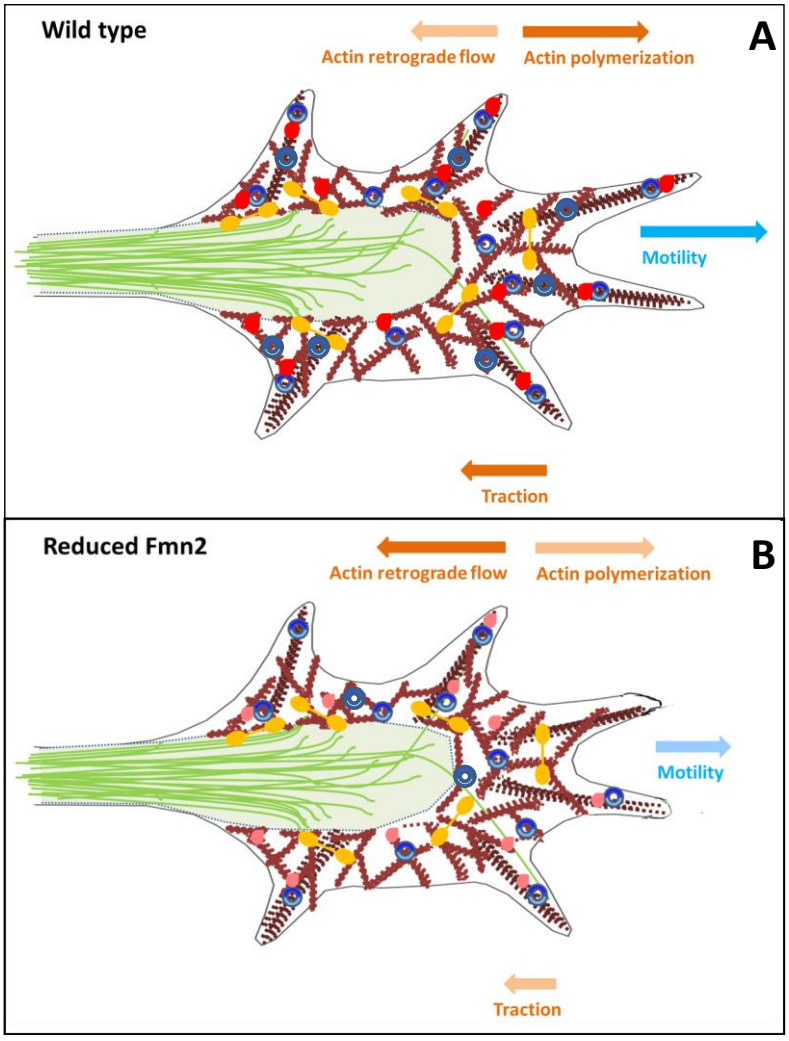
Wild type
Actin retrograde flow
Actin polymerization
A
Motility
Traction
Reduced Fmn2
Actin retrograde flow
Actin polymerization
B
Motility
Traction

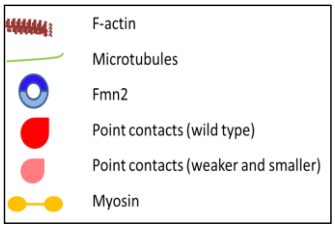
F-actin
Microtubules
Fmn2
Point contacts (wild type)
Point contacts (weaker and smaller)
Myosin

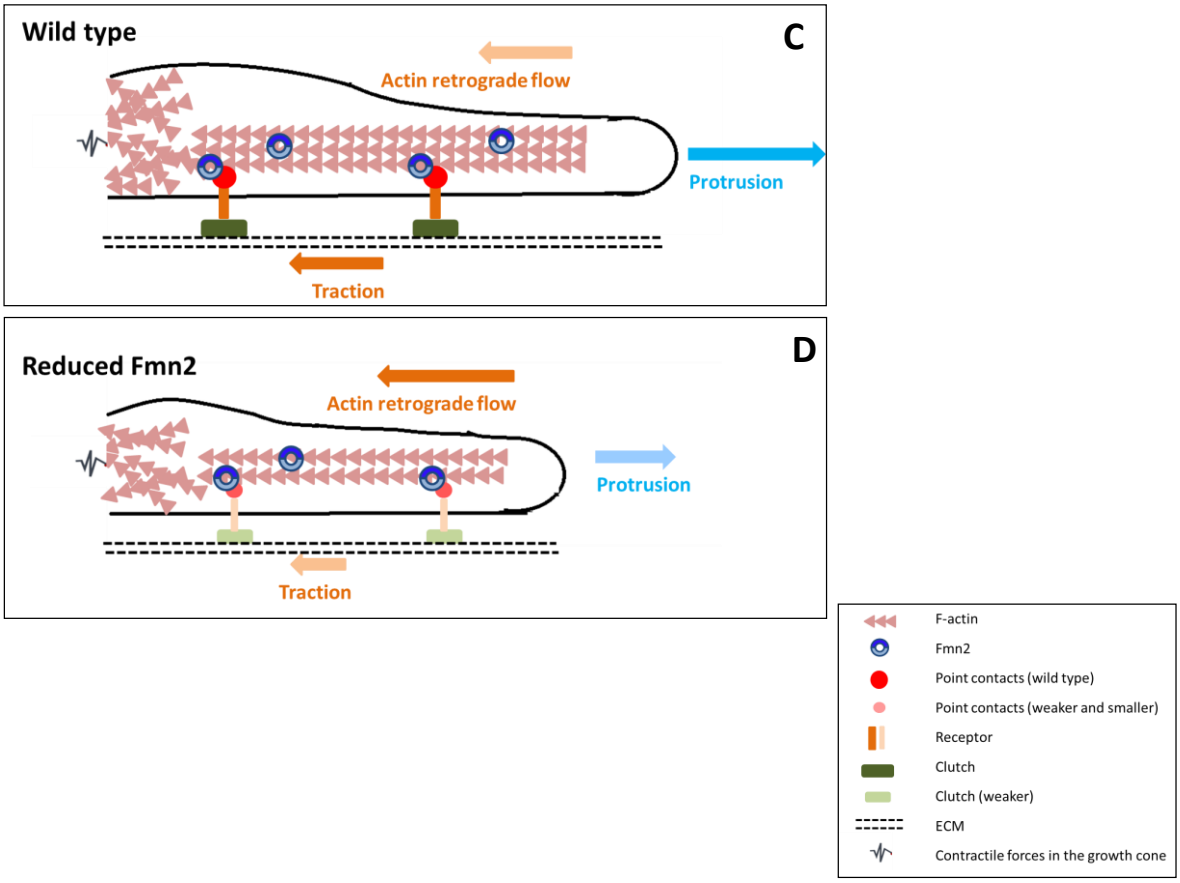

Figure 6.1: Model proposing the role of Fmn2 in growth cone motility. Fmn2 modulates point contact assembly and stability on ECM substrates as well as controls actin dynamics by regulating actin retrograde flow. The interaction of these two reflects in altered traction forces generated by neurons which in turn result in affected directed growth cone motility in the absence of Fmn2. (A) and (B) schematics showing differences in growth cone upon reduction of Fmn2. (C) and (D) schematics showing a closer view of the leading edge and compromised molecular clutch upon Fmn2 depletion.

Cell motility is essential for various cellular processes such as growth, repair and wound healing. A shared feature of these processes is that the cells must be able to apply forces onto their underlying substrates and generate traction in order to move forward. The molecular clutch is a popular model of cell motility proposed by Mitchison and Kirschner in 1988 which postulated that when actin retrograde flow is tugged to the underlying substrate of the cell (i.e. clutch is engaged) the actin polymerization takes over to result in movement of the cell. In order to achieve this, there must be a functional unit comprised of various proteins

that concurrently bind actin filaments and a membrane receptor that communicates with the underlying substrate. Initial evidence of molecular clutch model came from experiments in *Aplysia* growth cones highlighting the importance of actin retrograde flow and adhesion molecules such as apCAM (Lin and Forscher, 1995; Suter et al., 1998). Several studies in vertebrate growth cones, as well as other non-neuronal cell types, have now improved our understanding of molecular clutch. In order to relay the force generated by the actin network to the substrate, focal adhesion complexes are shown to play a very essential role. Integrin receptor-mediated sequential recruitment and activation of a variety of proteins form focal adhesions that directly attach the cell to the substrate. These complexes have been shown to recruit actin binding proteins such as talin, vinculin, and α-actinin which help them cross-link with the actin cytoskeleton. It has also been shown extensively in non-neuronal cells that the force of actin retrograde flow helps maturation of these focal adhesions and facilitates recruitment of actin binding proteins which further enhances the actin crosstalk with the focal adhesion complexes resulting in traction force generation necessary for the movement of the cell. Focal adhesion complexes are thought to be mechanosensory and they modulate their composition according to the underlying substrate. Their stabilization, maturation, and disassembly are also very well coordinated and this regulation is also shown to be influenced by actin dynamics (Case and Waterman, 2015).

As depicted in the schematic (Fig. 6.1) our studies in chick spinal neurons show localization of Fmn2 to actin structures in growth cone, depletion of which results in short-lived filopodia. However, unchanged processes like filopodial initiation and elongation rates indicate the role of Fmn2 in maintaining tip adhesion. This role of Fmn2 was further supported by parallel studies conducted in our lab which showed reduced bead-pulling by Fmn2 depleted neuronal filopodia on compliant substrates (Sahasrabudhe et al., 2016). Additionally, neuronal studies highlighted Fmn2 function in growth cone translocation by exhibiting compromised point contacts in Fmn2 deficient neurons. This suggests weakly engaged molecular clutch and can be further confirmed by an increase in the rate of actin retrograde flow observed in Fmn2 depleted neurons. A cumulative effect of this is weaker traction forces generated by Fmn2 knockdown neurons. Studies from fibroblasts showed localization of Fmn2 juxtaposed to focal adhesions and along contractile actin stress fibres. This could suggest the presence of Fmn2 within a complex that connects actin cytoskeleton to integrin-induced adhesions that facilitated their crosstalk. Cell spreading experiments in fibroblasts also indicate weak

adhesions and slipping off of the molecular clutch which supports the Fmn2 function across different cell types.

Taken together, the data suggest that Fmn2 might act a part of the functional unit that simultaneously communicates with actin architecture and focal complexes. However, it will be interesting to further dissect functional details of Fmn2 in the molecular clutch complex in order to understand its precise role in modulating the crosstalk. Apart from regulating the actin retrograde flow, Fmn2 is essential for stabilization of point contacts as indicated by pFAK (Y 397) which is vital to assembly and mechanotransduction at integrin-based adhesion sites. Our non-neuronal studies also show that Fmn2 regulates pFAK levels only on integrin binding ECM substrates, such as fibronectin indicating a possibility of its highly specific interaction in the focal adhesions. In neuronal growth cones and non-neuronal studies, talin and vinculin are two candidates that are indicated to act as a part of the molecular clutch as they are a part of the actin regulatory domain of the focal complexes. Talin is a protein that can bind both actin as well as integrin whereas vinculin binds to talin and is recruited in force dependent manner. As described in the earlier chapters, compromised point contacts in Fmn2 depleted neurons suggest that Fmn2 might be interacting with the actin-regulatory domain of focal complexes via actin interacting proteins like vinculin, relaying actin forces through the point contact complex onto the underlying substrate in form of traction forces. This interaction could be further tested by biochemistry studies among Fmn2 and vinculin. Furthermore, detailed microscopy studies of point contact proteins such as paxillin and vinculin with Fmn2 depleted background could improve our understanding of Fmn2 function in various phases of point contact assembly and maturation further revealing the mechanistic role of Fmn2. These studies and our existing knowledge of Fmn2 interaction with the actin cytoskeleton will serve as additional evidence for our model of Fmn2 as the molecular clutch.

7. Appendix

7.1 Spinal and dorsal root ganglia (DRG) neuronal culture and electroporation

Preparation of ECM coated plates

22 mm glass coverslips were glued on bottoms of drilled 35 mm plastic plates (Laxbro) using silicon glue (Dow Corning) and sterilized by 70% ethanol wash and UV treatment in the cell culture hood. These coverslip bottom plates were coated with 1mg/ml poly-L-lysine (Sigma) diluted in sterile phosphate buffered saline (137 mM NaCl, 2.7 mM KCl, 10 mM Na2HPO4, 1.8 mM KH2PO4) for 1 hour at 37oC. After washing the PLL with sterile 1X PBS the plates were coated with 20µg/ml fibronectin (Sigma) in PBS for 1 hour at 37oC. These plates were further used to culture the dissociated chick spinal neurons.

Spinal dissection and culture

Six-day old eggs (HH25/HH26) were utilised to harvest entire spinal cords of embryos. The embryos were dissected in sterile phosphate buffered saline (mentioned above) on a Silgard coated plate under a dissecting microscope inside a horizontal laminar flow hood. The dissected tissue was collected in an Eppendorf with embryonic medium (Leibovitz's media (Gibco) with 1X penicillin-streptomycin (Gibco)). The spinal cord was spun at 3000 rpm for 3 min at room temperature after which the embryonic medium was replaced with 1X trypsin-

EDTA (Lonza). The tissue was macerated in trypsin and incubated at 37^{o}C for 15-20 min. The further embryonic medium was added to the trypsin and the dissociated spinal cord was spun at 3000 rpm for 3 min. The cells were plated in 2 ml of basal culture medium (L-15 (Gibco), 1X PenStrep (Gibco), 10% heat-inactivated FBS (Gibco)) with 20ng/ml NGF (Invitrogen) supplement and incubated without CO2 at 37^{o}C for 24-36 hrs.

For electroporation, cells were resuspended in 100µl OptiMEM (Gibco) with 10 µg of plasmid.

The cell suspension with plasmid and morpholino was transferred to the electroporation cuvette and current was delivered under following conditions using NepaGene electroporator (NEPA 21 *In-vitro* and *In-vivo* electroporator).

Poring pulse:	Transfer pulse:
Voltage (V) – 125	Voltage (V) - 20
Pulse length (msec) – 5	Pulse length (msec) - 50
Pulse interval (msec) – 50	Pulse interval (msec) - 50
Number of pulses – 2	Number of pulses - 5
Decay rate (%) – 10	Decay rate (%) - 40
Polarity - +	Polarity - +/-

After electroporation, the cell suspension was transferred to a microfuge tube with 400 µl OptiMEM (Gibco) and plated on ECM coated coverslip bottom plates with 2 ml of basal culture media (mentioned above).

7.2 DRG Dissection and culture

Seven-day old eggs were utilised to harvest DRGs. The embryos were dissected in sterile phosphate buffered saline (mentioned above) on a Silgard coated plate under a dissecting microscope inside a horizontal laminar flow hood. The dissected tissue was collected in an Eppendorf with embryonic medium (Leibovitz's media (Gibco) with 1X penicillin-

streptomycin (Gibco)). The DRGs were spun at 3000 rpm for 3 min at room temperature after which the embryonic medium was replaced with 1X trypsin-EDTA (Lonza). The tissue was macerated in trypsin and incubated at 37oC for 15-20 min. The further embryonic medium was added to the trypsin and the dissociated spinal cord was spun at 3000 rpm for 3 min. The cells were plated in 2 ml of basal culture medium (F-12 (Lonza), 1X PenStrep (Gibco), 1X B27 (Invitrogen)) with 10ng/ml NGF (Invitrogen) supplement and incubated with CO2 at 37^{o}C for 24-36 hrs.

For electroporation, cells were resuspended in 100µl OptiMEM (Gibco) with 10 µg of plasmid and 100 µM morpholino.

(Standard morpholino sequence that was used as a negative control: CCTCTTACCTCAGTTACAATTTATA, Fmn2 morpholino sequence that was used: CCATCTTGATTCCCCATGATTTTTC).

The cell suspension with plasmid and morpholino was transferred to the electroporation cuvette and current was delivered under conditions mentioned above using NepaGene electroporator (NEPA 21 *In-vitro* and *In-vivo* electroporator).

After electroporation, the cell suspension was transferred to a microfuge tube with 400 µl OptiMEM (Gibco) and plated on ECM coated coverslip bottom plates with 2 ml of basal culture media using F-12 (mentioned above).

7.3 NGF induction

DRG neurons from chick embryo were cultured as mentioned earlier with pCAG-GFP and control morpholino or morpholino against gFmn2. They were subjected to 50 ng/ml NGF (Invitrogen) for every 15 min time interval until 60 min. After the NGF induction, the neurons were fixed using 4% PFA (Electron microscopy sciences) and 0.05% glutaraldehyde (Electron microscopy sciences) in PBS (mentioned earlier) for 10 min. The fixative was removed and cells were washed in PBS twice for 10 min each following which they were mounted in 80% glycerol.

7.4 *In ovo* injection and electroporation

To deliver the plasmid and morpholino in the developing spinal cord lumen, glass needles were made by pulling glass capillaries (Suter instruments BF 120-94-10) using a needle puller (Suter instruments model P-97) before the injections.

For injections, the hatched chicken eggs were incubated horizontally for 2 days. Embryos stage HH 14 were used to inject the plasmid and morpholino as during this stage the spinal cord lumen is open and thus the delivery is relatively easy. Before injections the eggs were punctured on one side with a sharp needle and about 10 – 12 ml albumin was removed using a syringe. The egg was windowed such that the embryo could be visualised on the surface. Following this, the glass needles pulled earlier were filled with morpholino and plasmid using injector (Harvard apparatus). The egg was placed under a dissection microscope and the spinal cord lumen was carefully injected using injector (Harvard apparatus); morpholinos could be visualised as they were tagged by FITC (control) or lissamine (gFmn2).

Once the entire spinal cord lumen was filled with the plasmid and morpholino then the spinal cord was electroporated using L-shaped electrodes (Nepa Gene CUY613P2) of Square wave Nepa Gene electroporator (CUY21SC). After delivery of the current, 1 ml of Leibovitz's media (Gibco) with 1X Pen-strep (Gibco) was added on to the embryo. The window in the egg was later sealed using sellotape and the egg was incubated for 2 days before further experiments.

7.5 Cryosections of spinal cord

The injected and electroporated embryos were harvested and fixed overnight in 4% PFA in PBS at 4^{o}C. Later the embryos were transferred to overnight sucrose gradient ranging from 10 – 30 % sucrose in PBS each at 4^{o}C. After the last sucrose gradient, the embryos were embedded in 15% polyvinylpyrrolidone (PVP) (Sigma) in PBS and stored at -80^{o}C.

15 µm thick sections of spinal cord were made using Leica cryotome at - 30^{o}C which were collected on glass coverslips coated with poly-L-lysine (Sigma). These sections were stored at 4^{o}C until further immunostaining.

7.6 Immunocytochemistry

Spinal cord sections from the cryotome were stored at 4^{o}C to ensure their proper attachment on the glass slide. Before starting the staining, the sections were washed in PBS for 15 min. After removing PBS, sections were permeabilized using 0.1% Triton-X in PBS for 30 min. After permeabilization, the sections were blocked in 3% BSA for 60 min. The blocking solution was replaced by an antibody against Axonin-I (23.4-5 DSHB) in 1:50 dilution in 3% BSA and incubated at 4^{o}C for 14-16 hrs. Subsequently, after removing primary antibody, the sections were washed 3 times with PBS+0.1% Triton-X, 15 times each. Later the sample was incubated at room temperature for 60 min in secondary antibody (Invitrogen) diluted 1:1000 in 3% PBS. After removing secondary antibody, the sections were washed again in PBST 3 times, 15 min each followed by one 15 min PBS wash. Lastly, the sections were mounted in mounting media containing DAPI.

7.7 Spinal cord open book preparation

After *in ovo* injection and electroporation, the embryos were harvested for open book spinal cord preparation. To be able to dissect the spinal cord in such a way that the neuronal trajectories can be observed at the midline, the embryos were mounted on the Silgard coated plate. The spinal cord was carefully opened using thin needles by breaking the roof plate. To maintain the shape of an open book, the spinal cord was intermittently washed with 4% PFA in PBS while carefully removing it from the neighbouring tissue. The final dissected spinal cord was pinned on the Silgard coated plate and fixed in 4% PFA in PBS overnight. Lastly, the spinal cord was mounted on a glass slide in PBS just prior to imaging.

7.8 Imaging

Paxillin labelled point contacts were imaged using a PlanApo 60x/1.4 oil immersion objective on an Olympus IX81 system with Hamamatsu ORCA-R2 CCD camera. Growth cones were imaged for 30 min with 3 sec interval in TIRF fluorescence for pCAG-paxillin mCherry.

The NGF induced DRG neurons were imaged using a PlanApo 63x/1.4 oil immersion objective on a Zeiss 710 inverted microscope. The growth cones were co-transfected with pCAG-GFP and morpholino thus only fluorescing growth cones were imaged.

For imaging spinal cord sections a PlanApo 20 x objective was used on Zeiss Apotome. The spinal cord open-book preparations were imaged on a PlanApo 20 x objectives was used on Zeiss 710 inverted microscope. The images were acquired with tiling mode to image the entire spinal cord and all the conditions were kept constant across treatments so that intensity can be analysed.

7.9 Analysis

The NGF induced growth cones were manually analysed using Fiji. GFP labelled growth cones were analysed by manually marking growth cone area, length of the growth cone and axonal filopodia.

The spinal cord sections and open book preparations were processed in Fiji. Analysis of signal intensity for pre and post-crossing neuronal trajectories was done by random selection of 3 similar areas on either side of the spinal cord halves.

7.10 Data representation and statistics

The data for NGF treated neurons were measured in Fiji and analysed and plotted in GraphPad Prism 5. Box and Whisker plots represent the spread of the data with the Tukey method. Outliers are represented outside the box as individual data points. All Box and Whisker plots were compared using the Mann-Whitney test. Statistical analysis was done in GraphPad Prism 5.

The analysis for spinal cord open book preparation was done in GraphPad Prism 5 where the bar graphs represent the average ratio of signal intensity from pre-crossing and post-crossing neurons. The errors bars represent the standard error calculated.

Publication

Sahasrabudhe, A., **Ghate, K.**, Mutalik, S., Jacob, A. and Ghose, A. (2016)

Formin-2 regulates stabilization of filopodial tip adhesions in growth cones and affects neuronal outgrowth and pathfinding *in vivo*. Development, 143, 449-460.

http://dev.biologists.org/content/143/3/449.long

Bibliography

1. Abercrombie, M., Heaysman, J.E.M., and Pegrum, S.M. (1971). The locomotion of fibroblasts in culture. IV. Electron microscopy of the leading lamella. Exp. Cell Res. *67*, 359–367.

2. Argiro, V., Bunge, M.B., and Johnson, M.I. (1984). Correlation between growth form and movement and their dependence on neuronal age. J. Neurosci. *4*, 3051–3062.

3. Argiro, V., Bunge, M.B., and Johnson, M.I. (1985). A quantitative study of growth cone filopodial extension. J. Neurosci. Res. *13*, 149–162.

4. Arthur, W.T., and Burridge, K. (2001). RhoA Inactivation by p190RhoGAP Regulates Cell Spreading and Migration by Promoting Membrane Protrusion and Polarity. *12*, 2711–2720.

5. Bachir, A.I., Zareno, J., Moissoglu, K., Plow, E.F., Gratton, E., and Horwitz, A.R. (2014). Integrin-associated complexes form hierarchically with variable stoichiometry in nascent adhesions. Curr. Biol. *24*, 1845–1853.

6. Balaban, N.Q., Schwarz, U.S., Riveline, D., Goichberg, P., Tzur, G., Sabanay, I., Mahalu, D., Safran, S., Bershadsky, A., Addadi, L., et al. (2001). Force and focal adhesion assembly: A close relationship studied using elastic micropatterned substrates. Nat. Cell Biol. *3*, 466–472.

7. Ballestrem, C., Erez, N., Kirschner, J., Kam, Z., Bershadsky, A., And, and Geiger, B. (2006). Molecular mapping of tyrosine-phosphorylated proteins in focal adhesions using fluorescence resonance energy transfer. J. Cell Sci. *119*, 866–875.

8. Bard, L., Boscher, C., Lambert, M., Mege, R.-M., Choquet, D., and Thoumine, O. (2008). A molecular clutch between the actin flow and N-cadherin adhesions drives growth cone migration. J. Neurosci. *28*, 5879–5890.

9. Bentley David., and T.-R.A. (1986). Disoriented pathfinding by pioneer neuron growth cones deprived of filopodia by cytochalasin treatment. Nature *323*, 712–715.

10. Berginski, M.E., and Gomez, S.M. (2013). The Focal Adhesion Analysis Server: a web tool for analyzing focal adhesion dynamics. F1000Research *68*, 4–8.

11. Bershadsky, A.D., Tint, I.S., and Neyfakh, A.A. (1985). Focal contacts of normal and RSV-transformed Quail cells characteristics distinguishing transformed cultured cells from their non-trans- containing contacts than low metastatic variants of the same tumor cells [15]. Immunofluorescence Staining of Cytosk. *158*, 433–444.

12. Bornschlögl, Thomas, Romero Stephane, Vestergaard Christian, Joanny Jean-Francois, V.N.G.T. and B.P. (2013). Filopodial retraction force is generated by cortical actin dynamics and controlled by reversible tethering at the tip. In PNAS, pp. 18928–18933.

13. Butler, J.P., Tolic-Norrelykke, I.M., Fabry, B., and Fredberg, J.J. (2002). Traction fields, moments, and strain energy that cells exert on their surroundings. AJP Cell Physiol. *282*, C595–C605.

14. Campellone, K.G., and Welch, M.D. (2010). A nucleator arms race: Cellular control

of actin assembly. Nat. Rev. Mol. Cell Biol. *11*, 237–251.

15. Case, L.B., and Waterman, C.M. (2015). Integration of actin dynamics and cell adhesion by a three-dimensional, mechanosensitive molecular clutch. Nat. Cell Biol. *17*, 955–963.

16. Chan, C.E., and Odde, D.J. (2008). Traction dynamics of filopodia on compliant substrates. Science (80-.). *322*, 1687–1691.

17. Chesarone, M.A., and Goode, B.L. (2009). Actin nucleation and elongation factors: mechanisms and interplay. Curr. Opin. Cell Biol. *21*, 28–37.

18. Chien, C. Bin, Rosenthal, D.E., Harris, W.A., and Holt, C.E. (1993). Navigational errors made by growth cones without filopodia in the embryonic Xenopus brain. Neuron *11*, 237–251.

19. Choi, C.K., Vicente-Manzanares, M., Zareno, J., Whitmore, L.A., Mogilner, A., and Horwitz, A.R. (2008). Actin and α-actinin orchestrate the assembly and maturation of nascent adhesions in a myosin II motor-independent manner. Nat. Cell Biol. *10*, 1039–1050.

20. Chrzanowska-wodnicka, M., and Burridge, K. (1996). Rho-stimulated contractility drives the formation of stress fibers and focal adhesions. J. Cell Biol. *133*, 1403–1415.

21. Cramer, L.P., Siebert, M., and Mitchison, T.J. (1997). Identification of novel graded polarity actin filament bundles in locomoting heart fibroblasts: Implications for the generation of motile force. J. Cell Biol. *136*, 1287–1305.

22. D. Pollard, T., and G. Borisy, G. (2003). Cellular motility driven by assembly and disassembly of actin filaments. Cell *21*, 453–465.

23. Dent, E.W., and Gertler, F.B. (2003). Cytoskeletal dynamics and transport in growth cone motility and axon guidance. Neuron *40*, 209–227.

24. Dent, E.W., and Meiri, K.F. (1992). GAP-43 phosphorylation is dynamically

regulated in individual growth cones. J. Neurobiol. *23*, 1037–1053.

25. Dent, E.W., Kwiatkowski, A. V, Mebane, L.M., Philippar, U., Barzik, M., Rubinson, D.A., Gupton, S., Van Veen, J.E., Furman, C., Zhang, J., et al. (2007). Filopodia are required for cortical neurite initiation. Nat. Cell Biol. *9*, 1347–1359.

26. Dent, E.W., Gupton, S.L., Gertler, F.B., Chédotal, A., Richards, L.J., Frank, B., Adams, R.H., Eichmann, A., Engle, E.C., Raper, J., et al. (2011). The growth cone cytoskeleton in axon.

27. Faix, J., and Rottner, K. (2006). The making of filopodia. Curr. Opin. Cell Biol. *18*, 18–25.

28. Fitzli, D., Stoeckli, E.T., Kunz, S., Siribour, K., Rader, C., Kunz, B., Kozlov, S. V., Buchstaller, A., Lane, R.P., Suter, D.M., et al. (2000). A direct interaction of axonin-1 with NgCAM-related cell adhesion molecule (NrCAM) results in guidance, but not growth of commissural axons. J. Cell Biol. *149*, 951–968.

29. Forscher, P., and S.S.J. (1988). Actions of Cytochalasins on the organization of actin filaments and microtubules in a neuronal growth cone. J. Cell Biol. *107*, 1505–1516.

30. Friedland, J., Lee, M., and Boettiger, D. (2009). Structure of integrin a 5 b 1 in complex with fibronectin. Science (80-.). *323*, 642–644.

31. Gardel, M.L., Schneider, I.C., Aratyn-Schaus, Y., and Waterman, C.M. (2010). Mechanical integration of actin and adhesion dynamics in cell migration. Annu. Rev. Cell Dev. Biol. *26*, 315–333.

32. Gauthier, Nils C., Fardin Marc A., Roca-Cusachs P., and S.M.P. (2011). Temporary increase in plasma membrane tension coordinates the activation of exocytosis and contraction during cell spreading. PNAS *108*, 14467–14472.

33. Geiger, B., Bershadsky, A., Pankov, R., and Yamada, K.M. (2001). Transmembrane extracellular matrix-cytoskeleton crosstalk. Nat. Rev. Mol. Cell Biol. *2*, 793–805.

34. Geiger, B., Spatz, J.P., and Bershadsky, A.D. (2009). Environmental sensing through

focal adhesions. Nat. Rev. Mol. Cell Biol. *10*, 21–33.

35. Giannone, G., Dubin-Thaler, B.J., Döbereiner, H.G., Kieffer, N., Bresnick, A.R., and Sheetz, M.P. (2004). Periodic lamellipodial contractions correlate with rearward actin waves. Cell *116*, 431–443.

36. Gomez, T.M., Roche, F.K., and Letourneau, P.C. (1996). Chick sensory neuronal growth cones distinguish fibronectin from laminin by making substratum contacts that resemble focal contacts. J. Neurobiol. *55455*.

37. Gupton, S.L., and Gertler, F.B. (2007). Filopodia: The fingers that do the walking. Sci. STKE *2007*, re5-re5.

38. Gupton, S.L., Eisenmann, K., Alberts, A.S., and Waterman-Storer, C.M. (2007). mDia2 regulates actin and focal adhesion dynamics and organization in the lamella for efficient epithelial cell migration. J. Cell Sci. *120*, 3475–3487.

39. Heath, J.P. (1983). Behaviour and structure of the leading lamella in moving fibroblasts.

40. Heath, J.P., and Dunn, G.A. (1978). Cell to substratum contacts of chick fibroblasts and their relation to the microfilament system. A correlated interference-reflexion and high-voltage electron microscope study Electron-microscopical studies of cultured non-muscle cells have demonstrated. Cell *212*, 197–212.

41. Higgs, H.N., and Peterson, K.J. (2005). Phylogenetic analysis of the formin homology 2 domain. Mol. Biol. Cell *16*, 1–13.

42. Holinstat, M., Knezevic, N., Broman, M., Samarel, A.M., Malik, A.B., and Mehta, D. (2006). Suppression of RhoA activity by focal adhesion kinase-induced activation of p190RhoGAP: Role in regulation of endothelial permeability. J. Biol. Chem. *281*, 2296–2305.

43. Hotulainen, P., and Lappalainen, P. (2006). Stress fibers are generated by two distinct actin assembly mechanisms in motile cells. J. Cell Biol. *173*, 383–394.

44. Huber, A.B., Kolodkin, A.L., Ginty, D.D., and Cloutier, J.-F. (2003). Signaling at the growth cone: Ligand-receptor complexes and the control of axon growth and guidance. Annu. Rev. Neurosci. *26*, 509–563.

45. Hyland, C., Mertz, A.F., Forscher, P., and Dufresne, E. (2014). Dynamic peripheral traction forces balance stable neurite tension in regenerating Aplysia bag cell neurons. Sci. Rep. *4*, 1–8.

46. Iskratsch, T., Yu, C.H., Mathur, A., Liu, S., Stévenin, V., Dwyer, J., Hone, J., Ehler, E., and Sheetz, M. (2013). FHOD1 is needed for directed forces and adhesion maturation during cell spreading and migration. Dev. Cell *27*, 545–559.

47. Iwasa, J.H., and Mullins, R.D. (2007). Spatial and temporal relationships between actin-filament nucleation, capping, and disassembly. Curr. Biol. *17*, 395–406.

48. Jiang, G., Giannone, G., Critchley, D.R., Fukumoto, E., and Sheet, M.P. (2003). Two-piconewton slip bond between fibronectin and the cytoskeleton depends on talin. Nature *424*, 334–337.

49. Jones, L.S. (1996). Integrins: possible functions in the adult CNS. Trends Neurosci. *19*, 68–72.

50. Kage, F., Winterhoff, M., Dimchev, V., Mueller, J., Thalheim, T., Freise, A., Brühmann, S., Kollasser, J., Block, J., Dimchev, G., et al. (2017). FMNL formins boost lamellipodial force generation. Nat. Commun. *8*.

51. Kamiguchi, H. (2007). The role of cell adhesion molecules in axon growth and guidance. Adv. Exp. Med. Biol. *621*, 95–103.

52. Kaufmann, N., Wills, Z.P., and Van Vactor, D. (1998). Drosophila Rac1 controls motor axon guidance. Development *125*, 453–461.

53. Kerstein, P.C., Jacques-Fricke, B.T., Rengifo, J., Mogen, B.J., Williams, J.C., Gottlieb, P.A., Sachs, F., and Gomez, T.M. (2013). Mechanosensitive TRPC1 channels promote calpain proteolysis of talin to regulate spinal axon outgrowth. J. Neurosci. *33*, 273–285.

54. Kerstein, P.C., Nichol IV, R.H., and Gomez, T.M. (2015). Mechanochemical regulation of growth cone motility. Front. Cell. Neurosci. *9*, 1–16.

55. Ketschek, A., and Gallo, G. (2010). Nerve growth factor induces axonal filopodia through localized microdomains of phosphoinositide 3-kinase activity that drive the formation of cytoskeletal precursors to filopodia. J. Neurosci. *30*, 12185–12197.

56. Ketschek, A., Jones, S., Spillane, M., Korobova, F., Svitkina, T., and Gallo, G. (2015). Nerve growth factor promotes reorganization of the axonal microtubule array at sites of axon collateral branching. Dev. Neurobiol. *75*, 1441–1461.

57. Koch, D., Rosoff, W.J., Jiang, J., Geller, H.M., and Urbach, J.S. (2012). Strength in the periphery: Growth cone biomechanics and substrate rigidity response in peripheral and central nervous system neurons. Biophys. J. *102*, 452–460.

58. Kolodkin, A.L., and Tessier-Lavigne, M. (2010). Mechanisms and molecules of neuronal wiring: A Primer. Cold Spring Harb Perspect Biol.

59. Kovac, B., Teo, J.L., Mäkelä, T.P., and Vallenius, T. (2013). Assembly of non-contractile dorsal stress fibers requires α-actinin-1 and Rac1 in migrating and spreading cells. J. Cell Sci. *126*, 263–273.

60. Kuo, J.C., Han, X., Hsiao, C. Te, Yates, J.R., and Waterman, C.M. (2011). Analysis of the myosin-II-responsive focal adhesion proteome reveals a role for β-Pix in negative regulation of focal adhesion maturation. Nat. Cell Biol. *13*, 383–395.

61. Lafont, F., Rouget, M., Rousselet, A., Valenza, C., and Prochiantz, A. (1993). Specific responses of axons and dendrites to cytoskeleton perturbations: J Cell Sci *104*, 433–443.

62. Law, R., Dixon-Salazar, T., Jerber, J., Cai, N., Abbasi, A.A., Zaki, M.S., Mittal, K., Gabriel, S.B., Rafiq, M.A., Khan, V., et al. (2014). Biallelic truncating mutations in FMN2, encoding the actin-regulatory protein formin 2, cause nonsyndromic autosomal-recessive intellectual disability. Am. J. Hum. Genet. *95*, 721–728.

63. Leader, B., and Leder, P. (2000). Formin-2, a novel formin homology protein of the cappuccino subfamily, is highly expressed in the developing and adult central nervous system. Mech. Dev. *93*, 221–231.

64. Leader, B., Lim, H., Carabatsos, M.J., Harrington, A., Ecsedy, J., Pellman, D., Maas, R., and Leder, P. (2002). Formin-2, polyploidy, hypofertility, and positioning of the meiotic spindle in mouse oocytes. Nat. Cell Biol. *4*, 921–928.

65. Lee, A.C., and Suter, D.M. (2008). Quantitative analysis of microtubule dynamics during adhesion-mediated growth cone guidance. Dev. Neurobiol. *68*, 1363–1377.

66. Lehtimaki J., Hakala M., L.P. (2016). Actin filament structures in migrating cells. Handb. Exp. Pharmacol.

67. Lin, Chi-hung, T.C.A., and F.P. (1994). Cytoskeletal reorganization underlying growth cone motility. Curr. Opin. Neurobiol. *4*, 640–647.

68. Lin, C., and Forscher, P. (1993). Cytoskeletal remodeling during growth cone-target interactions. J. Cell Biol. *121*, 1369–1383.

69. Lin, C.H., and Forscher, P. (1995). Growth cone advance is inversely proportional to retrograde F-actin flow. Neuron *14*, 763–771.

70. Livak, K.J., And, and Schmittgen, T.D. (2001). Analysis of relative gene expression data using real-time quantitative PCR and the 2(-Delta Delta C(T)) Method. In Methods, pp. 402–408.

71. Lo, C.M., Wang, H.B., Dembo, M., and Wang, Y.L. (2000). Cell movement is guided by the rigidity of the substrate. Biophys. J. *79*, 144–152.

72. Loudon, R.P., Silver, L.D., Yee, H.F., and Gallo, G. (2006). RhoA-kinase and myosin II are required for the maintenance of growth cone polarity and guidance by nerve growth factor. J. Neurobiol. *66*, 847–867.

73. Lowery, L.A., and Vactor, D. Van (2009). The trip of the tip: Understanding the growth cone machinery. Nat. Rev. Mol. Cell Biol. *10*, 332–343.

74. Mallavarapu, A., and Mitchison, T. (1999). Regulated actin cytoskeleton assembly at filopodium tips controls their extension and retraction. J. Cell Biol. *146*, 1097–1106.

75. Maness, P.F., and Schachner, M. (2007). Neural recognition molecules of the immunoglobulin superfamily : signaling transducers of axon guidance and neuronal migration. Nat. Neurosci. *10*.

76. Marsh, L., and Letourneau, P.C. (1984). Growth of neurites without filopodial or lamellipodial activity in the presence of cytochalasin B. J. Cell Biol. *99*, 2041–2047.

77. Matusek, T., Gombos, R., Szecsenyi, A., Sanchez-Soriano, N., Czibula, A., Pataki, C., Gedai, A., Prokop, A., Rasko, I., and Mihaly, J. (2008). Formin proteins of the DAAM subfamily play a role during axon growth. J. Neurosci. *28*, 13310–13319.

78. Medeiros, N.A., Burnette, D.T., and Forscher, P. (2006). Myosin II functions in actin-bundle turnover in neuronal growth cones. Nat. Cell Biol. *8*, 215–226.

79. Mitchison, T., and Kirschner, M. (1988). Cytoskeletal dynamics and nerve growth. Neuron *1*, 761–772.

80. Moissoglu, K., and Schwartz, M.A. (2006). Integrin signalling in directed cell migration. Biol. Cell *98*, 547–555.

81. Montaville, P., Jégou, A., Pernier, J., Compper, C., Guichard, B., Mogessie, B., Schuh, M., Romet-Lemonne, G., and Carlier, M.F. (2014). Spire and Formin 2 synergize and antagonize in regulating actin assembly in meiosis by a ping-pong mechanism. PLoS Biol. *12*, 1–20.

82. Moore, S.W., Biais, N., and Sheetz, M.P. (2009). Traction on immobilized Netrin-1 is sufficient to reorient axons. Science (80-.). *325*, 18–20.

83. Moore, S.W., Zhang, X., Lynch, C.D., and Sheetz, M.P. (2012). Netrin-1 attracts axons through FAK-dependent mechanotransduction. J. Neurosci. *32*, 11574–11585.

84. Moser, M. (2009). The tail of Integrins , Talin , and Kindlins. *895*, 895–900.

85. Mozhui, K., Ciobanu, D.C., Schikorski, T., Wang, X., Lu, L., and Williams, R.W. (2008). Dissection of a QTL hotspot on mouse distal chromosome 1 that modulates neurobehavioral phenotypes and gene expression. PLoS Genet. *4*.

86. Myers, J.P., and Gomez, T.M. (2011). Focal adhesion kinase promotes integrin adhesion dynamics necessary for chemotropic turning of nerve growth cones. J. Neurosci. *31*, 13585–13595.

87. Myers, J.P., Santiago-Medina, M., and Gomez, T.M. (2011). Regulation of axonal outgrowth and pathfinding by integrin-ECM interactions. Dev. Neurobiol. *71*, 901–923.

88. Nobes, C.D., and Hall, A. (1995). Rho, Rac, and Cdc42 GTPases regulate the assembly of actin stress fibers, lamellipodia, and filopodia. Cell *81*, 53–62.

89. Oakes, P.W., Beckham, Y., Stricker, J., and Gardel, M.L. (2012). Tension is required but not sufficient for focal adhesion maturation without a stress fiber template. J. Cell Biol. *196*, 363–374.

90. Pak, C.W., Flynn, K.C., and Bamburg, J.R. (2008). Actin-binding proteins take the reins in growth cones. Nat. Rev. Neurosci. *9*, 136–147.

91. Pepper, S., and Patricia, J.K. (2011). Mammary gland ECM remodeling, stiffness, and mechanosignaling in normal development and tumor progression. Cold Spring Harb. Perspect. Biol. *3*, 56–60.

92. Pfender, S., Kuznetsov, V., Pleiser, S., Kerkhoff, E., and Schuh, M. (2011). Spire-type actin nucleators cooperate with formin-2 to drive asymmetric oocyte division. Curr. Biol. *21*, 955–960.

93. Pinkstaff, J.K., Detterich, J., Lynch, G., and Gall, C. (1999). Integrin subunit gene expression is regionally differentiated in adult brain. J. Neurosci. *19*, 1541–1556.

94. Plotnikov, S. V, Pasapera, A.M., Sabass, B., and Waterman, C.M. (2012). Force fluctuations within focal adhesions mediate ECM-rigidity sensing to guide directed

cell migration. Cell *151*, 1513–1527.

95. Polackwich, R.J., Koch, D., McAllister, R., Geller, H.M., and Urbach, J.S. (2015). Traction force and tension fluctuations in growing axons. Front. Cell. Neurosci. *9*, 1–9.

96. Ponti, A., Machacek, M., Gupton, S.L., Waterman-Storer, C.M., and Danuser, G. (2004). Two distinct actin networks drive the protrusion of migrating cells. Science (80-.). *305*, 1782–1786.

97. Renaudin, A., Lehmann, M., Girault, J.A., and McKerracher, L. (1999). Organization of point contacts in neuronal growth cones. J. Neurosci. Res. *55*, 458–471.

98. Ridley, A.J. (2011). Life at the leading edge. Cell *145*, 1012–1022.

99. Riveline, D., Zamir, E., Balaban, N.Q., Schwarz, U.S., Ishizaki, T., Narumiya, S., Kam, Z., Geiger, B., And, and Bershadsky, A.D. (2001). Focal contacts as mechanosensors externally applied local mechanical force induces growth of focal contacts by an mDia1-dpendent and ROCK-independent mechanism. J. Cell Biol. *153*, 1175–1185.

100. Robles, E., and Gomez, T.M. (2006). Focal adhesion kinase signaling at sites of integrin-mediated adhesion controls axon pathfinding. Nat. Neurosci. *9*, 1274–1283.

101. Rosales-nieves, A.E., Johndrow, J.E., Keller, L.C., Magie, C.R., Pinto-santini, D.M., Parkhurst, S.M., Spire, T., and Capu, C. (2006). Coordination of microtubule and microfilament dynamics by Drosophila Rho1 , Spire and Cappuccino. Nat. Cell Biol. *8*.

102. Saez, A., Buguin, A., Silberzan, P., and Ladoux, B. (2005). Is the mechanical activity of epithelial cells controlled by deformations or forces? Biophys. J. *89*, 52–54.

103. Sahasrabudhe, A., Ghate, K., Mutalik, S., Jacob, A., and Ghose, A. (2016). Formin 2 regulates the stabilization of filopodial tip adhesions in growth cones and affects neuronal outgrowth and pathfinding in vivo. Development *143*, 449–460.

104. Sander, E.E., Ten Klooster, J.P., Van Delft, S., Van Der Kammen, R.A., and Collard, J.G. (1999). Rac downregulates Rho activity: Reciprocal balance between both GTPases determines cellular morphology and migratory behavior. J. Cell Biol. *147*, 1009–1021.

105. Sanger, J.W., Sanger, J.M., and Jockusch, B.M. (1983). Differences in the stress fibers between fibrblasts and epithelial cells. J. Cell Biol. *96*, 961–969.

106. Schaub, Sébastien., Bohnet Sophie., Laurent Valerie M., Meister Jean-Jacques., and V.A.B. (2007). Comparative maps of motion and assembly of filamentous actin and myosin II in migrating cells. Mol. Biol. Cell *18*, 3723–3732.

107. Schober, M., Raghavan, S., Nikolova, M., Polak, L., Pasolli, H.A., Beggs, H.E., Reichardt, L.F., and Fuchs, E. (2007). Focal adhesion kinase modulates tension signaling to control actin and focal adhesion dynamics. J. Cell Biol. *176*, 667–680.

108. Schuh, M., and Ellenberg, J. (2008). A new model for asymmetric spindle positioning in mouse oocytes. Curr. Biol. *18*, 1986–1992.

109. Schumacher, N., Borawski, J.M., Leberfinger, C.B., Gessler, M., and Kerkhoff, E. (2004). Overlapping expression pattern of the actin organizers Spir-1 and formin-2 in the developing mouse nervous system and the adult brain. Gene Expr. Patterns *4*, 249–255.

110. Shi, Q., And, and Boettiger, D. (2013). A novel mode for integrin-mediated signaling: tethering is required for phosphorylation of FAK Y397. Mol. Biol. Cell *14*, 4306–4315.

111. Short, C.A., Suarez-Zayas, E.A., and Gomez, T.M. (2016). Cell adhesion and invasion mechanisms that guide developing axons. Curr. Opin. Neurobiol. *39*, 77–85.

112. Small, J.V. (1988). The actin cytoskeleton. In Electron Microscopy Review, pp. 155–174.

113. Small, J.V., Rottner, K., Kaverina, I., and Anderson, K.I. (1998). Assembling an actin cytoskeleton for cell attachment and movement. Biochim. Biophys. Acta - Mol. Cell Res. *1404*, 271–281.

114. Spillane, M., Ketschek, A., Donnelly, C.J., Pacheco, A., Twiss, J.L., and Gallo, G. (2012). Nerve growth factor-induced formation of axonal filopodia and collateral branches Involves the intra-axonal synthesis of regulators of the actin-nucleating Arp2/3 complex. J. Neurosci. *32*, 17671–17689.

115. Stricker, J., Beckham, Y., Davidson, M.W., and Gardel, M.L. (2013). Myosin II-mediated focal adhesion maturation is tension insensitive. PLoS One *8*.

116. Suter, D.M., and Forscher, P. (2000). Substrate-cytoskeletal coupling as a mechanism for the regulation of growth cone motility and guidance. J. Cell Sci. *44*, 97–113.

117. Suter, D.M., and Forscher, P. (2001). Transmission of growth cone traction force through apcam-cytoskeletal linkages is regulated by src family tyrosine kinase activity. J. Cell Biol. *155*, 427–438.

118. Svitkina, T.M., Verkhovsky, A.B., McQuade, K.M., and Borisy, G.G. (1997). Analysis of the actin-myosin II system in fish epidermal keratocytes: Mechanism of cell body translocation. J. Cell Biol. *139*, 397–415.

119. Svitkina, T.M., Bulanova, E.A., Chaga, O.Y., Vignjevic, D.M., Kojima, S. ichiro, Vasiliev, J.M., and Borisy, G.G. (2003). Mechanism of filopodia initiation by reorganization of a dendritic network. J. Cell Biol. *160*, 409–421.

120. Sydor, A.M., Su, A.L., Wang, F., Xu, A., and Jay, D.G. (1996). Talin and vinculin play distinct roles in filopodial motility in the neuronal growth cone antibody loading by trituration methods of quantitation. Cell *134*, 1197–1207.

121. Symons, M.H., and Mitchison, T.J. (1991). Control of actin polymerization in live and permeabilized fibroblasts. J. Cell Biol.

122. Tadokoro, S., Shattil, S.J., Eto, K., Tai, V., Liddington, R.C., de Pereda, J.M., Ginsberg, M.H., and Calderwood, D. a (2003). Talin binding to integrin beta tails : A final common step in integrin. Science (80-.). *302*, 103–106.

123. Tee, Y.H., Shemesh, T., Thiagarajan, V., Hariadi, R.F., Anderson, K.L., Page, C., Volkmann, N., Hanein, D., Sivaramakrishnan, S., Kozlov, M.M., et al. (2015). Cellular chirality arising from the self-organization of the actin cytoskeleton. Nat. Cell Biol. *17*, 445–457.

124. Thoumine, O. (2008). Interplay between adhesion turnover and cytoskeleton dynamics in the control of growth cone migration. Cell Adh. Migr. *2*, 263–267.

125. Tojkander, S., Gateva, G., and Lappalainen, P. (2012). Actin stress fibers - assembly, dynamics and biological roles. J. Cell Sci. *125*, 1855–1864.

126. Tojkander, S., Gateva, G., Husain, A., Krishnan, R., and Lappalainen, P. (2015). Generation of contractile actomyosin bundles depends on mechanosensitive actin filament assembly and disassembly. Elife *4*, 1–28.

127. Toriyama, M., Kozawa, S., Sakumura, Y., and Inagaki, N. (2013). Conversion of a signal into forces for axon outgrowth through pak1-mediated shootin1 phosphorylation. Curr. Biol. *23*, 529–534.

128. Tse, J.R., and Engler, A.J. (2010). Preparation of Hydrogel Substrates with Tunable Mechanical Properties. Curr. Protoc. Cell Biol. 1–16.

129. Tsygankov, D., Bilancia, C.G., Vitriol, E.A., Hahn, K.M., Peifer, M., and Elston, T.C. (2014). CellGeo: A computational platform for the analysis of shape changes in cells with complex geometries. J. Cell Biol. *204*, 443–460.

130. Vallenius, T. (2013). Actin stress fibre subtypes in. Open Biol. *3*.

131. Vitriol, E.A., and Zheng, J.Q. (2012). Growth Cone Travel in Space and Time: The Cellular Ensemble of Cytoskeleton, Adhesion, and Membrane. Neuron 73, 1068–1080.

132. Webb, D.J., Donais, K., Whitmore, L.A., Thomas, S.M., Turner, C.E., Parsons, J.T., and Horwitz, A.F. (2004). FAK-Src signalling through paxillin, ERK and MLCK regulates adhesion disassembly. Nat. Cell Biol. *6*, 154–161.

133. Wiseman, P.W. (2004). Spatial mapping of integrin interactions and dynamics during cell migration by Image Correlation Microscopy. J. Cell Sci. *117*, 5521–5534.

134. Wolfenson, H., Iskratsch, T., and Sheetz, M.P. (2015). Early events in cell spreading as a model for quantitative analysis of biomechanical events. Biophys. J. *107*, 2508–2514.

135. Woo, S. (2006). Rac1 and RhoA promote neurite outgrowth through formation and stabilization of growth cone point contacts. J. Neurosci. *26*, 1418–1428.

136. Yaginuma, H., Shiga, T., Homma, S., Ishihara, R., Oppenheim, R.W., Bargmann, C.I., and Garriga, G. (1990). Identification of early developing axon projections from spinal interneurons in the chick embryo with a neuron specific beta-tubulin antibody: evidence for a new “pioneer” pathway in the spinal cord. Development *108*, 705–716.

137. Yamada, K.M., Spooner, B.S., and Wessells, N.K. (1970). Axon growth: roles of microfilaments and microtubules. Proc. Natl. Acad. Sci. *66*, 1206–1212.

138. Yamada, K.M., Spooner, B.S., and Wessells, N.K. (1971). Ultrastructure and function of growth cones and axons of cultured nerve cells. J. Cell Biol. *49*, 614–635.

139. Yang, C., and Svitkina, T. (2011). Filopodia initiation: Focus on the Arp2/3 complex and formins. Cell Adhes. Migr. *5*, 402–408.

140. Yu-Li, P.R.J. and W. (1997). Cell locomotion and focal adhesions are regulated by substrate. Proc. Natl. Acad. Sci. *94*, 13661–13665.

141. Yu, C., Law, J.B.K., Suryana, M., Low, H.Y., and Sheetz, M.P. (2011). Early integrin binding to Arg-Gly-Asp peptide activates actin polymerization and

contractile movement that stimulates outward translocation. Proc. Natl. Acad. Sci. *108*, 20585–20590.

142. Zaidel-Bar, R., Milo, R., Kam, Z., and Geiger, B. (2006). A paxillin tyrosine phosphorylation switch regulates the assembly and form of cell-matrix adhesions. J. Cell Sci. *120*, 137–148.

143. Zamir, E., Katz, M., Posen, Y., Erez, N., Yamada, K.M., Katz, B.Z., Lin, S., Lin, D.C., Bershadsky, A., Kam, Z., et al. (2000). Dynamics and segregation of cell-matrix adhesions in cultured fibroblasts. Nat. Cell Biol. *2*, 191–196.